Microbial Interactions: From Microbes to Metals

A DISSERTATION
SUBMITTED TO THE FACULTY OF
UNIVERSITY OF MINNESOTA
BY

Aunica Lea Kane

IN PARTIAL FULFILLMENT OF THE REQUIREMENTS
FOR THE DEGREE OF
DOCTOR OF PHILOSOPHY

Adviser: Jeffrey A. Gralnick

January 2016

Acknowledgements

It takes a village to raise a scientist, and I have been raised by some of the best. Thank you first and foremost to my advisor, Jeffrey Gralnick. Your love for science is contagious, and I am grateful for your years of support and encouragement. You promised in the beginning that if I continued to be excited about the science you could teach me the rest. You have more than lived up to your promise! My graduate school years have been some of the most fun and exciting years of my life, so thank you. Thank you also to Daniel Bond who is equally responsible for pushing me to become a better scientist. Thank you for the years of engaging conversations, for helping me to delve into all of the complexities of metabolism, and for always being willing to light something on fire!

I am equally grateful to all of the many talented people I was able to work alongside during my graduate career. Many of my lab mates have become more than friends, and I consider many of you to be like family. Thank you especially to Zara Summers. Not only are you an amazing friend, but you were a very important mentor through all of the ups and downs of graduate school. Thank you also to Nick Kotloski who is not only a great scientist, but is also a great friend. Thank you for all of your help and for our many, many, many science and life conversations. Fixing the HPLC hasn't been the same without you! I also must thank Caleb Levar for being a great friend and co-worker. Thanks for always making the MICaB retreat one of my favorite times of the year and for providing tasty refreshments any time I needed one! Our conversations on

science and life have meant a lot to me. Thank you also to Evan Brutinel. Your monocle-ness can never be replaced. Thanks for your support and encouragement! Miss Audrey Harris, thanks for being a great friend (not just a co-worker). You truly are a triple threat and you definitely made lab more fun! I miss our long walks and conversations on the way out each night. To Ben Bonis, thanks for making lab bananas! You are one of a kind, and I am so happy I was able to work alongside you for so many years. Brittany Bennett, thanks for making some great holiday memories and for all of the dance parties! I am counting on you to keep our lab traditions going! Eric (Kee Kee) Kees, thanks for being all-around awesome! Last, but certainly not least, thank you also to Jeff Flynn. You were the first person I met in the Gralnick lab, and I am so thankful for our friendship. Thank you for all of the support and for our many conversations over the years. To all of the newer members of the Gralnick lab, thank you for helping to keep the lab not only a place for great science, but also a place for fun.

I also want to thank the many, many undergraduates I was able to work with over the years. My very biggest thank you goes to Rachel Soble. You are such a talented and amazing young woman, and it has been such a pleasure to watch you grow over the past four years. I am so lucky that Jeff paired us up in the beginning. I could not have asked for anyone better! You are awesome, and I am going to miss you more than you will ever know! I can't wait to see all that you accomplish as you take the next step in graduate school, and I will be cheering for you the whole way!

Thank you also to my family and friends! I have the world's greatest support system. Dad, thanks for opening up the world of science to me, and for being the best dad in the world. Mom, thanks for always being there and being my biggest fan. I couldn't have done this without you two! Sheila, thank you for being more than just my step-mom! To Anna, Mitch, Sarah, LaRae and Zach, thank you for being the world's greatest siblings. Life has thrown a lot at our family over the past few years, and I am so lucky to have all of you. Thank you also to my best friend in the world, Sally Mielke. You are more than just my best friend; you are my family! I love all of you to the moon and back!

Dedication

This thesis is dedicated to my husband and best friend, Randall Kane. There aren't words to express how grateful I am for your love and support. There is no way I could have made it through all of this without you. I am the luckiest girl in the world, and there is no other person I would rather have made this journey with. Thank you for being my everything and my very best friend.

Abstract

Microbial communities are the major drivers of biochemical cycling and nutrient flux on the planet, yet despite their importance, the factors that influence and shape behavior and function of microbial ecosystems remain largely undefined. The knowledge gap existing for microbial communities stems partly from a focus of microbiologists on monoculture but also because studies of multispecies systems are impeded by their complexity and dynamic nature. Synthetic ecology, the engineering of rationally designed communities in well-defined environments, provides an innovative and robust approach to reduce the complexity inherent in natural systems and mimic microbial interaction in a controlled framework.

Synthetic ecology was used to engineer a co-culture using two previously non-interacting bacteria, *Shewanella oneidensis* and *Geobacter sulfurreducens*, both organisms important for multiple applications in biotechnology. The *S. oneidensis* and *G. sulfurreducens* co-culture provided a model laboratory co-culture to study microbial interactions and revealed that genetic mutations in metabolic pathways can provide the foundation to initiate cooperation and syntrophic relationships in multispecies ecosystems. Syntrophy between *S. oneidensis* and *G. sulfurreducens* was studied further using three-electrode bioreactors. Both *S. oneidensis* and *G. sulfurreducens* are capable of respiring insoluble terminal electron acceptors, a process termed extracellular respiration. During extracellular respiration, electrons produced during oxidative metabolism are transferred across both membranes to the outer surface of the bacterial cell where they

reduce terminal electron acceptors such as metal oxides. Extracellular respiration can be monitored in real time as current produced in bioreactors with electrodes serving as a proxy for metal oxides. The ability of both *S. oneidensis* and *G. sulfurreducens* to transfer electrons to their outer surface enabled the study of a process central to many syntrophic communities known as interspecies electron transfer – the transfer of reducing equivalents between organisms. Mutants in various electron transfer pathways revealed that interspecies electron transfer in an obligate *S. oneidensis/G. sulfurreducens* co-culture was mediated by soluble redox-active flavins secreted by *Shewanella* serving as electron shuttles between species.

The second half of this thesis focuses on *S. oneidensis* metabolism and interactions of microbes with metals. Microbial transfer of electrons to metals has a large impact on biogeochemical cycles and can also be harnessed for biotechnology applications in bioenergy and bioremediation. In order to effectively engineer *S. oneidensis* for these applications, it is imperative to understand how *Shewanella* gains energy from the oxidation of electron donors and the efficiency of electron transfer to metals and electrodes. Work in Chapter 4 revealed formate oxidation to be a central strategy under anaerobic conditions for energy conservation through the generation of proton motive force in *S. oneidensis*. Work in Chapter 5 quantified the effect of hydrogen metabolism on electron transfer reactions in *Shewanella* three-electrode bioreactors. Deletion of the hydrogenase large subunits, *hyaB* and *hydA*, in *Shewanella* resulted in higher current density and coulombic efficiency in single-chamber three-electrode

bioreactors by diverting electron flux to the anode instead of to hydrogen production. The final chapter of this thesis focused on harnessing microbial transformation of metals for bioremediation purposes. An engineered *Escherichia coli* strain containing a mercury resistance plasmid was constructed to facilitate the remediation of organic and ionic forms of mercury pollution. The engineered strain was then encapsulated using silica sol gel technology generating a bio-filtration material for use in bioremediation platforms.

Work in this thesis highlights the importance of microbial interactions, both with other organisms and with metals in the environment. Comprehensive knowledge on microbial interactions is important not only for a better understanding of ecosystem function but can also be harnessed for biotechnology applications. Microbial interactions and transformation of metals shape the world around us and have also facilitated use and further engineering of microorganisms for bioenergy and bioremediation technologies.

Table of Contents

List of Tables

List of Figures

Chapter 1 : Introduction on Microbial Communities

Microbial Communities

Microorganisms are ubiquitous across Earth's biosphere and total prokaryotic abundance measurements are estimated at 4-6 x 10^{30} cells representing the largest pool of nutrients in living organisms at 350-550 Pg of cellular carbon, 85-130 Pg of nitrogen, and 9-14 Pg of phosphorous (Whitman et al., 1998). The shear numbers estimated for prokaryotic abundance highlights their importance as drivers of biogeochemical cycling and nutrient flux via microbially catalyzed reactions (Falkowski et al., 2008). As such, microorganisms in the environment rarely act as individuals but instead as inherently complex and dynamic communities that interact and communicate with one another and the environment, yet factors that influence/determine behavior and function of microbial ecosystems remain largely undefined (De Roy et al., 2014).

Sequencing technologies have enabled initial analysis of microbial communities and allowed the characterization of species diversity in numerous environments ranging from communities in the ocean, soil, built environment, and the human microbiome (Huttenhower et al., 2012; Kembel et al., 2012; Rondon et al., 2000; Venter et al., 2004). To date, the Integrated Microbial Genomes (IMG) system lists a total of 42,658 genome datasets across all domains of life with 31,905 from prokaryotic organisms and 4242 metagenome datasets (img.jgi.doe.gov), and the National Center for Biotechnology Information (NCBI) currently lists a total of 55,096 prokaryotic genomes (ncbi.nlm.nih.gov). Yet, the vast quantities of sequencing data do not enable attribution of key functions within communities to individual members or the identification of active

members within natural communities (Franzosa et al., 2015). Isolation of individual organisms and –omics based studies have also enabled in-depth research into the genetic and physiological characteristics of microbes and advanced understanding of function and adaptation, but behavior in communities is often very different from behavior in pure culture laboratory conditions.

Studies on microbial communities are inherently limited by the complexity and dynamic nature of multispecies ecosystems. Further, the utility of methods to study communities is generally inversely proportional to overall complexity (Denef et al., 2010). Metagenomics, metatranscriptomics, and metaproteomics provide information on species diversity, expression profiles, and protein production, but it remains nearly impossible to assign functional roles to specific individual species (Zengler & Palsson, 2012). Current approaches also do not allow for comprehensive analysis of environmental fluctuations, interactions between members of a community, and detailed spatial organization, all which increase complexity of communities. In order to develop comprehensive understanding of communities, researchers must be able to formulate testable hypotheses, which necessitate reduced complexity and increased control.

Synthetic Microbial Communities

Synthetic biology encompasses applying rational engineering principles to the design of novel biological systems, and the extension of synthetic biology to engineering of whole consortia has ushered a new frontier in the study of microbial communities termed synthetic ecology (Dunham, 2007; Endy, 2005). Synthetic ecology is the rational

design of communities containing two or more members in well-controlled and defined environments (De Roy et al., 2014; Dunham, 2007). By deconstructing features of communities using a bottom-up approach, researchers are able to investigate fundamental principles involved in microbial interaction and metabolic networks, or design interactions with desired outputs and functions. Synthetic communities can serve as model systems in the lab to formulate and test hypotheses due to their reduced complexity, increased control, and the ability to identify specific community responses and interactions. Overall, synthetic systems enable researchers to mimic microbial interactions under controlled conditions and enable better understanding of how different variables affect community function.

Synthetic communities offer multiple benefits to researchers both in the laboratory and applied biotechnology settings. Model laboratory cultures enable studies on the evolution of cooperation, co-adaptation, and the emergence of novel metabolic networks over time (Harcombe, 2010; Hillesland & Stahl, 2010; Wintermute & Silver, 2010). Populations can also be designed to mimic a range of interactions from beneficial to detrimental to various members, and also enable exploration of the effect of cheaters, members of a community who enjoy the benefits of a costly behavior without contributing to it themselves, on community stability (Foster & Bell, 2012; Shou et al., 2007; Waite & Shou, 2012). Through control of the system, synthetic communities also enable the design of experiments to probe natural stability of ecosystems and their response to environmental perturbations such as bottlenecks and spatial arrangement

(Kim et al., 2008; Shou et al., 2007). In biotechnology applications, synthetic communities can perform tasks that may be too complex for monogenic populations, and division of labor can be engineered in communities to eliminate heavy metabolic burdens on individual strains (Brenner et al., 2008). Each step of a metabolic pathway can be engineered individually, and populations can be coordinated as a whole. Microbial consortia have also been shown to be more robust to environmental fluctuations over time (Brenner et al., 2008). Construction of simplified ecosystems with well-defined genetic backgrounds and identifiable cellular interactions also enable researchers to utilize communities as chasses or platforms to develop more complex communities.

Definitions of Bacterial Interactions

Interactions between organisms can be beneficial (+), neutral (0), or detrimental (-), meaning that for a pair of organisms (with no directionality implied) up to six types of pairwise interactions are possible and are often driven by metabolic interaction (Fig. 1). The first type assumes a neutral environment for both organisms (0/0) and represents no interaction between community members. Non-interaction is rare, as resources and space are generally limited in any community. More common is a type of interaction termed commensalism where one member benefits and the second remains neutral (0/+) (Faust & Raes, 2012; Grobkopf & Soyer, 2014). Food chains are examples of commensalism where the by-product of one organism is consumed by another. The food chain example also highlights the fact that true commensal relationships can be hard to accurately define since the “neutral” partner may derive an unknown benefit such as consumption of waste

products by the partner strain. Interactions that benefit all members of a community are defined as mutualisms (+/+) and further as syntrophy or obligate mutualisms if the beneficial exchange occurs through required bi-directional metabolic reactions (Dolfing, 2014; Morris et al., 2013). Both commensal and mutualistic relationships can be defined as cross-feeding if the metabolic output from one organism is utilized as a nutrient and/or energy source by another (Bull & Harcombe, 2009). Negative interactions, which are not covered further in this thesis, include classical predation models (-/+), amenalism (0/-) where one member is harmed without direct benefit to the other, and competition (-/-).

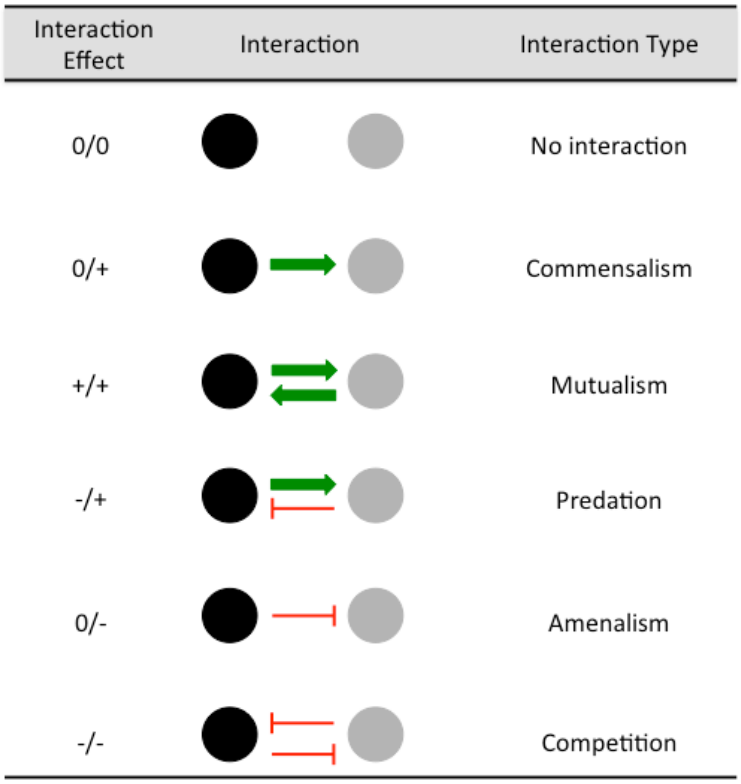

Figure 1.1: Six basic types of microbial interactions. Represented are the effects of interaction on individual strains (circles), which can be positive (+, green arrows), neutral (0, no line), or negative (-, red lines). Figure modified from (Grobkopf & Soyer, 2014).

Syntrophy and Interspecies Electron Transfer

Origin of the word syntrophy, as it applies to bacterial communities, is often incorrectly attributed to a 1978 study describing the exchange of sulfur compounds between phototrophic, sulfur-oxidizing and chemotrophic sulfate-reducing bacteria (Biebl & Pfennig, 1978). Syntrophism was described as early as 1946 by Joshua Lederberg in the 'Proceedings of Local Branches' section of the Journal of Bacteriology as the "growth of two distinct biochemical mutants in mixed culture as a result of the ability of each strain to synthesize the growth factor required by the other" (Lederberg, 1946). He found that mutants in different stages of the same metabolic pathway could promote each other's grow when cultured together, likely due to exchange of metabolites. Since Lederberg's description, the definition of syntrophy has become more complex and has spurred a few articles on correct use of the term (Dolfing, 2014; Morris et al., 2013). Concise terms are hampered by the fact that syntrophic communities can be described in terms of three different components: nutritional dependence, thermodynamics, and mutual cooperation. From the nutritional perspective, syntrophy describes two or more members of a community interacting to gain energy through combined metabolic strategies to catabolize compounds that either organism alone could not digest (Morris et al., 2013; Schink, 1997; Schink & Stams, 2006). With respect to thermodynamics, syntrophic degradation often requires the end products of the first partner to be kept at a low concentration for the overall reaction to be thermodynamically feasible (Dolfing, 2014; Morris et al., 2013; Schink, 1997; Schink & Stams, 2006; Sieber et al., 2012).

Finally, syntrophy requires cooperation or interdependence where each partner directly influences metabolism of the other (Dolfing, 2014; Morris et al., 2013; Schink, 1997; Schink & Stams, 2006; Sieber et al., 2012). For the sake of this thesis, syntrophy will be defined as proposed by Morris *et al.* (2013) simply as "obligately mutualistic metabolism."

Many syntrophic communities require the exchange of reducing equivalents between community members to catalyze reactions that no single member can accomplish alone. Oftentimes, cooperative exchange of electrons is required in these communities in order to gain energy and overcome thermodynamic barriers. The first interspecies electron transfer mechanisms studied were those mediated by hydrogen and formate. Various shuttling molecules like sulfur, cysteine, and humics have also been shown to mediate community electron transfer. More recently, strong evidence suggests that a direct mechanism mediated by *c*-type cytochromes and/or conductive pili may also exist in some communities. Interspecies electron transfer has also recently been shown to occur through conductive minerals serving as conduits between partner organisms. Each type will be discussed further in the following paragraphs.

Interspecies Hydrogen and Formate Transfer

Interspecies hydrogen transfer, the canonical method of interspecies electron transfer, is a process in which one organism oxidizes an organic compound coupled to the reduction of protons forming hydrogen that is consumed by a partner organism (Stams & Plugge, 2009). Due to the low redox potential of $2H^+/H_2$ ($E^{o'}$ = -414 mV), it is

energetically unfavorable to produce hydrogen from reducing equivalents such as NADH, and continuous generation requires a syntrophic hydrogen-consuming partner (Stams & Plugge, 2009). Interspecies hydrogen transfer was first described in the "*Methanobacillus omelianskii*" culture that was initially thought to be a single organism but was later determined to be a dual species co-culture containing an 'S organism' (which has since been lost) and the M.o.H strain (*Methanobacterium ruminantium*) (Bryant et al., 1967; Schink & Stams, 2006). The S strain converted ethanol to acetate, carbon dioxide, and hydrogen only in the presence of the M.o.H. strain, which consumed hydrogen for the reduction of carbon dioxide to methane (Bryant et al., 1967; Schink & Stams, 2006). Consumption of hydrogen by the M.o.H. strain, effectively keeping hydrogen concentrations low, shifted conversion of ethanol by the S strain (unfavorable at standard conditions) to be thermodynamically favorable (Bryant et al., 1967; Schink & Stams, 2006). Conversion of ethanol to methane could not be completed by either species alone but instead required syntrophic activities mediated by interspecies hydrogen transfer. Since the "*Methanobacillus omelianskii*" culture, interspecies hydrogen transfer has been determined to be important for methanogenic communities tied to the breakdown of complex organic compounds and may also mediate anaerobic oxidation of methane (AOM) though the exact mechanism of AOM is not yet fully understood (Schink, 1997; Schink & Stams, 2006; Sieber et al., 2012; Stams & Plugge, 2009).

As an alternative to hydrogen, microbial communities can exchange electrons through formate (Stams & Plugge, 2009). The low redox potential of formate ($E^{o'}$ = -420

mV) poses the same thermodynamic constraints as hydrogen on the formate-producing partner, and hence, reduction of carbon dioxide (as bicarbonate) requires a formate-consuming partner. Evidence for interspecies formate transfer arose in a syntrophic community where hydrogen transfer could not explain rates of ethanol degradation linked to methane formation (Thiele & Zeikus, 1988). Addition of hydrogen at levels making ethanol oxidation thermodynamically unfavorable by the community (even in the presence of a consuming partner) had no effect on ethanol oxidation or methane formation, and exogenous inhibition of methanogenesis resulted in the accumulation of formate (Thiele & Zeikus, 1988). Further evidence for interspecies formate transfer was provided by a propionate degrading co-culture where *Syntrophobacter fumaroxidans* only grew with methanogens capable of using both hydrogen and formate and not with methanogens only able to utilize hydrogen (Dong et al., 1994). Formate transfer may be preferred over hydrogen in some systems due to higher diffusion coefficient for formate enabling larger mass transfer to the methanogenic partner (Shrestha & Rotaru, 2014).

Interspecies Electron Transfer by Shuttles/Conductive Materials

Various shuttling compounds have also been implicated in interspecies electron transfer. Cysteine and other sulfur compounds have been shown to mediate electron transfer as well as the humic analog AQDS (Biebl & Pfennig, 1978; Kaden et al., 2002; Smith et al., 2015). Recently, conductive materials such as magnetite particles, graphite, granular activated carbon, and biochar have also been shown to serve as conduits facilitating electron transfer between community members (Chen et al., 2014; Kato et al.,

2012; Liu et al., 2012). Mediating electron transfer through carbon compounds could have important applications for stimulating methanogenesis in anaerobic digestors and wastewater systems (Kouzuma et al., 2015). Flavins acting as electron shuttles have also been shown to improve electron transfer to insoluble terminal electron acceptors by *Shewanella* (Brutinel & Gralnick, 2012; Coursolle et al., 2010; Kotloski & Gralnick, 2013; Marsili et al., 2008; von Canstein et al., 2008). The role of flavins in interspecies electron transfer is discussed further in Chapter three.

Direct Interspecies Electron Transfer

Ocean sediments are huge sources of methane and produce methane at amounts equivalent to approximately half of all natural sources. Methane is a potent greenhouse gas, and luckily the majority of methane produced in ocean sediments never reaches the ocean or atmosphere due to syntrophic breakdown of methane by microbial communitites (Alperin & Hoehler, 2010; Orcutt & Meile, 2008). Control of methane at the sea floor is performed by methanogenic archaea effectively running methanogenesis 'in reverse' (oxidizing methane and producing carbon dioxide and hydrogen) in a partnership with sulfate-reducing bacteria (Boetius et al., 2000; Orphan et al., 2001). The longstanding mystery of these communities stems from the fact that AOM rates observed in the environment cannot be explained solely by interspecies hydrogen or formate transfer or any other mechanisms requiring diffusion based transfer (Orcutt & Meile, 2008). Modeling studies hinted at a direct method for electron transfer between AOM

community members, yet with no ability to separate members or perform genetics-based studies, this has been hard to prove (Orcutt & Meile, 2008).

Recently a synthetic laboratory community composed of *Geobacter metallireducens* and *Geobacter sulfurreducens* provided strong evidence for direct interspecies electron transfer in syntrophic communities (Summers et al., 2010). In this system, *G. metallireducens* oxidizes ethanol only in the presence of *G. sulfurreducens* who can accept electrons produced by *G. metallireducens* and reduce the provided terminal electron acceptor fumarate, which *G. metallireducens* cannot use (Summers et al., 2010). The community formed large aggregates similar to environmental syntrophic communities, and deletions of the hydrogenase and formate dehydrogenase (Δ*hybL*Δ*fdnG*) in *G. sulfurreducens* still generated successful co-cultures with *G. metallireducens* (Rotaru et al., 2012; Summers et al., 2010). Deletion of *omcS*, an outer membrane mutliheme cytochrome associated with pili, and *pilA*, the structural pilin unit, prevented growth of the co-culture indicating that multiheme cytochromes and pili are involved in direct transfer of electrons between *G. metallireducens* and *G. sulfurreducens* (Summers et al., 2010). Recent evidence suggests multiheme cytochromes and pili may also play important roles in AOM communities (McGlynn et al., 2015; Wegener et al., 2015).

"Life is an electron looking for a place to land." – Daniel Bond

Electron transfer reactions are the energy currency of life. Movement of electrons from donor to acceptor molecules mediate energy production and are important for

shaping communities and environmental processes. The following thesis sections are dominated by the theme of electron transfer and how it mediates microbial interactions both with other species and their environment. Further introductory discussion focuses on electron transfer as it relates to respiration and unusual organisms able to respire, or breathe, insoluble compounds like metals. Laboratory techniques used to monitor these processes in the laboratory are also discussed.

Bacterial Respiration

Many bacteria thrive across a diverse range of environments due to the ability to couple the oxidation of compounds to the reduction of a variety of terminal electron acceptors. The process of transferring electrons to a terminal electron acceptor is termed respiration, and many bacteria are capable of respiring compounds other than oxygen such as organic acids, nitrogen oxides, sulfur oxyanions, and minerals. Free energy associated with coupled oxidation and reduction (redox) reactions can be converted to energy in the form of an electrochemical ion gradient across insulating membranes (Mitchell, 1961). The energy released by the flow of electrons in redox reactions is related to the difference in reduction potential between the donor and terminal electron acceptor. Electrons released during oxidation "flow" from the more negative potential electron donor to a more positive potential electron acceptor, and energy released during this process can be used to drive the translocation of protons across the cytoplasmic membrane. The difference in pH and separation of charge across an insulating membrane created by proton translocation can be harnessed by cells to perform work and is termed

the proton motive force (pmf). Pmf can be used to drive production of ATP, for cell motility, and to facilitate transport of molecules across the cytoplasmic membrane.

Proton translocation occurs either through the pumping of protons by various protein complexes involved in electron transport chains or through the cycling of redox loops. In the first example, low potential electron donors (NADH, $FADH_2$) generated during oxidative metabolism transfer electrons to a chain of proteins in the cytoplasmic membrane and electron flow through the chain facilitates proton pumping by some members. In the second example, proton translocation is facilitated by quinone-mediated redox loops. Quinones are lipid soluble molecules that can shuttle protons and electrons mediating their transfer between electron transport proteins. Coupling sites on the donor and acceptor proteins can occur at either the cytoplasmic or periplasmic side of the membrane and can facilitate proton movement across the membrane (Fig. 2). Depending on location of coupling sites, redox loops can also be net neutral or energy dissipating with respect to proton movement. Energy conservation through proton translocation mediated by redox loops is often vary important during anaerobic respiration as will be highlighted in Chapter 4.

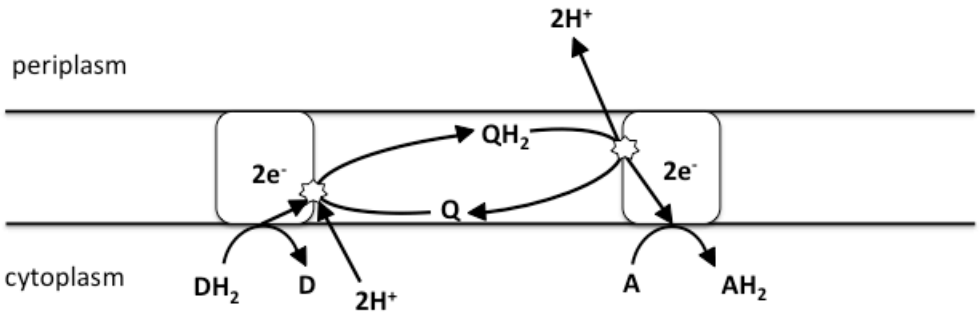

Figure 1.2: Generic configuration of a redox loop leading to translocation of protons across a membrane. Oxidation of the donor (D) and subsequent reduction of the acceptor (A) are connected via a redox loop that leads to translocation of protons due to the placement of coupling sites (stars) on opposite sides of the cytoplasmic membrane.

Extracellular Respiration

Respiratory chains are generally thought of as occurring at the cytoplasmic membrane, but some bacteria are able to extend these pathways and transfer electrons to the outer cell surface or beyond in a process termed extracellular respiration. The best-studied mechanisms of extracellular respiration are those involving the transfer of metabolic electrons to the reduction of extracellular metals. Unlike oxygen and soluble organic acceptors, Fe and Mn mineral oxides are insoluble at neutral pH, and respiration of such compounds necessitates specialized systems to transfer electrons across the cytoplasmic membrane, periplasm, and outer membrane (Gram negative metal reducers) or cell wall (Gram positive metal reducers). Transfer of electrons between bacteria and metals largely affect biogeochemical cycling as changes in redox state can alter solubility, bioavailability, toxicity, and partitioning of metals in the environment. The electrical connection between living organisms and metals has also been harnessed for multiple biotechnology applications. Microbial transfer of electrons to metals can

generate electrical current from the oxidation of waste in microbial fuel cells, be used to produce hydrogen in microbial electrolysis cells, or act as the input for bio-sensing technologies. Reversing this electron transfer process—driving electron transfer from metals back into microbes—can potentially be harnessed for electrosynthesis, where reducing power is used to produce value-added biofuels and biochemicals.

Since the discovery of microbially-catalyzed respiration of Fe and Mn oxides over 25 years ago, the bacteria *Shewanella* and *Geobacter* have served as the model organisms for extracellular respiration. Complete genome sequences for multiple species as well as well-defined genetics systems have aided in identifying important mechanisms for extracellular electron transport, a few of which are discussed next.

Shewanella

Shewanella species are Gram-negative, facultative anaerobic members of the γ-Proteobacteria found globally in redox-stratified aquatic and sediment environments (Fredrickson et al., 2008; Hau & Gralnick, 2007; Nealson & Scott, 2006). Their diverse distribution is due in part to their respiratory diversity. *Shewanella oneidensis*, the best-studied member of the genus, is able to respire over 20 organic and inorganic compounds as terminal electron acceptors including oxygen, fumarate, iron and manganese oxides, and electrodes (Hau & Gralnick, 2007; Nealson & Scott, 2006). Due in part to a number of promising applications in biotechnology, respiratory electron transfer has been intensely studied in *S. oneidensis* and the underlying physiology is well understood (Fredrickson et al., 2008; Hau & Gralnick, 2007). Electrons generated during anaerobic

metabolism are transferred from the quinone pool to the inner membrane tetraheme cytochrome CymA, which serves as the branch point to multiple terminal electron acceptor pathways (Marritt et al., 2012a; Myers & Myers, 2000). For respiration of soluble compounds such as fumarate, which can enter the periplasm, electrons are transferred from CymA to periplasmic terminal reductases (Nealson & Scott, 2006). During respiration of metals (either soluble or insoluble), electrons are transferred from CymA to the outer surface of the cell utilizing a mutli-heme cytochrome-porin complex collectively termed the Mtr (metal respiration) pathway (Beliaev & Saffarini, 1998; Beliaev et al., 2001; Coursolle & Gralnick, 2010; Coursolle et al., 2010; Hartshorne et al., 2009). At the cell surface, electrons can also be transferred to redox active flavin compounds that facilitate electron transfer between the cell and extracellular substrates (Brutinel & Gralnick, 2012; Kotloski & Gralnick, 2013; Marsili et al., 2008; von Canstein et al., 2008). Further description of *S. oneidensis* is provided as warranted in the introductory sections of subsequent chapters.

Geobacter

Geobacter species are Gram negative, members of the δ-Proteobacteria and are found in a variety of anaerobic sediments (Lovley et al., 2011). A hallmark of the *Geobacter* genus is the ability to exchange electrons with the extracellular environment, and they were the first organisms discovered to couple the oxidation of organic compounds to the reduction of Fe(III) oxide as terminal electron acceptor (Lovley et al., 1987; Lovley et al., 1993). Some of the electron acceptors utilized by *Geobacter* species

include Fe(III) and Mn(IV) oxides and chelates, toxic metals U(VI) and Tc(VII), fumarate, elemental sulfur, the humic acid analog AQDS, and electrodes (Lovley et al., 2011). Respiration of metals by *Geobacter* species play important roles in biogeochemical cycling and also affect cycling of the trace metals and nutrients like phosphate that can adsorb onto metal oxides (Lovley et al., 2004).

Unlike *Shewanella*, the full mechanism(s) of electron transport by *Geobacter* have not been elucidated. Genomes of *Geobacter* species contain, on average, approximately 80 cytochromes representing about 2% of protein coding regions (Butler et al., 2010; Methe et al., 2003). The vast majority of these cytochromes also contain more than one heme-binding motif (Butler et al., 2010; Methe et al., 2003). Despite this, comparative genomics studies have revealed that very few of the multiheme cytochromes are conserved across the *Geobacter* genus (Butler et al., 2010). Omics-based studies have also failed to highlight any one pathway, and genetics have been complicated by the fact that no one deletion has been shown to completely eliminate extracellular electron transfer (Aklujkar et al., 2013; Butler et al., 2010; Ding et al., 2006; Ding et al., 2008; Holmes et al., 2006; Rollefson et al., 2009).

Recently, two studies have identified distinct cytochromes involved in electron transport across the inner membrane of *G. sulfurreducens*, the model strain of the *Geobacter* genus. Using a combination of transposon mutagenesis and high-throughput Illumina sequencing known as Tn-seq, it was found that transposon disruption of *imcH* and *cbcL* resulted in respiratory phenotypes during the respiration of high and low

potential terminal electron acceptors, respectively (Levar et al., 2014; Zacharoff et al., 2016). Disruption of *imcH* by insertion of a kanamycin resistance cassette and a clean deletion of *cbcL* agreed with the transposon data providing evidence for at least two pathways for electron transport across the inner membrane indicating that *G. sulfurreducens* can adapt and respond to varying redox potentials in the environment (Levar et al., 2014; Zacharoff et al., 2016).

Three-Electrode Bioreactors

Extracellular respiration can be monitored in real-time in the laboratory using three-electrode bioreactors with electrodes serving as the terminal electron acceptor (Bond et al., 2002). In bioelectrochemical reactors, bacteria couple the oxidation of supplied electron donors to respiration of the working electrode (anode), which can be set at a user-defined potential via a potentiostat and reference electrode. Control of potential at the anode allows the electrode to serve as a proxy for the terminal electron acceptor/respiratory pathway being investigated. Electrons transferred from bacterial cells to the anode flow through the system to the cathode where they re-enter the reactor medium and complete the circuit. Electron flow through these systems is monitored as current produced over time via the potentiostat. A depiction of three-electrode bioreactors utilized in this thesis is provided in Figure 3.

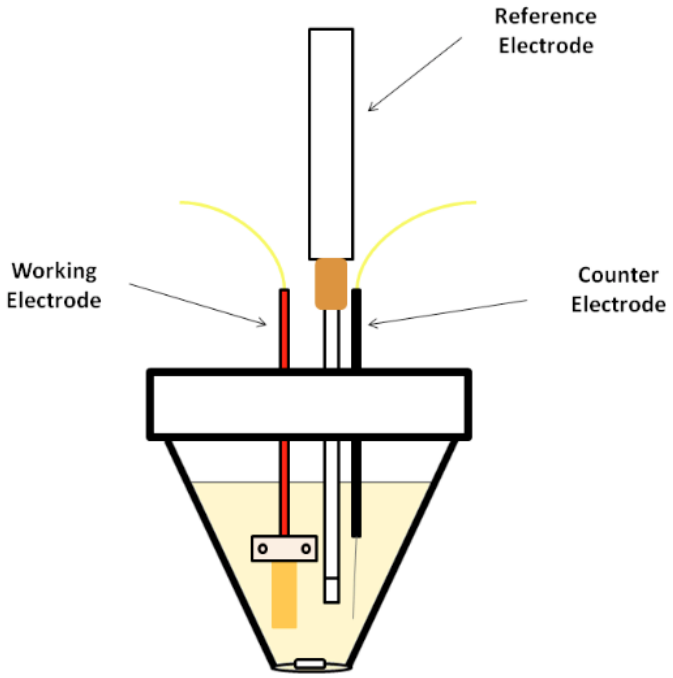

Figure 1.3: Schematic of a three-electrode bioreactor with an electrode serving as the terminal electron acceptor. Bacteria attached to electrode couple oxidation of supplied electron donors to the respiration of the electrode and electron flow is monitored as current produced over time. A potentiostat and reference electrode are utilized to control potential set at the working electrode and also to monitor electron flow as current between the working (anode) and counter (cathode) electrodes.

Thesis Summary

The overarching theme of the following thesis chapters is the role of electron transfer as a mediator of microbial interactions both with other organisms and compounds in the environment such as metals. Chapter 2 focuses on the characterization of a model laboratory co-culture of *S. oneidensis* and *G. sulfurreducens*. In this system, *S. oneidensis* has been engineered to consume glycerol and secrete acetate that can then be utilized as a carbon source by *G. sulfurreducens*. Both organisms couple oxidation of their respective carbon sources to the reduction of fumarate. The commensal nature of the *S. oneidensis*

and *G. sulfurreducens* co-culture was shifted to an obligate mutualism by deleting the fumarate reductase in *S. oneidensis* (Δ*fccA*) disabling its use of fumarate as terminal electron acceptor. Co-culturing *S. oneidensis* Δ*fccA* and *G. sulfurreducens* resulted in a shift in overall metabolic strategy and emergence of a novel approach to energy generation by the community. Instead of oxidizing glycerol, the community shifted to conversion of fumarate to malate and utilized ensuing malate as a carbon source. Targeted deletions were constructed to test various carbon utilization pathways in the obligate co-culture.

Chapter 3 focuses on use of the *S. oneidensis* and *G. sulfurreducens* co-culture in three-electrode bioreactors to test various mechanisms of interspecies electron transfer. In this co-culture, *S. oneidensis* oxidizes glycerol and produces acetate for *G. sulfurreducens* only if *G. sulfurreducens* accepts electrons generated by *S. oneidensis*. *S. oneidensis* must transfer electrons to *G. sulfurreducens* because gold electrodes were used as terminal electron acceptors in bioreactors, a surface *S. oneidensis* is unable to respire. A new mechanism, interspecies electron transfer via flavins electron shuttles, was found to mediate electron transfer in this community.

Chapter 4 focuses on a central mechanism important for energy conservation during anaerobic respiration by *S. oneidensis*. Formate is produced during anaerobic respiration of carbon sources entering at or above the level of pyruvate in *S. oneidensis*, and the genome of *S. oneidensis* encodes three complete formate dehydrogenase (FDH) complexes indicating importance of formate metabolism. Growth of *S. oneidensis* in

comparison to several mutant strains revealed that formate oxidation coupled to proton translocation via a redox-loop mechanism, as well as pumping of protons by the ATPase, are the main contributors to pmf under anaerobic conditions in *S. oneidensis*. Deletion of all three FDH gene regions also enabled growth of *Shewanella* on pyruvate in the absence of a terminal electron acceptor, a mode of growth not seen previously for the non-fermentative *S. oneidensis*.

Chapter 5 focuses on the effect of hydrogen metabolism on total current density and overall coulombic efficiency (charge recovered as electrical current) in *S. oneidensis* single-chamber, three-electrode bioreactors. In reactors, *S. oneidensis* is able to oxidize supplied carbon sources and use an electrode as terminal electron acceptor, but low efficiency calculations for *S. oneidensis* reactors previously indicate that it is able to divert electrons to other acceptors. Reduction of protons to molecular hydrogen represents an alternative electron transfer mechanism diverting electron transfer to electrodes in reactor systems. *S. oneidensis* is able to both consume and produce hydrogen via two periplasmically-oriented, membrane associated hydrogenases. Hydrogen is also produced abiotically at the cathode in single chamber electrodes further hampering efficiency calculations as oxidation of hydrogen by *S. oneidensis* can lead to current not attributable to carbon source oxidation and artificially high current density. In Chapter 5, we report high coulombic efficiencies achieved in *S. oneidensis* reactors through deletion of both hydrogenases and isolation and removal of hydrogen produced at the cathode.

Chapter 6 focuses on a project conducted by the 2014 University of Minnesota international Genetically Engineered Machine (iGEM) competition team. The team was awarded a gold medal and won the "Best Environment Project" division, which was described as one of top accomplishments for the College of Biological Sciences for 2014 by Dean Tom Hayes. In Chapter 6, we describe the engineering of *E. coli* to remediate both ionic and organic forms of mercury including the potent neurotoxin methylmercury using the *me*rcury *r*emediation (*mer*) operon. We also describe methods to encapsulate engineered strains in a silica-based material resulting in a biological-based filtration material. Encapsulated *E. coli* harboring the *mer* operon maintained ability to degrade methylmercury and represent a step toward using this technology for mercury remediation.

Chapter 2 : Shifting Metabolic Strategy From Commensalism to Obligate Mutualism in an Engineered Co-culture

Summary

Over the past century, microbiologists have mainly studied organisms in pure culture, yet in natural environments, the majority of microorganisms live in complex and highly dynamic multispecies communities. Natural communities are shaped by interactions among members as well as with the environment itself. To study multispecies interaction in the laboratory, specifically the emergence of cooperation, we constructed both a commensal community and an obligate mutualism using the previously non-interacting bacteria *Shewanella oneidensis* and *Geobacter sulfurreducens*. Incorporation of a glycerol utilization plasmid (pGUT2) enabled *S. oneidensis* to metabolize glycerol and produce acetate as a carbon source for *G. sulfurreducens* establishing a cross-feeding, commensal co-culture. In the commensal co-culture, both species coupled oxidative metabolism to the respiration of fumarate as the terminal electron acceptor. Deletion of the gene encoding fumarate reductase in the *S. oneidensis* pGUT2 strain shifted the co-culture with *G. sulfurreducens* to an obligate mutualism where neither species could grow in absence of the other. A shift in metabolic strategy from glycerol catabolism to malate metabolism was associated with obligate co-culture growth. Further targeted deletions in malate uptake and acetate generation pathways in *S. oneidensis* significantly inhibited co-culture growth with *G. sulfurreducens*. The engineered co-culture between *S. oneidensis* and *G. sulfurreducens* provides a model laboratory system to study the emergence of cooperation in bacterial communities, and

the shift in metabolic strategy observed in the obligate co-culture highlights the potential importance of genetic change in shaping microbial interactions in the environment.

Introduction

Microorganisms are the major drivers of biochemical and nutrient cycling in environments ranging from ocean sediments to the human microbiome, yet factors that influence the behavior and function of multispecies ecosystems remain largely undefined (Falkowski et al., 2008; Huttenhower et al., 2012; Raes & Bork, 2008; Venter et al., 2004). For the past century, microbiology has focused mainly on the isolation and study of individual species leading to in-depth studies on genetic and physiological characterization, but behavior of organisms as members of communities is often very different from behavior in pure laboratory cultures (Kaeberlein et al., 2002; Rappe & Giovannoni, 2003). Sequencing and community-based –omics studies have enabled the analysis of multispecies microbial communities answering questions such as 'who is there' and 'what functions are present,' yet they are limited in their ability to attribute key functions to individual species, identify active members, or provide an overall picture of how interaction shapes communities (Franzosa et al., 2015; Raes & Bork, 2008).

In natural settings, microorganisms rarely act as individuals, but instead as inherently complex and dynamic communities that interact and communicate with one another. Interaction can lead to obligate interdependence or syntrophy in communities where two or more members combine metabolic strategies to gain energy and catabolize compounds that neither species alone could digest (Morris et al., 2013; Schink, 1997;

Schink & Stams, 2006; Sieber et al., 2012). In syntrophic systems, the metabolism of one species is directly influenced by actions of the other and vice versa (Dolfing, 2014; Morris et al., 2013; Schink, 1997; Schink & Stams, 2006; Sieber et al., 2012). Interdependence between community members confounds their study because natural syntrophic communities oftentimes cannot be separated in the laboratory (Orcutt & Meile, 2008; Orphan, 2009). Inability to grow members separately also impedes studies on how syntrophy and obligate interactions emerge in multispecies ecosystems.

Synthetic ecology, the engineering of rationally designed communities in well-defined environments, provides an innovative and robust approach to reduce the complexity inherent in natural systems and mimic microbial interaction in a controlled framework (Brenner et al., 2008; De Roy, Marzorati et al., 2014; Grobkopf & Soyer, 2014). By distilling the salient features of communities into modular genetic and biochemical units, artificial consortia can be engineered from the bottom-up to serve as model systems enabling investigation of conditions that prime the emergence of microbial interactions and higher-order community function (De Roy et al., 2014; Grobkopf & Soyer, 2014). The construction of simplified, artificial ecosystems using organisms with well-defined genetic backgrounds provides a context in which to identify interaction within community metabolic networks. Developed synthetic communities can also be used as a chassis for the continued engineering of more complex ecosystems (De Roy et al., 2014; Song et al., 2014).

Here, we report the construction and characterization of model synthetic communities ranging from commensalism (one species benefits) to obligate mutualism (interdependence required for both species to benefit) using *Shewanella oneidensis* and *Geobacter sulfurreducens*, two bacteria chosen because i) they have no naturally-evolved metabolic interactions enabling us to monitor the emergence of cooperation in a population ii) a breadth of genetic tools available for both including: sequenced and annotated genomes (Heidelberg et al., 2002; Methe et al., 2003), full genetic systems (Chan et al., 2015; Coppi et al., 2001; Saltikov & Newman, 2003), and well-described metabolic networks (Flynn et al., 2012; Mahadevan et al., 2011; Pinchuk et al., 2009) and iii) the potential importance of this co-culture in biotechnology applications (Hau & Gralnick, 2007; Lovley et al., 2011). *S. oneidensis* and *G. sulfurreducens* serve as the model organisms for extracellular respiration, an ability to transfer electrons produced during oxidative metabolism across cellular membranes to insoluble terminal electron acceptors (Gralnick & Newman, 2007). Through extracellular respiration, *Shewanella* and *Geobacter* species respire a diverse array of substrates, including metals and electrodes, making these bacteria applicable – individually and potentially more in cooperative concert – to the remediation of environmental pollutants and to electricity production in microbial fuel cells (Hau & Gralnick, 2007; Lovley et al., 2011). A commensal co-culture was first engineered through incorporation of a cross-feeding mechanism between *S. oneidensis* and *G. sulfurreducens*. A targeted deletion in the respiratory pathway of *S. oneidensis* shifted the commensal co-culture to an obligate

mutualism where neither species could grow alone in the presence of the supplied carbon source. Importantly, the obligate co-culture also revealed a complete shift in metabolic strategy highlighting that mutations in metabolic pathways may play a substantial role in shaping microbial interactions in the environment.

Materials and Methods

Reagents

Enzymes were purchased from New England Biolabs (Ipswich, MA). Kits for PCR cleanup, gel purification, and plasmid preparations were purchased from Invitrogen (Carlsbad, CA). Chemicals were obtained from Sigma-Aldrich (St. Louis, MO) with the exception of glycerol, which was purchased from Fisher Chemical (Pittsburgh, PA). Medium components were purchased from Becton, Dickinson and Company (Sparks, MD).

Bacterial Strains and Culture Conditions

Strains and plasmids used in this study are listed in Table 2.2. Plasmid pGUT2 has been described previously (Flynn et al., 2010). *S. oneidensis* and *E. coli* strains were maintained at 30°C and 37°C, respectively, on Luria-Bertani (LB) medium solidified with 1.5% agar and supplemented with 50 μg/ml kanamycin when required. *G. sulfurreducens* was maintained at 30°C under strict anaerobic conditions using an anaerobic chamber with a 5% H_2/75%N_2/20%CO_2 atmosphere (Coy Lab Products; Grass Lake, MI) on basal medium (NB) plates containing the following per liter: 0.38 g KCl, 0.2 g NH_4Cl, 0.069 g $NaH_2PO_4 \cdot H_2O$, 0.04 g $CaCl_2 \cdot 2H_2O$, 0.2 g $MgSO_4 \cdot 7H_2O$, 2.0 g

$NaHCO_3$ (pH 6.8), 10 mL/L of a mineral mix (Hau et al., 2008) and supplemented with 0.1% trypticase (wt/vol), 1 mM cysteine, 20 mM acetate, 40 mM fumarate (NBFA+TC) and solidified with 1.5% agar.

Generation of Deletion Mutants

Oligonucleotide primers used to amplify portions of the *S. oneidensis* chromosome for deletion constructs are listed in Table 2.3. PCR products were cloned using standard laboratory molecular biology protocols. Regions flanking deletion targets were amplified using PCR and cloned into the pSMV3 suicide vector. In-frame gene deletions were generated using homologous recombination as previously described (Coursolle et al., 2010). Deletion constructs were moved *into S. oneidensis* by conjugal transfer from *E. coli* donor strain WM3064. All plasmid constructs and gene deletions were verified by sequencing (University of Minnesota Genomics Center).

Co-culture Growth Assays

All experiments were initiated with single colonies picked from freshly streaked -80°C 15% glycerol or 10% DMSO stocks on LB containing 50 μg/ml kanamycin or NBFA+TC plates for *S. oneidensis* and *G. sulfurreducens*, respectively. In preparation for growth assays, single colonies of *S. oneidensis* were grown shaken at 30°C in LB broth containing 50 μg/ml kanamycin for 16 hours and were then sub-cultured into *Shewanella* Basal Medium (SBM) containing 7 mM glycerol for 6 hours (pH 7.2; containing per 1 liter of medium: 0.225g K_2HPO_4, 0.225g KH_2PO_4, 0.46g NaCl, 0.225g $(NH_4)_2SO_4$, 0.117g $MgSO_4 \cdot 7H_2O$, 10 mM HEPES buffer, supplemented with 5 mL/L vitamin mix

and 5 mL/L mineral mix (Hau et al., 2008)). Single colonies of *G. sulfurreducens* were grown in an anaerobic chamber (5%:75%:20% H_2:N_2:CO_2) in 1 mL of basal medium (NB) supplemented with 20 mM acetate and 40 mM fumarate (NBFA) for 48 hours at 30°C. Following this initial growth, 1 mL of *G. sulfurreducens* was sub-cultured into 10 mL of NBFA medium in anaerobic culture tubes under a 80%:20% N_2:CO_2 headspace 24 hours prior to co-culture experiments.

For co-culture growth assays, *S. oneidensis* and *G. sulfurreducens* cultures were washed in their respective basal media, normalized to an optical density measured at 600 nm (OD_{600}) of 1, and sub-cultured in 15 mL of co-culture medium (CM) which contained per liter: 0.38 g KCl, 0.2 g NH_4Cl, 0.069 g $NaH_2PO_4 \cdot H_2O$, 0.04 g $CaCl_2 \cdot 2H_2O$, 0.2 g $MgSO_4 \cdot 7H_2O$, 2.0 g $NaHCO_3$ as buffer (pH 7.0), supplemented with 10 mL/L of mineral mix, 10 mL/L vitamin mix (Hau et al., 2008), 0.05% (w/v) casamino acids, 7 mM glycerol (+G) and 55 mM fumarate (+F) where indicated (CMFG, CMG, CMF). Cultures were grown stationary under a 20% CO_2/80% N_2 headspace using butyl rubber-stoppered glass tubes (Bellco; Vineland, NJ). Culture OD_{600} was monitored using a spectrophotometer (Spectronic 20D+; Thermo Fisher Corporation, Waltham, MA).

Monitoring Co-culture Growth Via Colony Forming Units

Culture samples were removed using degassed syringes, and serial dilutions were performed in LB or CMF medium to prevent cell lysis for *S. oneidensis* and *G. sulfurreducens*, respectively. To ensure optimal plating efficiency, *S. oneidensis* and *G.*

sulfurreducens dilutions were plated on aerobic LB and anaerobic NBFA+TC plates (75% N_2/20% CO_2/5% H_2) at 30°C, respectively (Coppi et al., 2001).

High Performance Liquid Chromatography

Metabolites were quantified by HPLC using Shimadzu Scientific equipment including an SCL-10A system controller, LC-10AT pump, SIL-10AF auto-injector, CTO-10A column oven, RID-10A refractive index detector (cell maintained at 40°C), and an SPD-10A UV-Vis detector (210nm). Mobile phase consisted of 0.015 N H_2SO_4 set at a flow rate 0f 0.400 mL min^{-1}. Injection volumes of 50 μL were separated on an Aminex HPX-87H column maintained at 46°C. Metabolite concentrations were determined by comparison with standard curves for each compound ($R^2 > 0.99$). Metabolite standards were run before and after unknown samples to ensure accuracy.

Results

To establish a co-culture system, a cross-feeding mechanism was engineered between *S. oneidensis* and *G. sulfurreducens* (Fig. 2.1). Incorporation of a glycerol utilization plasmid (pGUT2) enabled *S. oneidensis* to metabolize glycerol and secrete acetate (Flynn et al., 2010). *G. sulfurreducens*, unable to utilize glycerol as a carbon source, was then dependent on acetate secreted by *S. oneidensis* pGUT2 as a carbon source for growth (Lovley et al., 2011). As engineered, the complete oxidation of glycerol to carbon dioxide required the metabolic activity of both *S. oneidensis* pGUT2 and *G. sulfurreducens* and was coupled to fumarate respiration by both organisms (Fig. 2.1). The co-culture outlined in Figure 2.1 is described as commensal because co-culture

conditions are neither beneficial nor detrimental to *S. oneidensis* pGUT2 whereas *G. sulfurreducens* gains a direct benefit from co-culture growth with *S. oneidensis* pGUT2.

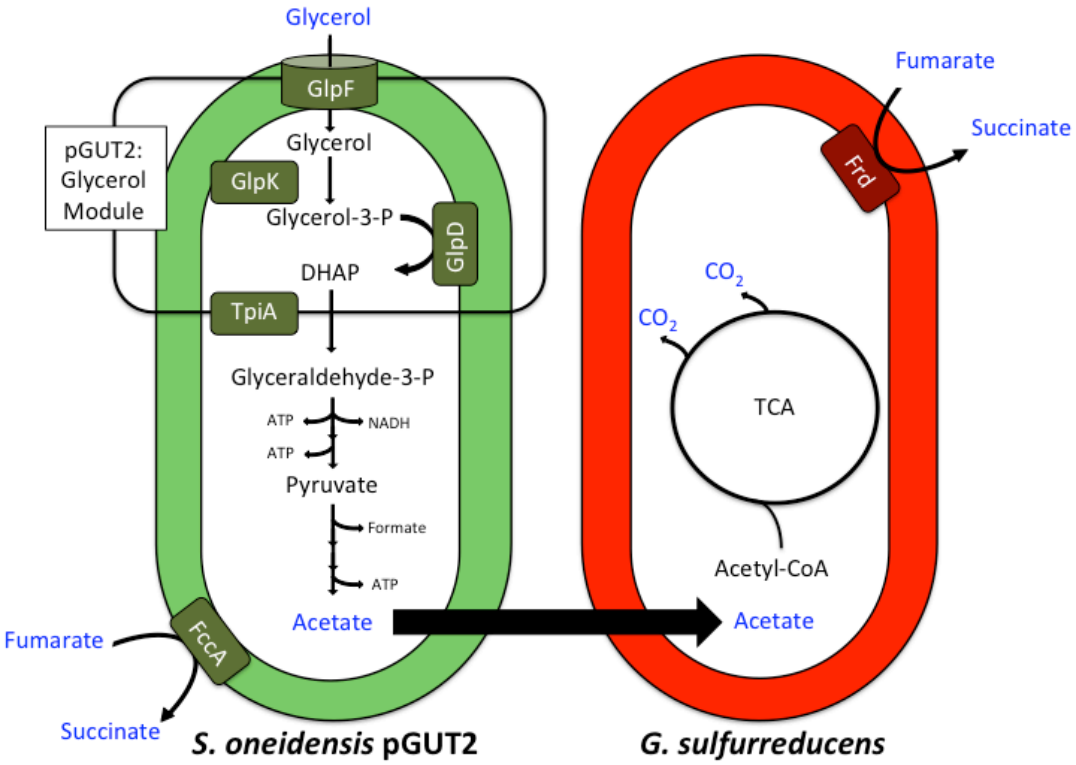

Figure 2.1: Metabolic interactions enabling co-culture growth of *S. oneidensis* pGUT2 and *G. sulfurreducens*. *S. oneidensis* oxidizes glycerol via an engineered glycerol utilization pathway encoded by the pGUT2 plasmid (GlpF, glycerol facilitator; GlpK, glycerol kinase; GlpD, glycerol-3-P dehydrogenase; TpiA, triose phosphate isomerase) and secretes acetate that is used as a carbon source by *G. sulfurreducens*. Cross-feeding of acetate from *S. oneidensis* pGUT2 to *G. sulfurreducens* is represented by the black arrow. In the commensal co-culture, both organisms couple metabolic oxidation reactions to the respiration of fumarate (FccA and Frd represent fumarate reductase in *S. oneidensis* and *G. sulfurreducens*, respectively). An obligate co-culture was engineered by eliminating fumarate respiration by *S. oneidensis* pGUT2 through deletion of *fccA*.

We began by characterizing growth of *S.* oneidensis pGUT2 and *G. sulfurreducens* in basal co-culture medium containing glycerol as carbon source and fumarate as terminal electron acceptor (CMGF). As predicted, when cultured separately, CMGF medium supported growth of *S. oneidensis* pGUT2 but not *G. sulfurreducens* due to its reliance on *S. oneidensis* pGUT2 for acetate (Fig. 2.2 A and B). Simultaneous growth of both species was only observed when *S. oneidensis* pGUT2 and *G. sulfurreducens* were cultured together in medium containing both glycerol and fumarate, and the co-culture reached a higher maximum OD_{600} then *S. oneidensis* pGUT2 cultured alone (Fig. 2.2A). To determine growth rates for each species in the co-culture, samples were removed periodically and serial dilutions were plated on medium selective for either species. Resulting colony forming units (CFU) were then determined and revealed an initial lag phase for *G. sulfurreducens* when co-cultured with *S. oneidensis* pGUT2 likely due to inhibition of *G. sulfurreducens* growth until secreted acetate concentrations were high enough to support growth (Fig. 2.2B). Growth of *S. oneidensis* pGUT2 was similar when cultured alone or in co-culture with *G. sulfurreducens* in CMGF medium (Fig. 2.2B).

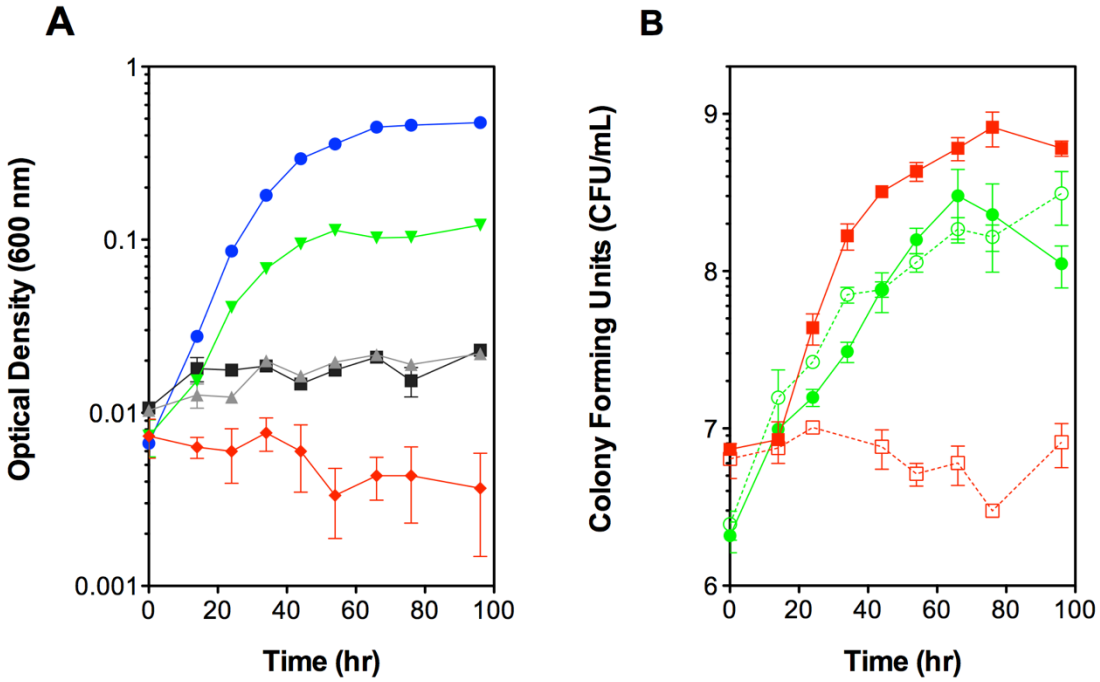

Figure 2.2: Growth of *S. oneidensis* pGUT2 and *G. sulfurreducens* alone and in co-culture in basal co-culture medium (CM) containing 7 mM glycerol (G) and/or 60 mM fumarate (F) as indicated. A) Growth measured as OD_{600} of the *S. oneidensis* pGUT2 + *G. sulfurreducens* co-culture in CMGF (blue circles), CMG (black squares), or CMF (grey triangles) medium as compared to *S. oneidensis* pGUT2 (green triangles) or *G. sulfurreducens* (red diamonds) grown singly in CMGF. Growth was not observed for *S. oneidensis* pGUT2 or *G. sulfurreducens* cultured alone in CMG or CMF, and data was removed for graph clarity. B) Growth monitored as colony forming units in CMGF medium for *S. oneidensis* pGUT2 (green circles) and *G. sulfurreducens* (red squares) grown alone (open symbols) or in co-culture (closed symbols). Reported values are averages for triplicate experiments with error represented as standard error of the mean (SEM).

To confirm that acetate was secreted by *S. oneidensis* pGUT2 and served as the carbon source for *G. sulfurreducens* in co-culture experiments, supernatant samples were analyzed by HPLC. Grown alone in CMGF medium, *S. oneidensis* pGUT2 consumed glycerol and secreted acetate at nearly stoichiometric ratios and coupled this oxidation to the reduction of fumarate as terminal electron acceptor subsequently producing succinate (Fig 2.3B, Table 2.1). Fumarate uptake by *S. oneidensis* pGUT2 grown alone was slightly

higher than the concentration of succinate produced, which indicated some utilization of fumarate by *S. oneidensis* cultures not associated with respiration (Table 2.1). Glycerol and fumarate concentrations remained largely unchanged for *G. sulfurreducens* grown alone in CMGF over the time course analyzed (Fig. 2.3C). Analysis of co-culture metabolites over time by HPLC revealed that glycerol was completely oxidized and coupled to fumarate reduction as predicted (Fig. 2.3A, Table 2.1). Acetate concentration increased initially in co-culture supernatants, but after reaching ~2 mM, was completely consumed, and no acetate was detected at the final time point in agreement with the prediction of acetate consumption by *G. sulfurreducens* (Fig. 2.3A, Table 2.1). In co-cultures, the concentration of fumarate utilized was slightly higher than predicted for the stoichiometric conversion of fumarate to succinate indicating that some fumarate was taken up by the co-culture in a process not linked to respiration (Table 2.1).

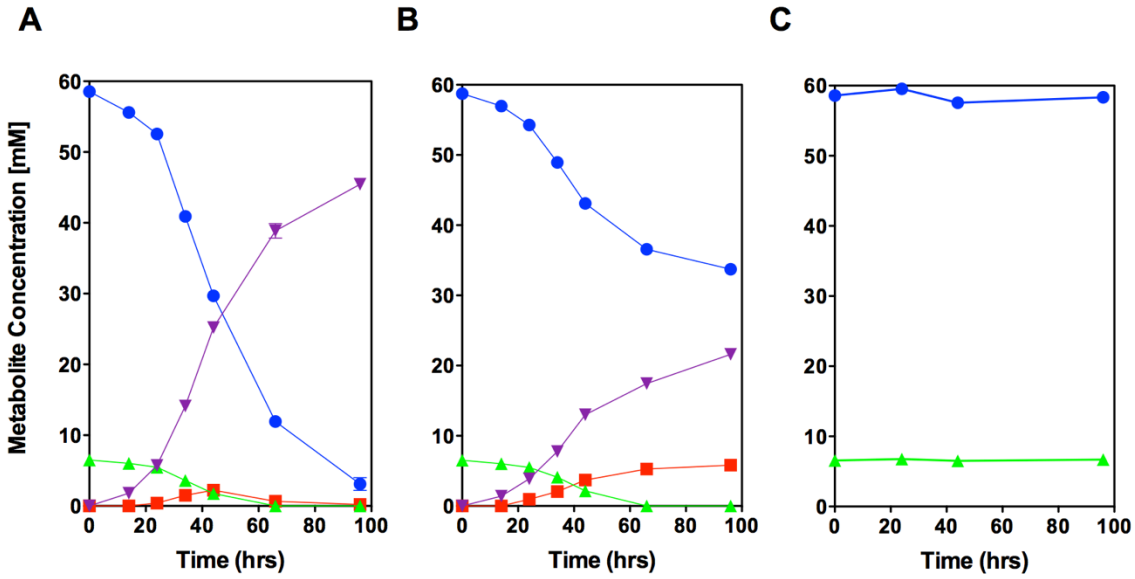

Figure 2.3: Metabolite profiles in A) *S. oneidensis* pGUT2 + *G. sulfurreducens* co-cultures B) *S. oneidensis* pGUT2 only and C) *G. sulfurreducens* only cultures in CMGF medium containing 7 mM glycerol and 60 mM fumarate. Metabolites include glycerol (green triangles), acetate (red squares), fumarate (blue circles), and succinate (purple inverted triangles). Reported values are for three independent experiments with error represented as SEM. Error bars associated with the above data were small, and hence are masked due to the symbol size used.

	***S. oneidensis* pGUT2 Grown Alone**	***S. oneidensis* pGUT2 and *G. sulfurreducens* Co-culture**
	Metabolite Conc. (mM)	**Metabolite Conc. (mM)**
Glycerol	- 6.5 ± 0.0	- 6.5 ± 0.0
Acetate	5.9 ± 0.1	ND
Fumarate	- 25.0 ± 0.4	- 55.4 ± 0.9
Succinate	21.6 ± 0.1	45.5 ± 0.2

Table 2.1: Concentration changes in metabolite profiles from initial to end time points for *S. oneidensis* pGUT2 grown singly or in co-culture with *G. sulfurreducens*. Metabolite concentrations changed by < 1% for *G. sulfurreducens* cultured alone, and hence were not included in the table. Initial concentrations measured in NBGF medium by HPLC were 6.5 ± 0.0 mM glycerol and 58.5 ± 0.1 mM fumarate. Reported concentrations are averages ± SEM from three independent experiments. ND; not detected.

An obligate interaction between *S. oneidensis* pGUT2 and *G. sulfurreducens* was created by deleting the gene encoding fumarate reductase (*fccA*) in the chromosome of *S. oneidensis* (strain referred to as *S. oneidensis* Δ*fccA* pGUT2) eliminating the ability of *S. oneidensis* to couple glycerol oxidation to the respiration of fumarate (Fig. 2.1). Growth in CMGF medium required the presence of both *S. oneidensis* Δ*fccA* pGUT2 and *G. sulfurreducens* and occurred over a much longer timescale (~80 days) as compared to the commensal *S. oneidensis* pGUT2 and *G. sulfurreducens* co-culture (~80 hours) (Fig. 2.4A versus Fig. 2.2A). Interestingly, growth was also observed for *S. oneidensis* Δ*fccA* pGUT2 and *G. sulfurreducens* co-cultured in basal medium lacking glycerol (CMF). Selective plating was again utilized to determine growth of each species in co-culture revealing that both *S. oneidensis* Δ*fccA* pGUT2 and *G. sulfurreducens* grew similarly when co-cultured in CMGF or CMF medium (Fig 2.4B). *S. oneidensis* Δ*fccA* pGUT2 populations experienced an initial drop in cell numbers followed by a moderate rise after approximately 40 days of co-culture incubation with *G. sulfurreducens* both in CMGF and CMF media (Fig 2.4B). In contrast, *G. sulfurreducens* CFUs increased steadily amounting to ~3.5 doublings both in CMGF and CMF media (Fig. 2.4B).

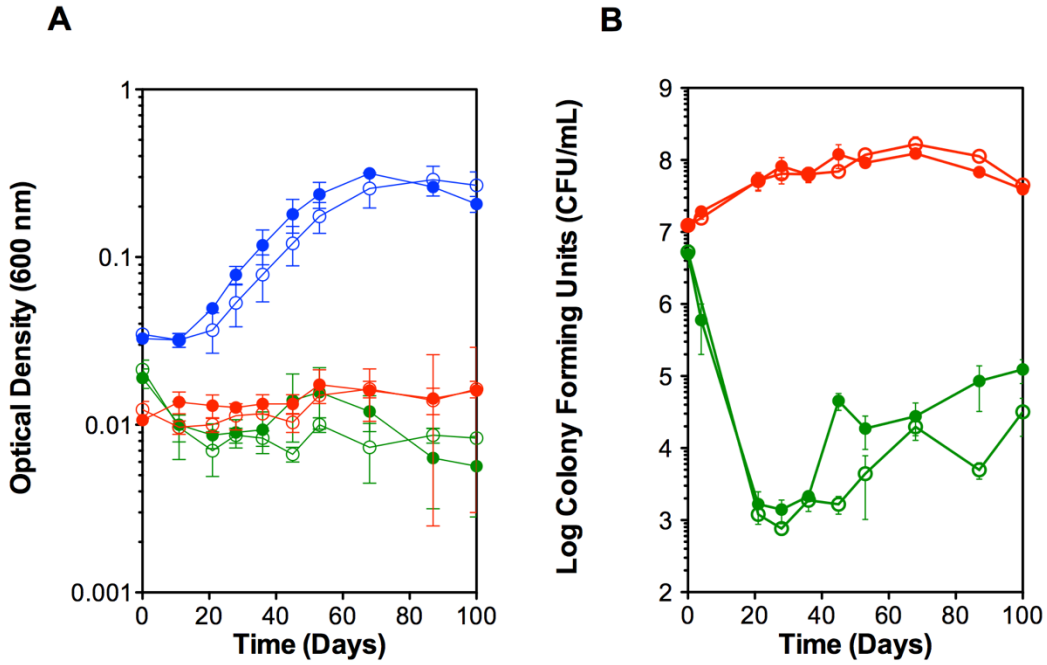

Figure 2.4: Obligate growth of *S. oneidensis* Δ*fccA* pGUT2 and *G. sulfurreducens* in basal co-culture medium (CM) containing 7 mM glycerol and 60 mM fumarate (CMGF, closed symbols) or co-culture medium supplemented only with 60 mM fumarate (CMF, open symbols). A) Growth measured as OD_{600} for *S. oneidensis* Δ*fccA* pGUT2 and *G. sulfurreducens* in co-culture (blue), and for *S. oneidensis* Δ*fccA* pGUT2 (green) and *G. sulfurreducens* (red) cultured alone. B) Growth measured as colony forming units for *S. oneidensis* Δ*fccA* pGUT2 (green) and *G. sulfurreducens* (red) in co-culture in CMGF (closed symbols) and CMF (open symbols) media. Reported values are averages for triplicate experiments with error bars representing SEM.

Growth of *S. oneidensis* Δ*fccA* pGUT2 and *G. sulfurreducens* co-cultures in medium lacking glycerol (CMF) indicated a shift in metabolic strategy and usage of a carbon source other than glycerol. To determine carbon source utilization by the obligate *S. oneidensis* Δ*fccA* pGUT2/*G. sulfurreducens* co-culture, supernatant samples were analyzed by HPLC. Indeed, glycerol concentration decreased <0.5 mM in co-cultures of *S. oneidensis* Δ*fccA* pGUT2 and *G. sulfurreducens* in CMGF medium over 100 days (Fig. 2.5A). Instead of using glycerol as carbon source, the *S. oneidensis* Δ*fccA* pGUT2/*G.*

sulfurreducens co-culture converted fumarate to malate, and malate was then consumed after concentrations reached ~40 mM (Fig. 2.5A). Malate was also produced and subsequently consumed by the *S. oneidensis* Δ*fccA* pGUT2/*G. sulfurreducens* co-culture in CMF medium highlighting the metabolic shift to malate catabolism (Fig. 2.5B). Succinate concentration rose in co-cultures both in CMGF and CMF media as malate was consumed (Fig. 2.5A andB). Growth related to malate metabolism required *S. oneidensis* Δ*fccA* pGUT2 and *G. sulfurreducens* to be cultured together as neither species was able to grow alone in CMGF or CMF medium (Fig. 2.4A). Supernatant from *S. oneidensis* Δ*fccA* pGUT2 and *G. sulfurreducens* cultured alone showed that both organisms were able to convert fumarate to malate, likely catalyzed by fumarase, yet at rates slower than occurred in the co-culture (Fig 2.5 C-F). *S. oneidensis* Δ*fccA* pGUT2 cultured alone was not able to consume malate, and only produced trace amounts of succinate in CMGF medium (Fig. 2.5 C and D). Low concentrations of succinate were also produced by *G. sulfurreducens* cultured alone in CMGF and CMF medium, but were produced at a significantly slower rate than by the co-culture (Fig. 2.5 E and F). Fumarate has been shown previously to serve as an additional carbon source in the presence of acetate by *G. sulfurreducens* (Yang et al., 2010).

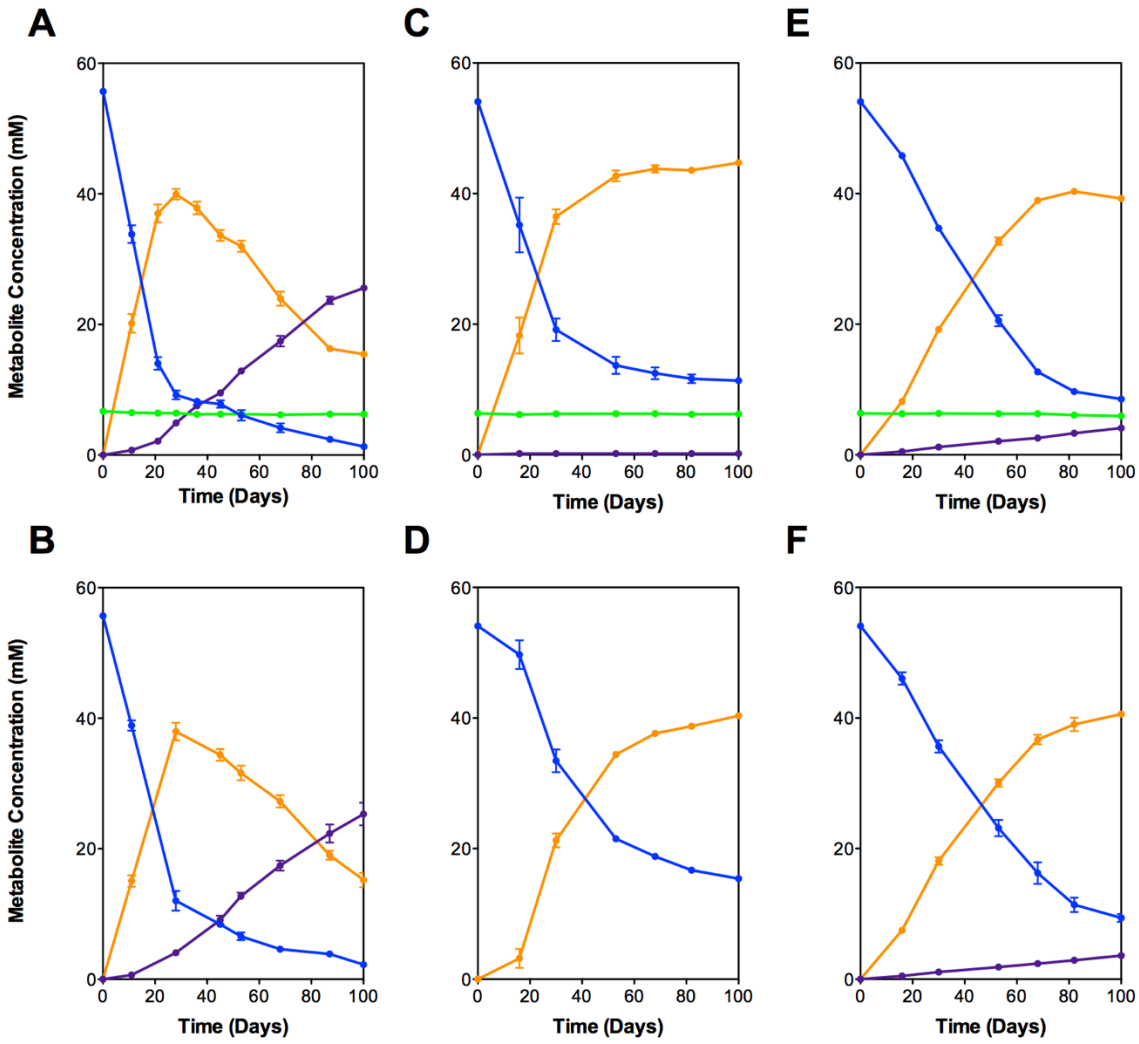

Figure 2.5: Metabolite profiles in *S. oneidensis* Δ*fccA* pGUT2/*G. sulfurreducens* co-cultures in A) CMGF medium or B) CMF medium; *S. oneidensis* Δ*fccA* pGUT2 cultured alone in C) CMGF medium or D) CMF medium; and *G. sulfurreducens* cultured alone in E) CMGF medium or F) CMF medium. Media contained 7 mM glycerol and/or 60 mM fumarate as indicated. Metabolites include glycerol (green triangles), acetate (red squares), fumarate (blue circles), and succinate (purple inverted triangles). Reported values represent mean ± SEM metabolite concentrations (mM) measured for three independent experiments.

To determine if the obligate *S. oneidensis* Δ*fccA* pGUT2/*G. sulfurreducens* co-culture was dependent on acetate transfer from *Shewanella* to *Geobacter*, as was determined for the commensal co-culture, targeted deletions were made in the metabolic

pathway linked to acetate production by *Shewanella*. *S. oneidensis* generates acetate from a variety of carbon sources via the acetate kinase/phosphotransacetylase (Ack/Pta) pathway (Hunt et al., 2010; Flynn et al., 2012), so to significantly diminish acetate secretion by *S. oneidensis* Δ*fccA* pGUT2, we deleted *pta* from the chromosome (strain referred to as *S. oneidensis* Δ*fccA*Δ*pta* pGUT2). Growth yield, in CMGF and more so in CMF media, was severely diminished for co-cultures initiated with *S. oneidensis* Δ*fccA*Δ*pta* pGUT2 and *G. sulfurreducens* as compared to co-cultures containing *S. oneidensis* Δ*fccA* pGUT2 and *G. sulfurreducens* after 100 days of incubation (Fig. 2.6 versus Fig. 2.4). Interestingly, increase in OD_{600} of the *S. oneidensis* Δ*fccA*Δ*pta* pGUT2/*G. sulfurreducens* co-culture occurred following a sharp increase in *S. oneidensis* Δ*fccA*Δ*pta* pGUT2 in the co-culture (after an initial population decline) (Fig. 2.6A and B). CFU counts for *G. sulfurreducens* increased slightly following the CFU increase for *S. oneidensis* Δ*fccA*Δ*pta* pGUT2 (Fig. 2.6B).

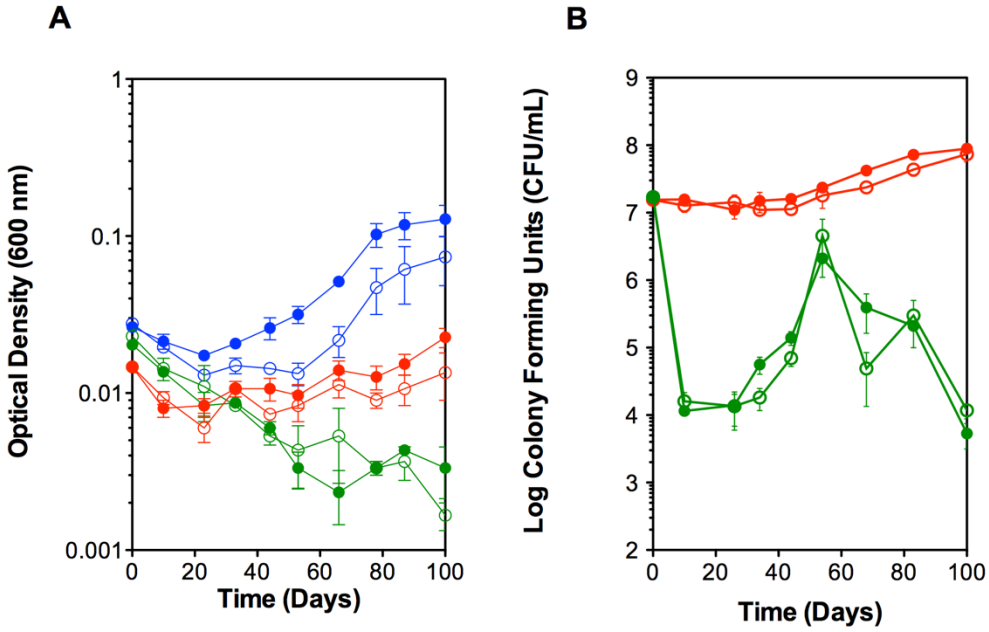

Figure 2.6: Obligate growth of *S. oneidensis* Δ*fccA*Δ*pta* pGUT2 and *G. sulfurreducens* in basal co-culture medium (CM) containing 7 mM glycerol and 60 mM fumarate (CMGF, closed symbols) or co-culture medium supplemented only with 60 mM fumarate (CMF, open symbols). A) Growth measured as OD_{600} for the *S. oneidensis* Δ*fccA*Δ*pta* pGUT2/*G. sulfurreducens* co-culture (blue), and for *S. oneidensis* Δ*fccA*Δ*pta* pGUT2 (green) and *G. sulfurreducens* (red) cultured singly. B) Growth measured as colony forming units for *S. oneidensis* Δ*fccA*Δ*pta* pGUT2 (green) and *G. sulfurreducens* (red) in co-culture. Reported values are averages for triplicate experiments with error bars representing SEM.

Conversion of fumarate to malate was significantly slowed for the *S. oneidensis* Δ*fccA*Δ*pta* pGUT2/*G. sulfurreducens* co-culture as compared to the original obligate *S. oneidensis* Δ*fccA* pGUT2/*G. sulfurreducens* co-cultures, and malate concentration did not decline until ~60 days mirroring growth measured by OD_{600}. Subsequent succinate production was also greatly diminished in the *S. oneidensis* Δ*fccA*Δ*pta* pGUT2/*G. sulfurreducens* co-culture as compared to *S. oneidensis* Δ*fccA* pGUT2/*G. sulfurreducens* co-cultures over the time period monitored both in CMGF and CMF media (Fig. 2.7A and B). Taken together, results from the *S. oneidensis* Δ*fccA*Δ*pta* pGUT2/*G.*

sulfurreducens co-culture (Fig. 2.6A) compared to the *S. oneidensis* Δ*fccA* pGUT2/*G. sulfurreducens* co-culture (Fig. 2.4A) indicated that deletion of *pta* inhibited co-culture growth. HPLC analysis of supernatant from cultures with *S. oneidensis* Δ*fccA*Δ*pta* pGUT2 cultured alone indicated that fumarate conversion to malate occurred at a slower rate in CMF medium as compared to CMGF medium though glycerol levels remained largely unchanged in CMGF medium (Fig. 2.7C and D). It is possible that the presence of 7 mM glycerol acts as a cell protectant in CMGF, and may explain why growth of the *S. oneidensis* Δ*fccA*Δ*pta* pGUT2 and *G. sulfurreducens* was also inhibited more in CMF than CMGF media (Fig. 2.6A).

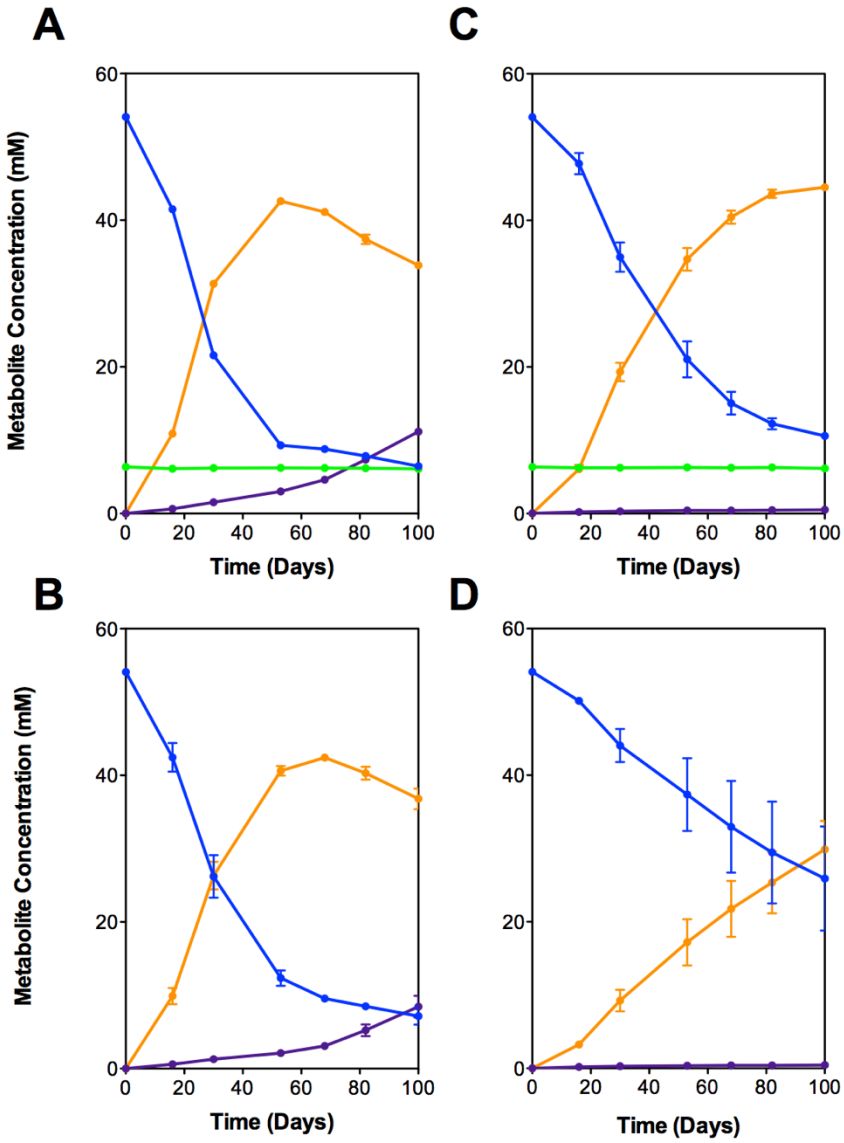

Figure 2.7: Metabolite profiles in *S. oneidensis* Δ*fccA*Δ*pta* pGUT2/*G. sulfurreducens* co-cultures in A) CMGF medium or B) CMF medium; *S. oneidensis* Δ*fccA*Δ*pta* pGUT2 cultured alone in C) CMGF medium or D) CMF medium. Media contained 7 mM glycerol and/or 60 mM fumarate as indicated. Metabolites include glycerol (green triangles), acetate (red squares), fumarate (blue circles), and succinate (purple inverted triangles). Reported values represent mean ± SEM metabolite concentrations (mM) measured for three independent experiments.

Due to inhibited co-culture growth by deletion of *pta* in *Shewanella*, we hypothesized that growth in the original *S. oneidensis* Δ*fccA* pGUT2/*G. sulfurreducens*

obligate co-culture was due to uptake of malate and production of acetate by *Shewanella*. *Shewanella* encodes pathways to convert malate to pyruvate via malic enzymes MaeB and SfcA, or phosphoenolpyruvate (PEP) through concerted malate dehydrogenase and PEP carboxykinase activity. PEP and pyruvate could then be catabolized via central metabolic pathways producing acetate. Growth was inhibited in co-cultures containing *S. oneidensis* Δ*fccA*Δ*maeB*Δ*sfcA*Δ*pckA* pGUT2 and *G. sulfurreducens* similar to co-cultures containing the *S. oneidensis* Δ*fccA*Δ*pta* pGUT2 strain (Fig. 2.8A and Fig. 2.6A). The *S. oneidensis* Δ*fccA*Δ*maeB*Δ*sfcA*Δ*pckA* pGUT2 population initially decreased in co-culture with *G. sulfurreducens* followed by an increase in CFUs around ~40 hours (Fig 2.8B) similar to the growth pattern observed for *S. oneidensis* Δ*fccA*Δ*pta* pGUT2 (Fig. 2.6B). CFU counts for *G. sulfurreducens* increased slightly following CFU increase by *S. oneidensis* Δ*fccA*Δ*maeB*Δ*sfcA*Δ*pckA* pGUT2 (Fig. 2.8B). Malate consumption and succinate production were also significantly slower for the *S. oneidensis* Δ*fccA*Δ*maeB*Δ*sfcA*Δ*pckA* pGUT2/*G. sulfurreducens* co-cultures as compared to the original *S. oneidensis* Δ*fccA* pGUT2/*G. sulfurreducens* co-culture in CMGF and CMF media (Fig. 2.9A and B). Co-cultures were also initiated between *G. sulfurreducens* and *S. oneidensis* containing deletions both in pathways for malate consumption and acetate production (*S. oneidensis* Δ*fccA*Δ*pta*Δ*maeB*Δ*sfcA*Δ*pckA* pGUT2), and growth and metabolite profiles were not significantly different from co-cultures containing either *S. oneidensis* Δ*fccA*Δ*pta* pGUT2 or *S. oneidensis* Δ*fccA*Δ*maeB*Δ*sfcA*Δ*pckA* pGUT2 (data not shown).

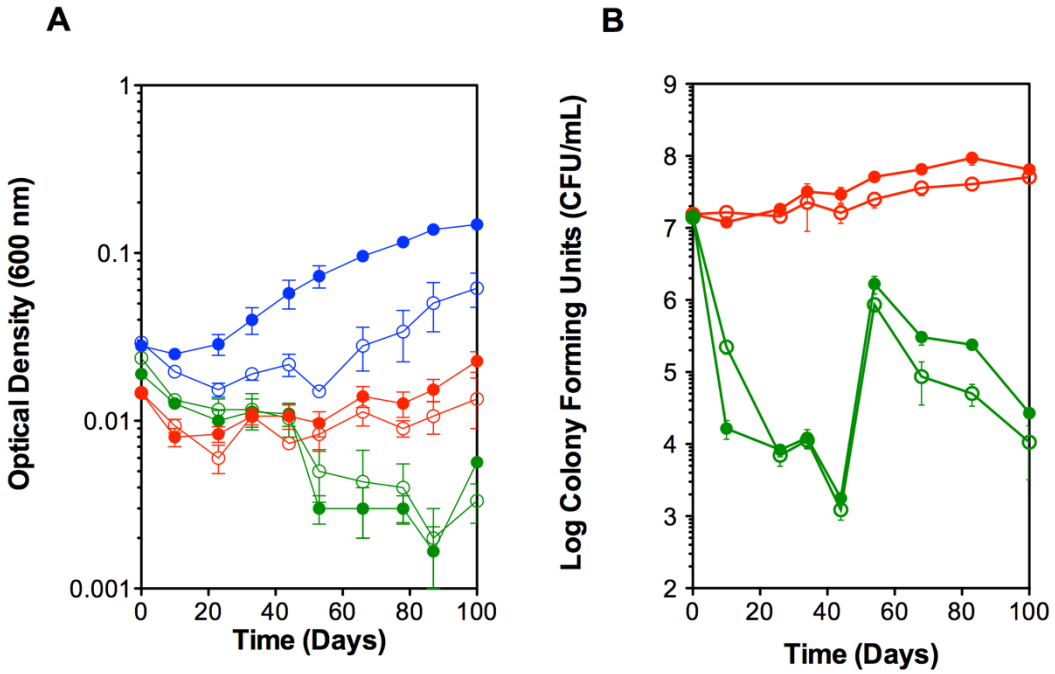

Figure 2.8: Obligate growth of *S. oneidensis* Δ*fccA*Δ*maeB*Δ*sfcA*Δ*pckA* pGUT2 and *G. sulfurreducens* in basal co-culture medium (CM) containing 7 mM glycerol and 60 mM fumarate (CMGF, closed symbols) or co-culture medium supplemented only with 60 mM fumarate (CMF, open symbols). A) Growth measured as OD_{600} for the *S. oneidensis* Δ*fccA*Δ*maeB*Δ*sfcA*Δ*pckA* pGUT2/*G. sulfurreducens* co-culture (blue), and for *S. oneidensis* Δ*fccA*Δ*maeB*Δ*sfcA*Δ*pckA* pGUT2 (green) and *G. sulfurreducens* (red) cultured singly. B) Growth measured as CFU/mL media for *S. oneidensis* Δ*fccA*Δ*maeB*Δ*sfcA*Δ*pckA* pGUT2 (green) and *G. sulfurreducens* (red) in co-cultures. Reported values are averages for triplicate experiments with error bars representing SEM.

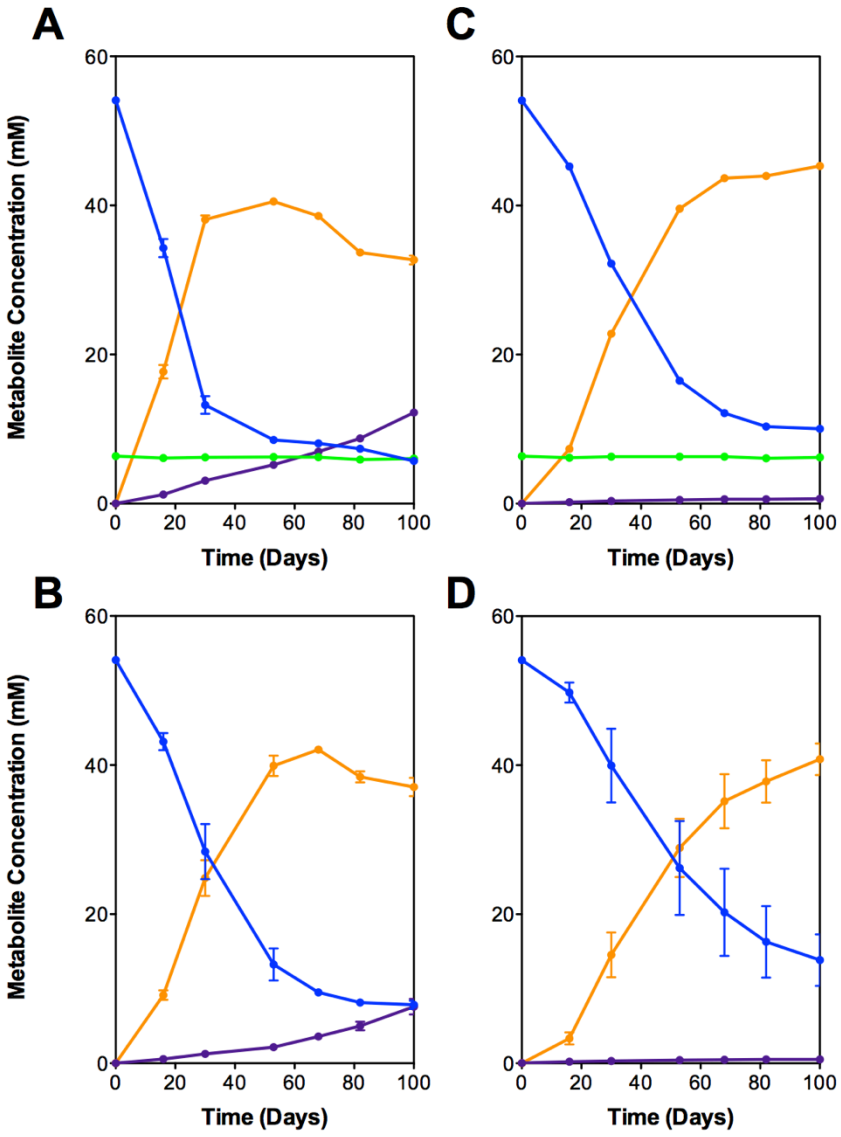

Figure 2.9: Metabolite profiles in *S. oneidensis* Δ*fccA*Δ*maeB*Δ*sfcA*Δ*pckA* pGUT2/*G. sulfurreducens* co-cultures in A) CMGF medium or B) CMF medium; *S. oneidensis* Δ*fccA*Δ*maeB*Δ*sfcA*Δ*pckA* pGUT2 cultured alone in C) CMGF medium or D) CMF medium. Media contained 7 mM glycerol and/or 60 mM fumarate as indicated. Metabolites include glycerol (green triangles), acetate (red squares), fumarate (blue circles), and succinate (purple inverted triangles). Reported values represent mean ± SEM metabolite concentrations (mM) measured for three independent experiments.

Finally, because growth rates of all co-cultures were slightly faster in CMGF medium as compared to CMF medium (Fig. 2.4A, 2.6A, and 2.8A), an obligate co-culture was initiated between *S. oneidensis* Δ*fccA* without the pGUT2 plasmid and *G. sulfurreducens* to determine if faster growth rates in CMGF medium were associated with activity encoded by pGUT2. Growth rate and yield were similar between co-cultures containing *S. oneidensis* Δ*fccA* with or without the pGUT2 plasmid and both had slightly higher growth rates in CMGF medium than in CMF (Fig. 2.4A versus Fig. 2.10A). Metabolite profiles were also similar for co-cultures of *G. sulfurreducens* with *S. oneidensis* Δ*fccA* with or without the pGUT2 plasmid (Fig. 2.5A and B versus Fig. 2.11A and B). Results from co-cultures containing *S. oneidensis* Δ*fccA* lacking the pGUT2 plasmid indicated that co-culture growth in CMGF and CMF media was not due to activity mediated by pGUT2.

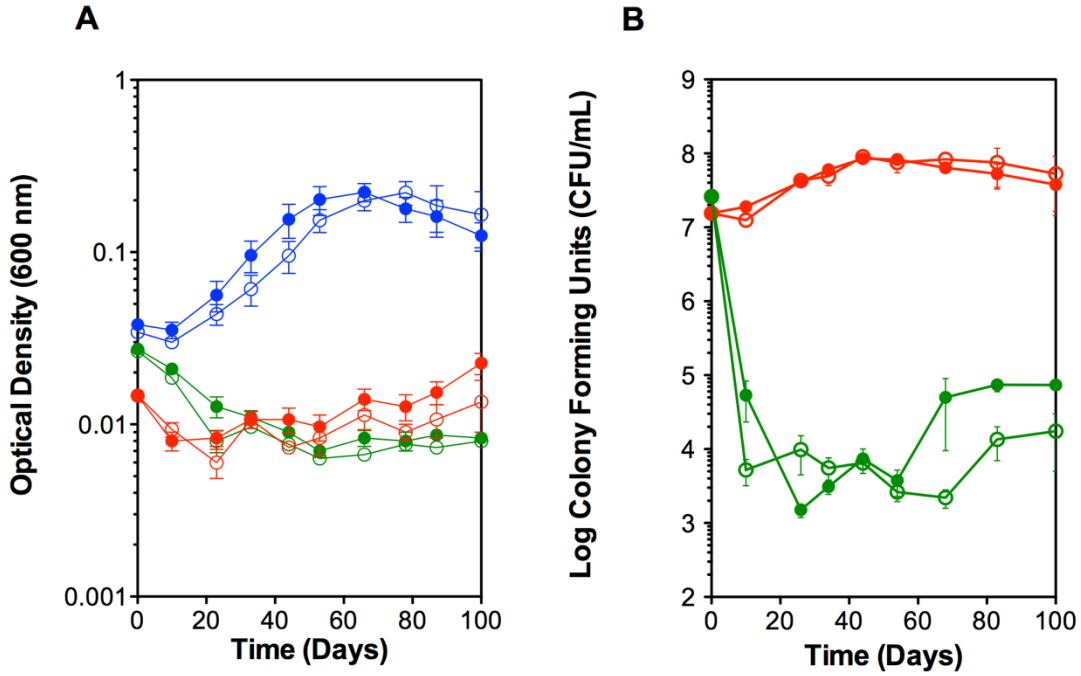

Figure 2.10: Obligate growth of *S. oneidensis* Δ*fccA* and *G. sulfurreducens* in basal co-culture medium (CM) containing 7 mM glycerol and 60 mM fumarate (CMGF, closed symbols) or co-culture medium supplemented only with 60 mM fumarate (CMF, open symbols). A) Growth measured as OD_{600} for the *S. oneidensis* Δ*fccA*/*G. sulfurreducens* co-culture (blue), and for *S. oneidensis* Δ*fccA* (green) and *G. sulfurreducens* (red) cultured singly. B) Growth measured as colony forming units for *S. oneidensis* Δ*fccA* (green) and *G. sulfurreducens* (red) co-cultures. Reported values are averages for triplicate experiments with error bars representing SEM.

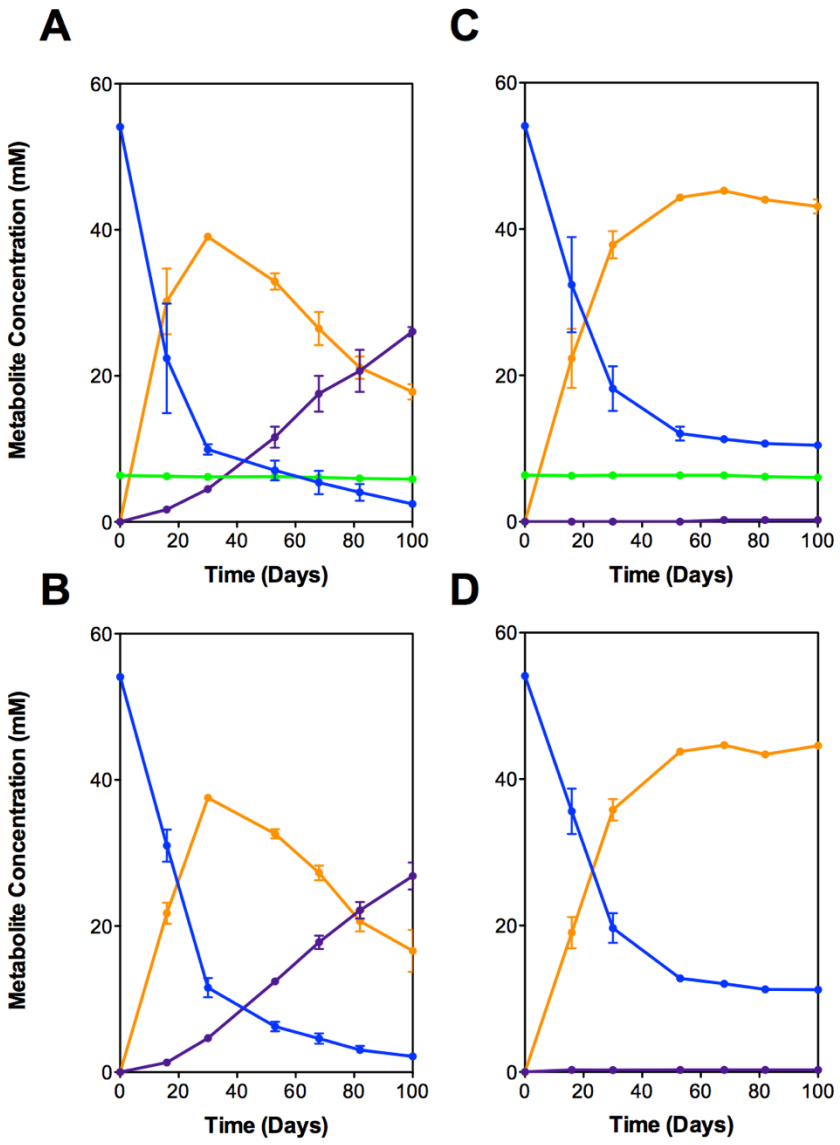

Figure 2.11: Metabolite profiles in *S. oneidensis* Δ*fccA*/*G. sulfurreducens* co-cultures in A) CMGF medium or B) CMF medium; *S. oneidensis* Δ*fccA* cultured alone in C) CMGF medium or D) CMF medium. Media contained 7 mM glycerol and/or 60 mM fumarate as indicated. Metabolites include glycerol (green triangles), acetate (red squares), fumarate (blue circles), and succinate (purple inverted triangles). Reported values represent mean ± SEM metabolite concentrations (mM) measured for three independent experiments.

Strain	Description	Reference
***Escherichia coli* strain UQ950**	DH5α host for cloning: F- *(argF-lac)169 80dlacZ58(M15) glnV44(AS) rfbD1 gyrA96(NalR) recA1 endA1 spoT1 thi-1 hsdR17 deoR pir+*	(Saltikov & Newman, 2003)
***Escherichia coli* strain WM3064**	DAP auxotroph used for conjugation: *thrB1004 pro thi rpsL hsdS lacZM15 RP4-1360 (araBAD)567 dapA1341::[erm pir(wt)]*	(Saltikov & Newman, 2003)
***Shewanella oneidensis* strain MR-1**	Wild type	(Venkateswaran et al., 1999)
***Shewanella oneidensis* pGUT2**	Wild type *Shewanella* containing the glycerol utilization plasmid	(Flynn et al., 2010)
Shewanella oneidensis* Δ*fccA	*Shewanella* containing an in-frame deletion of the fumarate reductase *fccA*	This study
***Shewanella oneidensis* Δ*fccA* pGUT2**	*Shewanella* containing the glycerol utilization plasmid; in-frame deletion of the fumarate reductase *fccA*	This study
***Shewanella oneidensis* Δ*fccA*Δ*pta* pGUT2**	*Shewanella* containing the glycerol utilization plasmid; in-frame deletions of the fumarate reductase *fccA* and phosphotransacetylase *pta*	This study
***Shewanella oneidensis* Δ*fccA*Δ*maeB*Δ*sfcA*Δ*pckA* pGUT2**	*Shewanella* containing the glycerol utilization plasmid; in-frame deletions of genes encoding the fumarate reductase *fccA*, malic enzymes *maeB* and *sfcA*, and phosphoenolpyruvate carboxykinase *pckA*	This study
***Geobacter sulfurreducens* strain PCA**	Wild type	(Caccavo et al., 1994)

Table 2.2: Strains used in this study.

Primer Name	DNA Sequence (5' to 3') or Reference
Primers used to delete *fccA*	
FccA_1	NNactagtTGCAGCGGTGCTATTAAG
FccA_2	NNgaattcCATTGCGCCAGAGATCAG
FccA_3	NNgaattcATCGCGGGTGCATCTGCC
FccA_4	NNgagctcATGGCAGGCTGATAGGC
Primers used to delete *pta*	(Hunt et al., 2010)
Primers used to delete *maeB*	
maeB_Up_F	CGATggatccGTGGTGCATGTCACCCATTCTACAC
maeB_Up_R	CGATactagtGTGGCTCGTTTCAGCGGGTTTAG
maeB_Dn_F	CGATactagtGAAGCGGTACCTGCAAGTGTCC
maeB_Dn_R	CGATgagctcGTCATACTGAGGCCCGACTGAG
Primers used to delete *sfcA*	
sfcA_Up_F	CGATggatccGGCGGTAATCAATGGCAA
sfcA_Up_R	CGATactagtGGGCAAATTCGACCAGTT
sfcA_Dn_F	CGATactagtAAAACTGGCCGCAGCTTT
afcA_Dn_R	CGATgagctcTGTGCCATCGAGTCTT
Primers used to delete *pckA*	
pckA_Up_F	CGATggatccGGCGGTAATCAATGGCAA
pckA_Up_R	CGATactagtGGGCAAATTCGACCAGTT
pckA_Dn_F	CGATactagtAAAACTGGCCGCAGCTTT
pckA_Dn_R	CGATgagctcAAGACTCGATGGCACA

Table 2.3: Primers utilized in this study.

Discussion

Natural microbial populations are continuously influenced by changing biological, chemical, and physical factors (Little et al., 2008). The dynamics of natural communities combined with their enormous diversity and the fact that many microorganisms cannot be grown in the laboratory has confounded the study of multispecies ecosystems (Little et al., 2008; Whitman et al., 1998). Obligate interactions among community members have been posed as one reason for recalcitrance to laboratory culture by many microorganisms (D'Onofrio et al., 2010; Kaeberlein et al., 2002). Interaction in multispecies communities often involves exchange of metabolites and small molecules, and synthetic model laboratory communities have provided a powerful tool to begin to study how interaction and overall cooperation can emerge in multispecies ecosystems (Bull & Harcombe, 2009; Harcombe, 2010; Hillesland & Stahl, 2010; Hillesland et al., 2014; Pande et al., 2014; Summers et al., 2010; Wintermute & Silver, 2010). Here, we describe construction of synthetic model communities ranging from commensalism to obligate mutualism using the bacteria *S. oneidensis* and *G. sulfurreducens*. Because *S. oneidensis* and *G. sulfurreducens* were originally isolated from different environments, their co-culture enabled us to monitor the emergence of cooperation from the initial point of contact (Caccavo et al., 1994; Venkateswaran et al., 1999). We show here also that a targeted deletion in the respiratory pathway of *S. oneidensis* altered interaction requiring obligate cooperation with *G. sulfurreducens* and completely shifted the metabolic strategy of the community. It is known that gene loss

can lead to obligate interaction (Pande et al., 2014), and that population bottlenecks can lead to mutation or loss of essential genes (Nilsson et al., 2005). The obligate co-culture between *S. oneideneis* Δ*fccA* pGUT2 and *G. sulfurreducens* provides a model laboratory system to monitor how metabolic strategy may shift in environments due to gene loss and provide a possible explanation for the emergence of obligate interaction in multispecies communities. While little is known about how cooperation emerges in natural environments, adaptive genetic loss or mutation may lead to metabolic synergy and context-dependent obligate interaction (Harcombe, 2010; Morris et al., 2012; Pande et al., 2014; Shou et al., 2007).

To engineer cooperation between *Shewanella* and *Geobacter*, we began by constructing a commensal, one-way cross-feeding mechanism into the community. Incorporation of the pGUT2 plasmid enabled *S. oneidensis* to metabolize glycerol and secrete acetate as a carbon source for *G. sulfurreducens* (Fig. 2.1). Because *G. sulfurreducens* could not utilize glycerol, it was reliant on *S. oneidensis* to produce its carbon source. Both species coupled oxidative metabolic reactions to the respiration of fumarate (Fig. 2.1, Fig. 2.3). Complete oxidation of glycerol required the presence of both species, and highest growth yield per mole glycerol used was achieved when both *S. oneidensis* pGUT2 and *G. sulfurreducens* were cultured together (Fig. 2.2A). Selective plating enabled monitoring of individual species within co-cultures and revealed, as predicted, that growth of *G. sulfurreducens* in basal co-culture medium containing glycerol and fumarate required the presence and metabolic activity of *S. oneidensis,* as *G.*

sulfurreducens was unable to growth in this medium alone (Fig. 2.2B). *S. oneidensis* pGUT2 growth was similar when cultured alone or in co-culture with *G. sulfurreducens* indicating that *S. oneidensis* did not receive an appreciable benefit from consumption of its waste product acetate by *G. sulfurreducens* (Fig 2.2B).

A deletion of the fumarate reductase (*fccA*) in *S. oneidensis* pGUT2, leaving it unable to respire fumarate, shifted the engineered co-culture from a commensal to an obligate interaction as neither *S. oneidensis* Δ*fccA* pGUT2 nor *G. sulfurreducens* were able to grow in basal co-culture medium containing glycerol and fumarate alone (Fig. 2.4A). Surprisingly, growth was also seen for the obligate co-culture in medium containing only fumarate (Fig. 2.4A). Analysis of *S. oneidensis* Δ*fccA* pGUT2/*G. sulfurreducens* co-culture supernatants revealed that glycerol was not utilized (Fig 2.5A) and activity mediated by the pGUT2 plasmid was not required for obligate co-culture growth (Fig 2.10A). Instead, fumarate was converted to malate, and malate was subsequently consumed by the *S. oneidensis* Δ*fccA* pGUT2/*G. sulfurreducens* co-culture highlighting a complete shift in metabolic strategy between the commensal and obligate co-cultures (Fig. 2.5A and B). Mutations inhibiting acetate production (Δ*pta*) or malate uptake into central metabolic intermediates (Δ*maeB*Δ*sfcA*Δ*pckA*) in the *S. oneidensis* Δ*fccA* pGUT2 background significantly inhibited growth with *G. sulfurreducens* (Fig 2.6A and 2.8A). Inhibition of growth by co-cultures containing *S. oneidensis* ΔfccA pGUT2 with additional deletion of *pta*, or combined *maeB*/*sfcA*/*pckA* deletions indicate that obligate co-culture growth likely involved malate uptake by *Shewanella* leading to

production of either pyruvate or PEP subsequently metabolized to acetate, which then served as carbon source for *G. sulfurreducens*. Interestingly, malate uptake and catabolism by *Shewanella* is not redox-balanced as outlined above, and the presence of *G. sulfurreducens* to accept reducing equivalents from *Shewanella* strains may explain co-culture growth. Transfer of reducing equivalents between species enabling the catabolic breakdown of compounds that neither species alone can digest is a hallmark of many syntrophic communities (Schink, 1997; Schink & Stams, 2006; Sieber et al., 2012; Stams & Plugge, 2009). Further elucidation of transfer of reducing equivalents from *Shewanella* to *Geobacter* will be highlighted through experiments in the following chapter of this thesis.

Acknowledgements

I would like to thank Rachel Soble for her help in conducting experiments in this chapter.

Chapter 3 *: Interspecies Electron Transfer Mediated by Flavins in a Synthetic Co-culture of Shewanella oneidensis and Geobacter sulfurreducens*

Summary

Interspecies electron transfer is required by many syntrophic communities in order to catabolize compounds that single species alone cannot digest. While syntrophic relationships are critical to many biogeochemical cycles, the obligate nature of interaction poses limitations to their study. To study syntrophy in the laboratory, we constructed a synthetic ecosystem in electrochemical reactors using *Shewanella oneidensis* and *Geobacter sulfurreducens*—two bacteria chosen because of their unusual extracellular electron transfer pathways. In the absence of oxygen, both species can transfer electrons to their outer cell surface enabling use of insoluble metals and electrodes as terminal electron acceptors. *S. oneidensis* also secretes redox-active flavins which act as soluble electron shuttles. The ability of *S. oneidensis* and *G. sulfurreducens* to transfer electrons extracellularly allowed us to engineer an obligate co-culture metabolically linked to an electrode and monitor metabolic rates in real-time using three-electrode bioreactors. Co-culture reactors contained glycerol, a carbon source only used by *S. oneidensis* containing a glycerol utilization plasmid (pGUT2), and a gold electrode serving as the terminal electron acceptor that could only be used by *G. sulfurreducens*. As engineered, *S. oneidensis* pGUT2 supplied a carbon source for *G. sulfurreducens* only if *G. sulfurreducens* accepted metabolic electrons from *S. oneidensis* pGUT2 and transferred them to the electrode. Interspecies electron transfer by this community could have occurred through one or more mechanisms: transfer of hydrogen, formate, flavin electron shuttles, and direct cell-to-cell contact. To determine the mechanism(s) used, gene

deletion and insertion mutants were made to disrupt each pathway. Real-time current production was greatly diminished for communities where flavin transfer was eliminated indicating flavin electron shuttles were the primary route for interspecies electron transfer between *S. oneidensis* pGUT2 and *G. sulfurreducens*.

Introduction

Microorganisms catalyze a diverse array of chemical reactions during the breakdown of organic matter and often do so through cooperation with other organisms. Cooperation is most apparent during anaerobic degradation of organic matter where organisms may be dependent on other community members to fulfill certain metabolic roles (Schick & Stams, 2006). Syntrophy represents a community structure in which two or more members interact to gain energy through combined metabolic strategies to catalyze the breakdown of compounds that neither species alone can digest (Schink & Stams, 2006; Sieber et al., 2012; Stams & Plugge, 2009). Syntrophic communities are fundamental to the global carbon cycle, yet detailed mechanistic understanding of cooperation and exchange within many of these communities remains enigmatic (Alperin & Hoehler, 2010; McGlynn et al., 2015; Orcutt & Meile, 2008; Sieber et al., 2012; Stams & Plugge, 2009; Wegener et al., 2015).

Electron transfer reactions are the energy currency of life, and exchange of reducing equivalents, a process termed interspecies electron transfer, is fundamental to the function and activity of many syntrophic communities (Stams & Plugge, 2009). Canonical mechanisms of interspecies electron transfer include hydrogen and formate

transfer. Here, the oxidation of organic carbon by one organism is coupled to the reduction of protons or carbon dioxide forming hydrogen or formate provided a consuming partner keeps their concentrations low (Rotaru et al., 2012; Sieber et al., 2012; Stams & Plugge, 2009). Besides hydrogen and formate transfer, laboratory cultures are being used to describe a plethora of additional compounds and mechanisms mediating interspecies electron transfer including: sulfur compounds (Biebl & Pfennig, 1978; Kaden et al., 2002; Milucka et al., 2012), humic analogs (Liu et al., 2012; Smith et al., 2015), conductive materials (Chen et al., 2014; Kato et al., 2012; Liu et al., 2012), and direct cell-to-cell contact thought to be mediated by mutiheme cytochromes and/or pili (McGlynn et al., 2015; Summers et al., 2010; Wegener et al., 2015).

Despite their importance in oxidation-reduction (redox) reactions, the role of flavins as electron shuttles in interspecies electron transfer has yet to be studied. Flavins can participate in both one- and two-electron transfer reactions making them extremely versatile and ubiquitous in redox processes, and flavin-binding proteins represent 1-3% of genes in bacterial and eukaryotic genomes (Abbas & Sibirny, 2011). A multitude of roles for extracellular flavins have come to light recently. Extra-cytoplasmic flavins can mediate acquisition and assimilatory uptake of Fe(II) by various bacteria, fungi, and plants (Abbas & Sibirny, 2011; Balasubramanian et al., 2010; Crossley et al., 2007; Dmytruk et al., 2006; Fassbinder et al., 2000; Rodriguez-Celma et al., 2011; Stenchuk et al., 2001; Worst et al., 1998). Riboflavin has also been shown to stimulate respiration and shoot formation in symbiotic *Sinorhizobium*-alfalfa populations (Phillips et al, 1999;

Yang et al., 2002). Secreted flavins can also act as soluble redox-active shuttles stimulating reduction of insoluble terminal electron acceptors by *S. oneidensis* and *Geothrix fermentans* (Brutinel & Gralnick, 2012; von Canstein et al., 2008; Marsili et al., 2008; Mehta-Kolte & Bond, 2012).

Here, we report an additional role for extracellular flavins as mediators of interspecies electron transfer in a model laboratory culture of *Shewanella oneidensis* and *Geobacter sulfurreducens*. *S. oneidensis* and *G. sulfurreducens* serve as the model organisms for extracellular respiration—the ability to transfer metabolic electrons to the outer cell surface for respiration of insoluble terminal electron acceptors such as iron oxides and electrodes—and hence, are prime organisms for the study of interspecies electron transfer (Gralnick & Newman, 2007; Hau & Gralnick, 2007; Lovley et al., 2011). Co-cultures were initiated by incorporating a glycerol utilization plasmid (pGUT2) in *S. oneidensis* enabling it to oxidize glycerol and secrete acetate as a carbon source for *G. sulfurreducens*. Co-cultures were grown in three-electrode reactors with a gold electrode serving as the terminal electron acceptor. *S. oneidensis* is unable to respire gold electrodes (Kane et al., 2013), and in order to continue oxidizing glycerol and provide acetate for *G. sulfurreducens,* must transfer metabolic electrons to *G. sulfurreducens* who then transfers electrons to the gold electrode. The genomes of *S. oneidensis* and *G. sulfurreducens* encode multiple pathways that could be utilized for interspecies electron transfer and targeted gene deletions were used to probe various pathways. Electron transfer to gold electrodes was significantly inhibited in co-cultures

when flavin secretion by *Shewanella* was eliminated, and was restored to near wild-type levels in the presence of exogenously supplied flavins indicating interspecies electron transfer mediated by flavin electron shuttles. Interestingly, interspecies electron transfer was not completely inhibited through deletion of hydrogen, formate, and flavin-mediated pathways indicating a possibility for direct electron transfer by the *S. oneidensis* pGUT2/*G. sulfurreducens* co-culture.

Methods

Bacterial Strains and Culture Conditions

Medium components for bacterial cultures were purchased from Becton, Dickinson and Company (Sparks, MD). Chemicals serving as carbon sources or electron acceptors were purchased from Sigma-Aldrich (St. Louis, MO) with the exception of glycerol, which was purchased from Fisher Chemical (Pittsburgh, PA).

S. oneidensis and *E. coli* strains were maintained at 30°C and 37°C, respectively, on lysogeny broth (LB) medium solidified with 1.5% agar and supplemented with 50 μg/ml kanamycin when required. *G. sulfurreducens* was maintained at 30°C under strict anaerobic conditions using an anaerobic chamber with a 5%:75%:20% H_2:N_2:CO_2 atmosphere (Coy Lab Products; Grass Lake, MI) on basal medium (NB) plates containing the following per liter: 0.38 g KCl, 0.2 g NH_4Cl, 0.069 g $NaH_2PO_4 \cdot H_2O$, 0.04 g $CaCl_2 \cdot 2H_2O$, 0.2 g $MgSO_4 \cdot 7H_2O$, 2.0 g $NaHCO_3$ (pH 6.8), 10 mL/L of a mineral mix (Hau et al., 2008) and supplemented with 0.1% trypticase (wt/vol), 1 mM cysteine, 20

mM acetate, 40 mM fumarate (NBFA+TC) and solidified with 1.5% agar. Strains and plasmids used in this study are listed in Table 3.1.

All experiments were initiated with single colonies picked from freshly streaked -80°C 15% glycerol or 10% DMSO stocks on LB containing 50 μg/ml kanamycin or NBFA+TC plates for *S. oneidensis* and *G. sulfurreducens*, respectively. In preparation for bioreactor assays, single colonies of *S. oneidensis* were grown shaken at 30°C in LB broth containing 50 μg/ml kanamycin for 16 hours and were then sub-cultured into *Shewanella* Basal Medium (SBM) containing 7 mM glycerol for 6 hours (pH 7.2) containing per 1 liter of medium: 0.225g K_2HPO_4, 0.225g KH_2PO_4, 0.46g NaCl, 0.225g $(NH_4)_2SO_4$, 0.117g $MgSO_4 \cdot 7H_2O$, 10 mM HEPES buffer, supplemented with 5 mL/L vitamin mix and 5 mL/L mineral mix (Hau et al., 2008). From aerobic SBM cultures, a 1:100 dilution was performed in anaerobic SBM medium containing 7 mM glycerol and 60 mM fumarate, and anaerobic *S. oneidensis* strains containing pGUT2 were grown shaken at 250 rpm at 30°C to mid exponential phase in preparation for bioreactor experiments. Single colonies of *G. sulfurreducens* were grown in an anaerobic chamber (5%:75%:20% H_2:N_2:CO_2) in 1 mL of NB medium supplemented with 20 mM acetate and 40 mM fumarate (NBFA) for 48 hours at 30°C. Following this initial growth, 1 mL of *G. sulfurreducens* was sub-cultured into 10 mL NBFA in anaerobic culture tubes under an 80%:20% N_2:CO_2 headspace 24 hours prior to co-culture experiments. *S. oneidensis* and *G. sulfurreducens* cultures were then washed twice, and re-suspended in CMG

medium supplemented with 60 mM NaCl to an optical density of 0.4. From these cell suspensions, 7 mL *S. oneidensis* and 3 mL *G. sulfurreducens* were added to reactors.

Generation of Knock-Out/Knock-In Strains

Enzymes were purchased from New England Biolabs (Ipswich, MA). Kits for PCR cleanup, gel purification, and plasmid preparations were purchased from Invitrogen (Carlsbad, CA). Oligonucleotide primers used to amplify portions of the *S. oneidensis* and *G. sulfurreducens* chromosomes for deletion or addition plasmids are listed in Table 3.2. PCR products were cloned using standard laboratory molecular biology protocols.

For deletions in *S.* oneidensis, regions flanking deletion targets were amplified using PCR and cloned into the pSMV3 suicide vector. In-frame gene deletions were generated using homologous recombination as previously described (Coursolle et al., 2010). To add *gfpmut3** to the chromosome of *S. oneidensis,* a gene-insertion plasmid (pAK1) was first constructed by cloning into pSMV3 homologous regions targeting a chromosomal insertion site located 7 bp downstream of the gene encoding *glmS,* a region previously targeted for gene addition in *Shewanella* (Teal et al., 2006). $P_{A1/O3/O4}$-*gfpmut3** amplified from plasmid pURR25 was addeded between the *glmS* target flanks generating plasmid pAK2 and was incorporated into the chromosome of *S. oneidensis* by homologous recombination as previously described (Coursolle et al., 2010; Teal et al., 2006). Gene knock-out and knock-in constructs were moved *into S. oneidensis* by conjugal transfer from *E. coli* donor strain WM3064. All plasmid constructs and gene deletions were verified by sequencing (University of Minnesota Genomics Center).

For gene replacement of *fdnG* in *G. sulfurreducens*, a fragment was generated by overlap PCR using primers in Table 3.2 to create a kanamycin resistance cassette flanked by ~500 bp regions homologous to regions upstream and downstream of *fdnG*. The Δ*fdnG*::*Km* fragment was then electroporated into *G. sulfurreducens* and mutants were selected on NBFA plates containing 200 μg/mL kanamycin as described previously (Levar et al., 2014; Lloyd et al., 2003). Disruption of *fdnG* by the kanamycin cassette was confirmed by PCR.

Fe(III) Oxide Reduction Assays

For Fe(III) oxide reduction, late-log-growth-phase *G. sulfurreducens* cells were inoculated to an OD_{600} of 0.005 into medium containing 50 mM ferrihydrite as the electron acceptor and 20 mM acetate as the electron donor as previously described (Levar et al., 2014). Samples were removed from tubes using a degassed syringe and were dissolved in 0.5 N HCl overnight. Fe(II) concentrations were measured via a modified FerroZine assay (Levar et al., 2014).

Electrochemical Analysis

Bio-electrochemical reactors and gold electrodes were constructed as described previously (Kane et al., 2013). Reactors consisted of a 25 mL glass cone and Teflon top modified to hold electrodes and a gas line port (Bioanalytical Systems; West Lafayette, IN). Anaerobic conditions were maintained by flushing reactors with humidified 80% N_2/20% CO_2 gas mix purified of impurities using a heated copper column. The working electrode consisted of a silicon wafer electroplated with 1000 Å of gold(111) machined to

2.54 cm x 0.635 cm. Gold electrodes were cleaned for 20 minutes before use in piranha solution (3:1 conc. sulfuric acid: 30% hydrogen peroxide). A platinum wire served as the counter electrode and was cleaned for 24 hours in 1 N HCl prior to use. The reference consisted of an Ag/AgCl electrode in 3M KCl connected to the system via a glass capillary tube filled with 1% agarose in a 0.1 M KCl solution and capped with a vycor frit. After addition of bacterial cultures, gold electrodes were poised at 0.24 V vs. standard hydrogen (SHE) and electrochemical data was monitored using a 16-channel VMP® potentiostat (Bio-Logic, Claix, France). Reactors were stirred and maintained at 30°C using a circulating water bath.

Results and Discussion

Syntrophic co-cultures were initiated between *S. oneidensis* and *G. sulfurreducens* through an engineered cross-feeding mechanism and reliance on interspecies electron transfer to balance oxidation of the supplied carbon source glycerol. Incorporation of a glycerol utilization plasmid (pGUT2) enabled *S. oneidensis* to utilize glycerol as a carbon source and subsequently produce acetate (Fig. 3.1). *G. sulfurreducens*, unable to metabolize glycerol (Lovley et al., 2011), relied on acetate secreted by *S. oneidensis* pGUT2 as a carbon source (Fig. 3.1). In turn, *S. oneidensis* pGUT2 relied on interspecies electron transfer to *G. sulfurreducens* because co-cultures were inoculated in three-electrode bioreactors containing gold electrodes as the sole terminal electron acceptor, a surface *S. oneidensis* cannot respire but *G. sulfurreducens* can (Liu et al., 2010; Kane et al., 2013). Hence, *S. oneidensis* pGUT2 and *G. sulfurreducens* were mutually dependent

on one another and oxidation of glycerol coupled to respiration of gold electrodes required combined metabolic activity of both organisms (Fig. 3.1).

Current is only produced in gold-electrode bioreactors containing glycerol when *S. oneidensis* pGUT2 and *G. sulfurreducens* are cultured together

Electron transfer to gold electrodes was measured in real-time as current production in three-electrode bioreactors. In these systems, *S. oneidensis* pGUT2 and *G. sulfurreducens* form biofilms on the gold electrode surface (anode) transferring to it electrons produced by the oxidation of glycerol, which are monitored as current produced over time using a potentiostat (see Material and Methods). As predicted, no current was produced by *S. oneidensis* pGUT2 or *G. sulfurreducens* when either was cultured alone in three-electrode bioreactors containing gold anodes and glycerol as carbon source over the time course monitored (Fig. 3.2). Current was produced in three-electrode bioreactors containing co-cultured *S. oneidensis* pGUT2 and *G. sulfurreducens* after approximately ~15 hours and increased exponentially over time reaching a maximum current density of ~120 $\mu A/cm^2$ after 2 days (Fig. 3.2). A current density of 120 $\mu A/cm^2$ is ~10-fold higher than is typically achieved from *S. oneidensis* reactors (with graphitic carbon as anode) and ~4-fold lower than is generally observed from *G. sulfurreducens* reactors (Kotloski et al., 2013; Levar et al., 2014). As current production only occurred when *S. oneidensis* pGUT2 and *G. sulfurreducens* were co-cultured, we next sought to determine roles of various mechanisms hypothesized to mediate interspecies electron transfer.

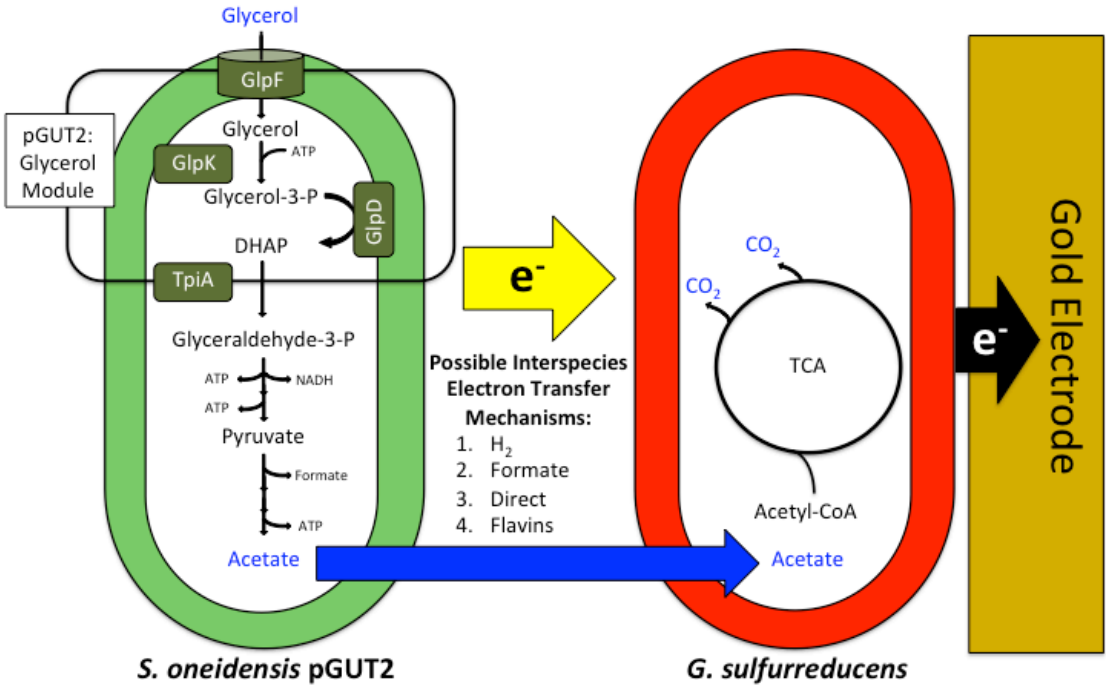

Figure 3.1: Diagram of the syntrophic co-culture of *S. oneidensis* pGUT2 and *G. sulfurreducens* in three-electrode bioreactors with gold anodes serving as terminal electron acceptor and glycerol as carbon source. Incorporation of a glycerol utilization plasmid containing *glpF*, *glpK*, *glpD*, and *tpiA*, which encode a glycerol facilitator, glycerol kinase, glycerol-3-phosphate dehydrogenase, and triosephosphate isomerase, respectively, enables *S. oneidensis* pGUT2 to catabolize glycerol and secrete acetate as a carbon source for *G. sulfurreducens* (large blue arrow). Electrons produced by *S. oneidensis* pGUT2 during glycerol oxidation must be transferred to *G. sulfurreducens* as *S. oneidensis* cannot respire gold electrodes. *G. sulfurreducens* then transfers electrons to the gold electrode. Interspecies electron transfer mechanisms tested in this system include transfer via hydrogen, formate, flavin shuttles, or direct cell-to-cell contact.

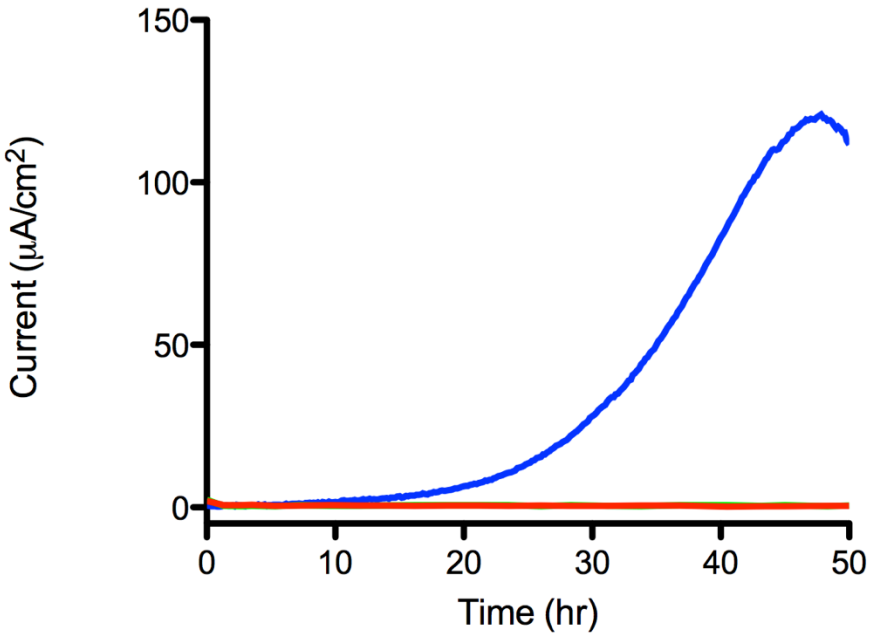

Figure 3.2: Co-cultures containing both *S. oneidensis* pGUT2 and *G. sulfurreducens* are required for current production in three-electrode bioreactors containing gold electrodes as terminal electron acceptor and 7 mM glycerol as carbon source. Current density (μA/cm^2) measured for co-cultures of *S. oneidensis* pGUT2 and *G. sulfurreducens* (blue), and *S. oneidensis* pGUT2 (green) or *G. sulfurreducens* (red) cultured alone. Gold electrodes were poised at 0.24 mV vs. SHE and representative data are shown from experiments performed in triplicate.

The majority of electron transfer to gold electrodes by *S. oneidensis* pGUT2/*G. sulfurreducens* co-cultures is mediated by flavin electron shuttles

Targeted gene deletion and gene insertion mutants were used to determine mechanisms of interspecies electron transfer utilized by the *S. oneidensis* pGUT2/*G. sulfurreducens* co-culture. Four potential mechanisms existed for interspecies electron transfer between *S. oneidensis* pGUT2 and *G. sulfurreducens* and included transfer via hydrogen, formate, flavin electron shuttles, or direct cell-to-cell contact. To eliminate interspecies electron transfer via hydrogen, *hydA* and *hyaB*, the two hydrogenases

encoded in the genome of *S. oneidensis* pGUT2 were deleted (Meshulam-Simon et al., 2007) (strain referred to as SOΔ*hyd* pGUT2). Hydrogenases are enzymes that catalyze the reversible reduction of protons to hydrogen, and deletion of *hydA* and *hyaB* have been shown to eliminate both hydrogen production and utilization by *S. oneidensis* (Meshulam-Simon et al., 2007). Co-cultured with *G. sulfurreducens*, the SOΔ*hyd* pGUT2 strain initiated current production earlier and reached a slightly higher maximum current density of ~135 μA/cm^2 as compared to *S. oneidensis* pGUT2 (Fig. 3.3), indicating that larger electron flux was directed towards the electrode by the co-culture when hydrogenases were deleted in *S. oneidensis*.

We next examined current production in co-cultures incapable of transferring electrons via formate. Formate is produced under anaerobic conditions by *S. oneidensis* when grown on carbon sources that enter central metabolism at or above the level of pyruvate through the action of pyruvate formate lyase (Flynn et al., 2012; Hunt et al., 2010; Pinchuk et al., 2011). Because formate production by *S. oneidensis* cannot be eliminated under our experimental conditions, formate utilization by *G. sulfurreducens* was eliminated by replacing the gene encoding the catalytic subunit of the formate dehydrogenase (*fdnG*) in *G. sulfurreducens* with a kanamycin resistance cassette (strain referred to as GSΔ*fdn).* Co-cultures containing GSΔ*fdn* and *S. oneidensis* pGUT2 produced current at a slower rate and to significantly lower maximum densities as compared to the original *S. oneidensis* pGUT2/*G. sulfurreducens* co-culture (Fig. 3.3). Results obtained with the GSΔ*fdn* strain are not conclusive of interspecies electron

transfer because this strain was also severely deficient in current production as compared to wild-type *G. sulfurreducens* in reactors containing acetate (data not shown), indicating that diminished current was due to strain defects and not necessarily due to hampered interspecies electron transfer. A new *fdnG*::Km gene insertion mutant has been constructed in *G. sulfurreducens* to conduct further co-culture experiments.

To determine the role of flavins as mediators during interspecies electron transfer, flavin secretion was eliminated in *S. oneidensis* by deleting the flavin exporter *bfe* (strain referred to as SOΔ*bfe*). Bfe transports flavin adenine dinucleotide (FAD) across the cytoplasmic membrane where it is then cleaved to flavin mononucleotide (FMN) and adenosine monophosphate (AMP) through the activity of UshA (Covington et al, 2010; Kotloski & Gralnick, 2013). FMN excreted from the cell can then act as an electron shuttle and has been shown to increase reduction of insoluble terminal electron acceptors by *S. oneidensis* (Kotloski & Gralnick, 2013). Current production was significantly diminished in co-cultures containing SOΔ*bfe* and *G. sulfurreducens* reaching a maximum density of only ~25 μA/cm^2, and the population crashed after 24 hours (Fig. 3.3). Co-culture results with the SOΔ*bfe* strain indicated that approximately 80% of current produced by the original *S. oneidensis* pGUT2/*G. sulfurreducens* was due to flavin-mediated electron transfer, which is a similar percentage attributed to flavin-mediated respiration of other insoluble electron acceptors by single *S. oneidensis* cultures (Kotloski & Gralnick, 2013; Marsili et al., 2008). To determine if current density could be restored, 1 μM of exogenous FMN was added to co-culture reactors containing

SOΔ*bfe* and *G. sulfurreducens*. Addition of 1 μM FMN resulted in a maximum current density of ~100 μA/cm^2 and current production was initiated much sooner than in the original *S. oneidensis* pGUT2/*G.sulfurreducens* co-culture (Fig. 3.3). Addition of 1 μM exogenous FMN did not fully restore current density in the SOΔ*bfe*/*G. sulfurreducens* co-culture to levels achieved by the original *S. oneidensis* pGUT2/*G.sulfurreducens* co-culture (~100 μA/cm^2 vs ~120 μA/cm^2). It is possible that higher concentrations of FMN are needed to fully restore maximum current density in SOΔ*bfe*/*G. sulfurreducens* co-cultures.

To further test the hypothesis that flavins could mediate interspecies electron transfer between *Shewanella* and *Geobacter*, we conducted experiments to test the ability of *G. sulfurreducens* to utilize FMN during extracellular respiration. To monitor rates of respiration by *G. sulfurreducens* in the presence and absence of flavins, *G. sulfurreducens* was cultured alone in NB medium containing 50 mM Fe(III) as ferrihydrite and 20 mM acetate with and without the addition of 10 μM FMN. Fe(III) respiration was then measured as the production of the reduced species Fe(II) in medium samples. The presence of FMN in *G. sulfurreducens* cultures significantly increased the respiration rate enabling *G. sulfurreducens* to fully reduce supplied ferrihydrite after ~175 hours. In contrast, after ~175 hours, wild-type *G. sulfurreducens* without FMN was only able to reduce ~13 mM ferrihydrite (Fig. 3.4). Increased respiratory rates of *G. sulfurreducens* in the presence of FMN, the flavin moiety secreted by *Shewanella*, further

supports evidence that flavins can mediate interspecies electron transfer in *S. oneidensis* pGUT2/*G. sulfurreducens* co-cultures.

Strong evidence has also emerged recently that interspecies electron transfer can occur through direct cell-to-cell contact likely mediated through mutiheme cytochromes and/or pili (McGlynn et al., 2015; Summers et al., 2010; Wegener et al., 2015). Direct electron transfer mechanisms pose a challenge to laboratory models, as many of the components mediating direct electron transfer also affect mechanisms for associating with other community members (i.e. pili mediating attachment to other cells). Our system faces similar challenges. Extracellular electron transfer by *S. oneidensis* to insoluble acceptors such as electrodes occurs via a multiheme cytochrome/porin complex collectively referred to as the Mtr pathway (Beliaev & Saffarini, 1998; Beliaev et al., 2001; Bretschger et al., 2007; Coursolle et al., 2010; Hartshorne et al., 2009; Marritt et al., 2012). If *S. oneidensis* is capable of direct interspecies electron transfer, it would be predicted to also occur via the Mtr pathway, but this cannot be tested separately from flavin-mediated interspecies electron transfer as the Mtr pathway is also required to reduce flavins (Coursolle et al., 2010). To circuitously test the possibility of a direct mechanism of interspecies electron transfer between *S. oneidensis* pGUT2 and *G.* sulfurreducens, the mechanisms for hydrogen, formate, and flavin mediated electron transfer were eliminated. Both hydrogenases and the flavin exporter were deleted from *S. oneidensis* (strain referred to as SOΔ*hyd*Δ*bfe* pGUT2) and co-cultured with the strain of *G. sulfurreducens* unable to utilize formate, GSΔ*fdn*. Maximum current density was

significantly diminished in the SOΔ*hyd*Δ*bfe* pGUT2/ GSΔ*fdn* co-culture reaching only ~8 μA/cm^2 after 2 days (Fig. 3.3). While ~8 μA/cm^2 is significantly less than produced by the original *S. oneidensis* pGUT2/*G. sulfurreducens* co-culture, production of any current by the SOΔ*hyd*Δ*bfe* pGUT2/ GSΔ*fdn* co-culture may indicate a small portion of interspecies electron transfer mediated by a direct cell-to-cell mechanism. Further information on direct cell-to-cell transport mechanisms in other syntrophic co-cultures may highlight other systems to target in order to test this hypothesis.

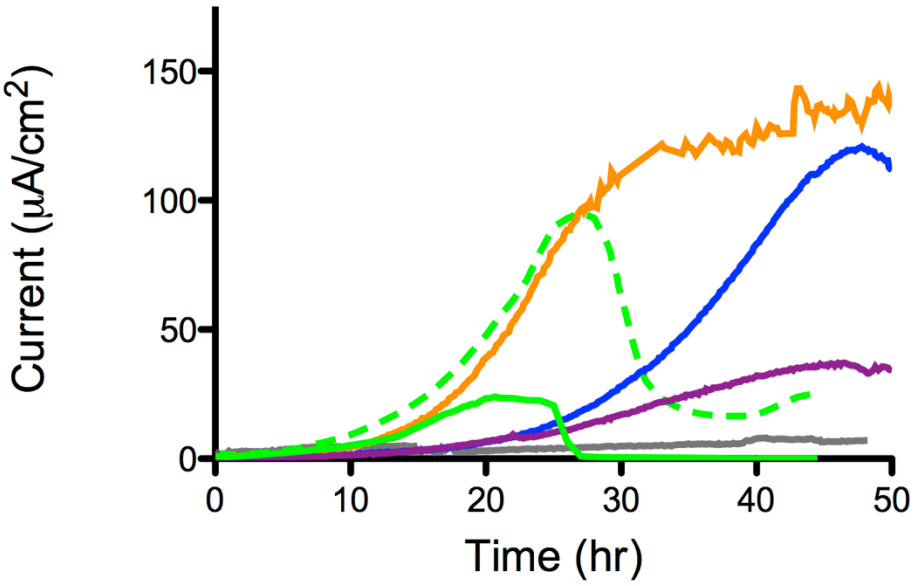

Figure 3.3: Interspecies electron transfer is dominated by flavin electron shuttles in obligate co-cultures of *S. oneidensis* pGUT2 and *G. sulfurreducens* in three-electrode bioreactors with gold anodes and 7 mM glycerol. Current density (μA/cm^2) measured for co-cultures of *S. oneidensis* pGUT2 and *G. sulfurreducens* (blue), SOΔ*hyd* pGUT2 and *G. sulfurreducens* (orange), *S. oneidensis* pGUT2 and GSΔ*fdn* (purple), SOΔ*bfe* pGUT2 and *G. sulfurreducens* (solid green), SOΔ*hyd*Δ*bfe* pGUT2 and GSΔ*fdn* (grey). The dashed green line represents current density measured for the SOΔ*bfe* pGUT2 and *G. sulfurreducens* co-culture in the presence of 1 μM exogenous FMN. Gold electrodes were poised at 0.24 mV vs. SHE and representative data are shown from duplicate experiments.

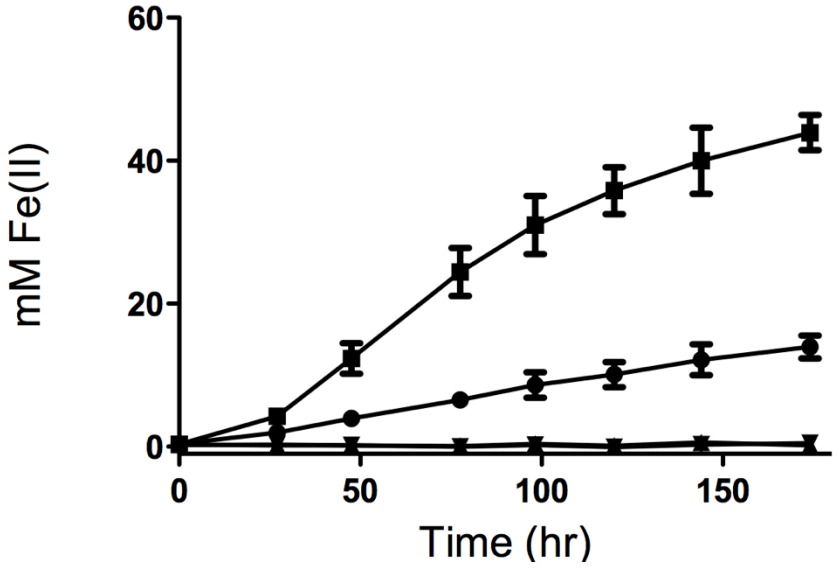

Figure 3.4: *G. sulfurreducens* utilizes FMN as an electron shuttle. Fe(III) respiration by *G. sulfurreducens* cultures in the presence (squares) or absence (circles) of 10 μM FMN measured as the production of Fe(II) over time in NB medium containing 20 mM acetate and 50 mM ferrihydrite. Abiotic medium controls are also included in the presence (inverted triangles) or absence (triangles) of FMN. Data represent the mean of experiments performed in triplicate with error bars representing standard error.

Conclusions and Future Directions

We have provided strong evidence that flavins mediate interspecies electron transfer in co-cultures of *S. oneidensis* pGUT2 and *G. sulfurreducens* in three-electrode bioreactors containing a gold electrode as terminal electron acceptor and glycerol as carbon source. Current is only produced in gold-electrode reactors containing glycerol when *S. oneidensis* pGUT2 and *G. sulfurreducens* are cultured together and is severely diminished when flavin transfer is eliminated (Fig 3.2 and Fig. 3.3). Exogenously supplied FMN restores current density in SOΔ*bfe* pGUT2/*G. sulfurreducens* to levels near that of the original *S. oneidensis* pGUT2/*G. sulfurreducens* co-culture (Fig. 3.3). We have also shown that *G. sulfurreducens* can utilize FMN as a redox shuttle, as FMN addition increased respiration of ferrihydrite by *G. sulfurreducens* (Fig. 3.4). Further

experiments are warranted to substantiate conclusions regarding interspecies electron transfer mechanisms between *S. oneidensis* pGUT2 and *G. sulfurreducens* as many of the reactor experiments have only been performed in duplicate. Also, experiments utilizing the GSΔ*fdn* strain must be conducted again as the strain itself was defective as compared to wild-type *G. sulfurreducens* for either biofilm formation or extracellular respiration of electrodes. A new GSΔ*fdn* strain has been constructed.

The interdependence and hypothesized direction of electron flow from *S. oneidensis* pGUT2 to *G. sulfurreducens* and finally to the gold electrode leads us also to hypothesize that spatial structure may play a role mediating cooperation in co-culture reactors. To study spatial arrangement of *S. oneidensis* and *G. sulfurreducens* we will image future electrode-attached biofilms using confocal microscopy. The *S. oneidensis* pGUT2 strain contains a chromosomal insertion of *gfpmut3** enabling imaging. Biofilm communities will be fixed in glutaraldehyde and counterstained using DAPI. Blue and green image channels from confocal microscopy will be merged to determine localization of *S. oneidensis* pGUT2 and *G. sulfurreducens* on gold electrodes.

The engineered syntrophic community using *S. oneidensis* pGUT2 and *G. sulfurreducens* has a multitude of applications beyond the study of interspecies electron transfer. In its current form, the *S.* oneidensis pGUT2/*G. sulfurreducens* co-culture enables the conversion of glycerol, a waste product of biodiesel production, to the generation of current using microbial fuel cell systems. Further, because we engineered the community using *Shewanella* and *Geobacter*, we have a co-culture composed of

organisms with defined genetic backgrounds and full genetic systems. As such, the *S. oneidensis* pGUT2/*G. sulfurreducens* co-culture can serve as a chassis community that can be further engineered to incorporate additional strains or genetic modules for biotechnology applications requiring bacteria interfaced with electrodes. For example, both *S. oneidensis* and *G. sulfurreducens* have garnered interest for use in electrosynthesis applications, a process where electrodes in bioreactors serve as electron donors instead of as terminal electron acceptors. Electrodes serving as electron donors drive current into biofilms that can be used as the reductive power to generate C-C bonds making this process applicable to biofuel and bio-product synthesis. *S. oneidensis* is an attractive model organism for electrosynthesis due to its amenable genetic system, clearly defined electron transport pathways, and its trophic level placement over complete oxidizers like *Geobacter* (i.e. secretion of acetate (2C) instead of CO_2). *G. sulfurreducens* is of interest to electrosynthesis applications as it produces robust, thick biofilms and nearly 40-fold higher current density than *S. oneidensis*, yet the exact pathway(s) for electron transfer in *G. sulfurreducens* have not been fully elucidated (Levar et al., 2014). An engineered co-culture designed to interface with electrodes enables exploitation of the benefits provided by each strain overcoming many of their inherent limitations.

Acknowledgements

I would like to thank Caleb Levar for conducting the iron reduction experiment shown in Figure 3.4.

Strain/Plasmid	Description	Reference
***Escherichia coli* strain UQ950**	DH5α host for cloning: F-*(argF-lac)169 80dlacZ58(*M15*) glnV44(*AS*) rfbD1 gyrA96(*NalR*) recA1 endA1 spoT1 thi-1 hsdR17 deoR pir+*	(Saltikov & Newman, 2003)
***Escherichia coli* strain WM3064**	DAP auxotroph used for conjugation: *thrB1*004 *pro thi rpsL hsdS lacZM15* RP4-1360 *(araBAD)567 dapA*1341::[*erm pir(wt)*]	(Saltikov & Newman, 2003)
***Shewanella oneidensis* strain MR-1**	Wild type	(Venkateswaran et al., 1999)
***Shewanella oneidensis* pGUT2**	*Shewanella* with a chromosomal insertion of *gfpmut3** containing the glycerol utilization plasmid	**This Study**
SOΔ*hyd* pGUT2	*Shewanella* with a chromosomal insertion of *gfpmut3** containing the glycerol utilization plasmid; Δ*hydA*Δ*hyaB*	**This Study**
SOΔ*bfe* pGUT2	*Shewanella* with a chromosomal insertion of *gfpmut3** containing the glycerol utilization plasmid; Δ*bfe*	**This Study**
SOΔ*hyd*Δ*bfe* pGUT2	*Shewanella* with a chromosomal insertion of *gfpmut3** containing the glycerol utilization plasmid; Δ*hydA*Δ*hyaB*Δ*bfe*	**This Study**
***Geobacter sulfurreducens* strain PCA**	Wild type	(Caccavo et al., 1994)
GSΔ*fdn*	*G. sulfurreducens* Δ*fdnG::Km*^{R}	**This Study**
pSMV3	9.1-kb suicide vector; *oriR6K mobRP4, sacB, Km*^{r}*, Ap*^{r}	(Coursolle & Gralnick, 2010)
pBBR1mcs-2	5.0-kb broad-host-range vector for cloning; *Km*^{r}	(Kovach et al., 1995)
pGUT2	pBBR1MCS-2 containing *glpD, glpF, glpK*, and *tpiA*	(Flynn et al., 2010)
pAK1	Gene knock-in construct targeting 7-bp downstream of the *glmS* gene	**This Study**
pAK2	pAK1 containing Plac$_{A1/O4/O3}$ *gfpmut3**	**This Study**

Table 3.1: Strains and plasmids utilized in this study.

Primer Name	DNA Sequence (5' to 3') or Reference
Primers used to delete *hydA*	
Hyd_Up_F	GCATgggcccGCATTATCAATTCACCATAAACCC
Hyd_Up_R	GCATactagtATTAATCTTGATCAGCCC
Hyd_Dn_F	GCATactagtGTGAAATCAGCCTCTGTC
Hyd_Dn_R	GCATgagctcTTTTGCTAGGCTGTCGTCCTTG
Primers used to delete *hyaB*	
Hya_Up_F	GCATgggcccGTGGCCGTTTTGATGCAG
Hya_Up_R	GCATactagtTTTCAGTATGACTTCAATACC
Hya_Dn_F	GCATactagtGATGCTGTCAATGCCCTG
Hya_Dn_R	GCATgagctcATGCGGGTTTCAGAATGG
Primers used to delete *bfe*	(Kotloski & Gralnick, 2013)
Primers used to generate the *fdnG::Km^r* fragment	
Kan_F	AAGCGAACCGGAATTGCCAGCT
Kan_R	TCAGAAGAACTCGTCAAGAAGG
GSU0777KP1	GACCCGCTTGAGCACTTCG
GSU0777KP2	AGCTGGCAATTCCGGTTCGCTTTACATCCCCCTTAGGTGTCAG
GSU0777KP3	GCCTTCTTGACGAGTTCTTCTGAGACAGCGGCAACGTCCTG
GSU0777KP4	GCGGGATCGAGGCCGTTC

Table 3.2: Primers used in this study.

Chapter 4 : Formate Metabolism in Shewanella oneidensis Generates Proton Motive Force and Prevents Growth Without an Electron Acceptor

Summary

Shewanella oneidensis strain MR-1 is a facultative anaerobe that thrives in redox-stratified environments due to its ability utilize to a wide array of terminal electron acceptors. Conversely, electron donors utilized by *S. oneidensis* are more limited and include products of primary fermentation such as lactate, pyruvate, formate, and hydrogen. Lactate, pyruvate, and hydrogen metabolism in *S. oneidensis* have been described previously, but little is known about the role of formate oxidation in the ecophysiology of these bacteria. Formate is produced by *S. oneidensis* by pyruvate formate lyase during anaerobic growth on carbon sources that enter metabolism at or above the level of pyruvate, and the genome contains three gene clusters predicted to encode three complete formate dehydrogenase complexes. To determine the contribution of each complex to formate metabolism, strains lacking one, two, or all three annotated formate dehydrogenase gene clusters were generated and examined for growth rate and yield on a variety of carbon sources. Here, we report that formate oxidation contributes both to growth rate and yield of *S. oneidensis* through the generation of proton motive force. Exogenous formate also greatly accelerated growth on N-acetylglucosamine, a carbon source normally utilized very slowly by *S. oneidensis* under anaerobic conditions. Surprisingly, deletion of all three formate dehydrogenase gene clusters enabled growth of *S. oneidensis* using pyruvate in the absence of a terminal electron acceptor – a mode of growth never before observed in these bacteria. Our results demonstrate that formate

oxidation is a fundamental strategy under anaerobic conditions for energy conservation in *S. oneidensis*.

Importance

Shewanella have garnered interest in biotechnology due to an ability to respire extracellular terminal electron acceptors such as insoluble metals and electrodes. Much effort has gone into studying proteins required for extracellular respiration, but how electrons enter this pathway from oxidative metabolism remains understudied. Here, we quantify the role of formate oxidation in *Shewanella oneidensis* anaerobic physiology. Formate oxidation contributes to growth rate and yield of *S. oneidensis* on a variety of carbon sources by generating proton motive force. We also demonstrate growth of *Shewanella* on pyruvate without a terminal electron acceptor when all formate dehydrogenase gene clusters are deleted. Advances in understanding *S. oneidensis* anaerobic metabolism are important for its use and engineering applications in bioenergy, biocatalysis and bioremediation.

Introduction

Shewanella oneidensis (hereafter referred to as MR-1) is a model environmental bacterium that thrives in redox-stratified environments due to its ability to couple the oxidation of organic carbon or hydrogen to a diverse array of terminal electron acceptors (Fredrickson et al., 2008; Hau & Gralnick, 2007; Nealson & Scott, 2006). Electron acceptors utilized by MR-1 range from soluble organics such as fumarate to insoluble

extracellular metal oxides and electrodes (Nealson & Scott, 2006). The respiratory diversity of MR-1 has led to its use in a number of promising applications in biotechnology, and because of this, extracellular electron transfer by MR-1 has been well studied (Fredrickson et al., 2008; Hau & Gralnick, 2007). Electrons produced by MR-1 during anaerobic metabolism drive reduction of the quinone pool and are subsequently transferred to the inner membrane-anchored *c*-type cytochrome CymA (Marritt et al., 2012). CymA serves as a central hub in the inner membrane from which electrons can be transferred to multiple terminal electron acceptors such as FccA during fumarate respiration (Fig. 4.1A) or a multi-subunit porin-cytochrome complex collectively termed the Mtr pathway during extracellular respiration (Beliaev & Saffarini, 1998; Beliaev et al., 2001; Hartshorne et al., 2009; Marritt et al., 2012; Myers & Myers, 2000). This elegant system of electron transport in MR-1 is dependent on the generation of electrons from the oxidation of organic carbon sources, yet how electrons flow from organic carbon to these respiratory pathways has been understudied. Moreover, quinone cycling by the CymA redox loop facilitates not only electron transfer but should, under some conditions, contribute to the generation of proton motive force (PMF) through the translocation of protons across the inner membrane (Marritt et al., 2012; Simon et al., 2008). A better understanding of how *Shewanella* gains energy from the oxidation of organic carbon is imperative to facilitate rational engineering for applications in biotechnology, bioremediation, and synthetic biology.

In anoxic environments, MR-1 oxidizes lactate, pyruvate, formate, hydrogen, and some amino acids for anaerobic respiration, likely forming syntrophic partnerships with fermentative microorganisms (Nealson & Scott, 2006). The underlying physiology of lactate, pyruvate and hydrogen utilization has been described (Brutinel & Gralnick, 2012; Meshulam-Simon et al., 2007; Pinchuk et al., 2009), but little is known about the role of formate in MR-1. Formate oxidation has been linked to the reduction of a variety of metals and azo dyes using *in vitro* assays (Carpentier et al., 2003; De Windt et al., 2006; Hong & Gu, 2010; Myers et al., 2000; Ruebush et al., 2006), and formate is the only carbon compound shown to elicit a chemotactic response by MR-1 (Nealson et al., 1995). Formate oxidation likely plays a significant role in energy conservation in MR-1 by providing the thermodynamic driving force required for reduction of CymA by the menaquinol pool and subsequent translocation of protons across the cytoplasmic membrane (Marritt et al., 2012; Simon et al., 2008).

Formate is critical for metabolism of many facultative anaerobic microorganisms. A prominent fermentation product of many obligate and facultative anaerobes, secretion of formate facilitates internal redox balancing during mixed acid fermentation. Formate secretion is pronounced in the Enterobacteriaceae, accounting for up to a third of the carbon secreted from fermented sugar substrates (Leonhartsberger et al., 2002). Due to the relatively low redox potential (-420 mV at pH 7.0), formate also serves as an important energy source for many microorganisms during aerobic or anaerobic respiration. The oxidation of formate (CHOO- at pH 7.0) results in the generation of two

reducing equivalents, a proton, and a molecule of carbon dioxide, and is typically carried out by a formate dehydrogenase (FDH) complex in the cytoplasmic membrane (Jormakka et al., 2002). Oxidation occurs in the periplasm to avoid acidification of the cytoplasm, and electrons are transferred through the FDH complex to menaquinone along with protons from the cytoplasmic side of the inner membrane (Jormakka et al., 2002). The genome of MR-1 contains gene clusters predicted to encode three complete FDH complexes and a single gene cluster predicted to encode a formate hydrogenlyase complex (FHL) (Fig. 4.1B), raising a number of questions regarding the role formate in the ecophysiology of the genus *Shewanella*. Here we demonstrate that formate, of endogenous and/or exogenous origin, contributes to the growth rate and yield of MR-1 through the generation of PMF. Notably, formate greatly accelerates anaerobic growth of MR-1 on N-acetylglucosamine (NAG) – a carbon source typically utilized slowly under anaerobic conditions. Deletion of all three FDH operons also enables anaerobic growth of *S. oneidensis* on pyruvate without the addition of a terminal electron acceptor, suggesting the existence of a feedback mechanism, or an inability to turn over reducing equivalents, which prevents MR-1 from growing when the menaquinone pool is fully reduced.

Materials and Methods

Bacterial Strains and Culture Conditions

Strains and plasmids used in this study are listed in Table 4.3. *Escherichia coli* strains used for cloning and conjugal transfer were maintained on lysogeny broth (LB) agar plates supplemented with 50 μg/mL kanamycin and/or 250 μM 2,6-diaminopimelic

acid as necessary. During routine propagation, *S. oneidensis* was maintained on LB agar containing 50 μg/mL kanamycin as necessary. For growth assays, strains were grown in *Shewanella* basal medium containing 5 mL/L vitamin mix, 5 mL/L mineral mix (Hau & Gralnick, 2007), and 0.05% casamino acids (hereafter referred to as SBM) supplemented with lactate, pyruvate, NAG, formate, and/or fumarate when indicated. Growth assays were performed as follows. Strains stored in 15% glycerol at -80°C were freshly streaked onto LB agar plates and incubated for ~16h at 30°C. Single colonies were used to inoculate LB medium shaken at 250 rpm at 30°C for 6-8 hours and were then sub-cultured in aerobic SBM shaken for ~16 hours at 30°C. Cells were then washed twice and added to Balch tubes stoppered with butyl rubber containing an argon headspace to a final optical density of ~0.02 (OD_{600}) (Balch & Wolfe, 1976).

Reagents and Materials

Enzymes were purchased from New England Biolabs (Ipswich, MA). Kits for gel purification and plasmid mini preps were purchased from Invitrogen (Carlsbad, CA). All related reactions were carried out according to manufacturer instructions. Media components were purchased from Becton, Dickinson and Company (Sparks, MD), and chemicals were purchased Sigma-Aldrich (St. Louis, MO).

Generation of Deletion Mutants

Oligonucleotide primers used to amplify portions of the MR-1 chromosome for deletion constructs are listed in Table 4.4. PCR products were cloned using standard laboratory molecular biology protocols. Regions flanking deletion targets were amplified

using PCR and cloned into the pSMV3 suicide vector. In-frame gene deletions were generated using homologous recombination as previously described (Coursolle et al., 2010). Deletion constructs were moved *into S. oneidensis* by conjugal transfer from *E. coli* donor strain WM3064. All plasmid constructs and gene deletions were verified by sequencing (University of Minnesota Genomics Center).

High Performance Liquid Chromatography

Metabolites were quantified by HPLC using Shimadzu Scientific equipment including an SCL-10A system controller, LC-10AT pump, SIL-10AF auto-injector, CTO-10A column oven, RID-10A refractive index detector, and an SPD-10A UV-Vis detector. Mobile phase consisted of 15 mN H_2SO_4 set at a flow rate of 0.400 mL min^{-1}. Injection volumes of 50 μL were separated on an Aminex HPX-87H column maintained at 30°C.

Sequence Analysis

Homologs of the FDH alpha subunits SO4509 and SO4513 were identified for other members of the Shewanellaceae via BLAST (http://blast.ncbi.nlm.nih.gov) and a gene bidirectional best-hit search using the JGI database (www.img.jgi.doe.gov). Resulting coding regions were aligned via Muscle (Edgar, 2004) and evolutionary analyses were conducted in MEGA6 (Tamura et al., 2013). From this alignment, a bootstrapped maximum likelihood (300 replicates) tree based on the General Time Reversible model was constructed using MEGA6 (Felsenstein, 1985; Nei & Kumar, 2000). Initial trees for the heuristic search were obtained automatically by applying

Neighbor-Join and BioNJ algorithms to a matrix of pairwise distances estimated using the Maximum Composite Likelihood (MCL) approach, and then selecting the topology with superior log likelihood value. A discrete Gamma distribution was used to model evolutionary rate differences among sites (5 categories (+G, parameter = 0.8571)). The rate variation model allowed for some sites to be evolutionarily invariable ([+I], 34.8331% sites). The analysis involved 87 nucleotide sequences. Codon positions included were 1st+2nd+3rd+Noncoding. All positions with less than 95% site coverage were eliminated. That is, fewer than 5% alignment gaps, missing data, and ambiguous bases were allowed at any position. There were 2842 positions in the final dataset.

Results

The chromosome of MR-1 contains multiple gene regions predicted to encode proteins involved in formate metabolism including three putative FDH complexes. Region SO0101-0103 is annotated as *fdnGHI*, a predicted nitrate inducible FDH similar to the canonical Fdh-N in *E. coli* (Fig. 4.1B). Gene regions SO4508-4511 and SO4512-4515 are annotated as *fdhXABC*, and are predicted to encode two individual, but related FDH complexes similar to Fdh-O of *E. coli* (Fig. 4.1B). FdhX is a member of an uncharacterized protein family and may be a small subunit or accessory protein of FDH, while the *fdhABC* genes encode the α, β, and γ subunits of FDH, respectively. A putative FHL complex is also predicted as part of the *hyd* locus (SO3920-3926) though SO3922 is annotated as a γ subunit and does not contain the catalytic component required to oxidize formate (Fig. 4.1B). The catalytic domain required for FHL may be encoded by an

orphan α subunit encoded by SO0988 (Fig. 4.1B). Interestingly, SO0988 does not encode a twin-arginine translocation pathway signal sequence and is therefore predicted to be cytoplasmic. Domain analysis indicates that the N-terminal portion of the protein encoded by SO0988 is predicted to contain multiple Fe-S cluster domains while the latter half is 58% similar at the amino acid level to Fdh-H, the catalytic subunit of the *E. coli* FHL complex. The MR-1 genome also contains a predicted bidirectional formate transporter FocA encoded by SO2911 directly upstream of the regions encoding pyruvate formate lyase (PflB) and its activating enzyme PflA (Fig. 4.1B). The preponderance of FDH gene clusters encoded in the MR-1 genome is unusual and warranted additional investigation regarding their phylogeny and dispersal across other sequenced *Shewanella*.

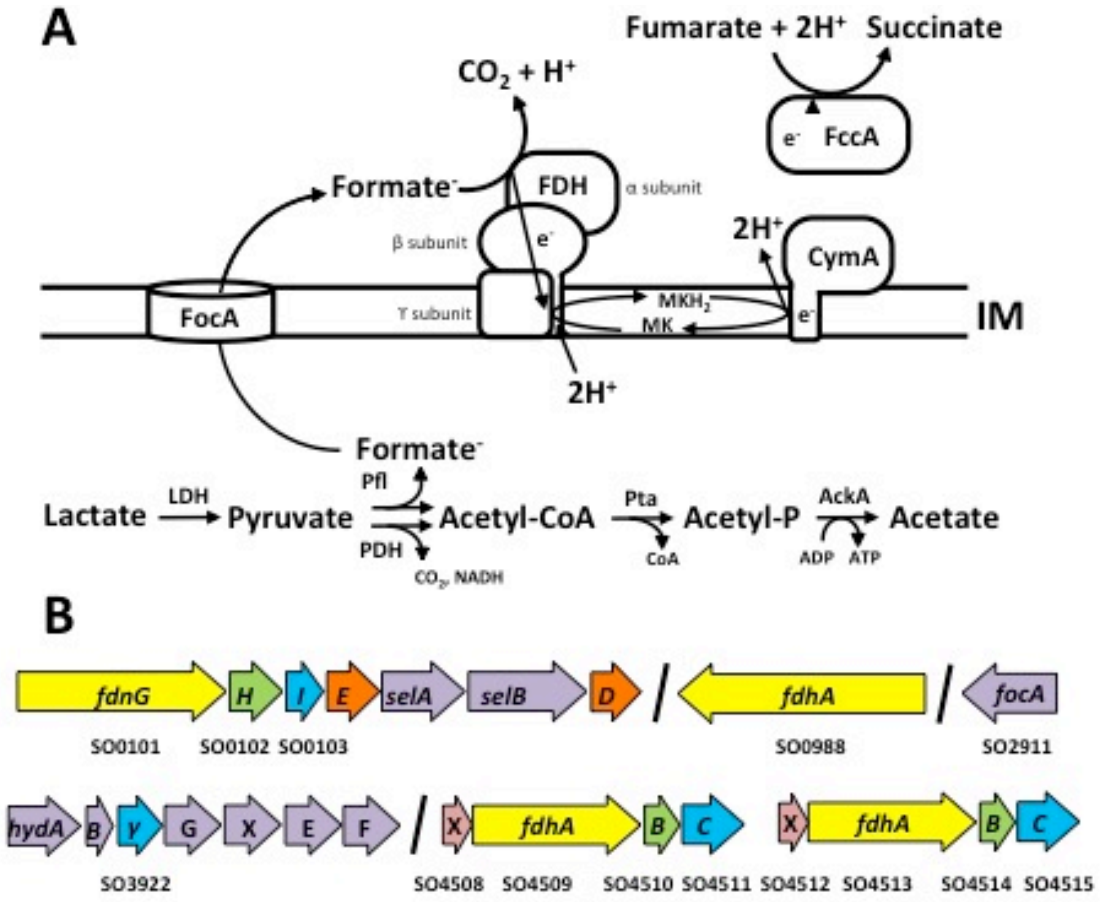

Figure 4.1:Formate metabolism pathway and genetic loci in *Shewanella oneidensis.* (A) Anaerobic formate metabolism in *S. oneidensis* MR-1. Model depicts oxidation of lactate (or pyruvate) as the sole carbon and energy source coupled to reduction of fumarate via the periplasmic fumarate reductase FccA. (B) Genomic organization of genes directly involved in formate metabolism in MR-1. Genes encoding the α-, β-, and γ-subunit of an FDH complex are colored yellow, green, and blue, respectively. Genes *fdhX*, which encode small proteins of unknown function are colored pink. Accessory genes involved in FDH complex maturation are colored orange and genes involved in cofactor maturation (*selAB*), formate transport (*focA*), and the putative formate hydrogenlyase (*hydAB*) are colored purple.

Phylogenetic Analysis of FdhA Across the *Shewanellaceae*

The tandem *fdhXABC* gene clusters (SO4508-4511 and SO4512-4513) in MR-1 have arisen from a gene duplication event, sharing 68% identity at the nucleotide level over the entire length. At the amino acid level, the FdhX pairs are 46% identical (57% similar), FdhA pairs are 74% identical (85% similar), FdhB pairs are 88% identical (94%

similar), and the FdhC pairs are 54% identical (70% similar). To look further into the history of the duplicated FDH region, a phylogenetic tree was created using *fdhA* nucleotide sequences (aligned by codons) for all sequenced *Shewanella* available in the JGI database (img.jgi.doe.gov). *fdhA* was chosen for phylogenetic analysis because it encodes the catalytic subunit of the FDH complex, and it is also the largest gene in the operon (~ 3kb) providing the most information on sequence divergence. The resulting tree outlining the phylogenetic lineage of the *fdhA* sequences results in three main clades (highlighted in blue, green, and red text in Fig. 4.2). Clades highlighted in blue and green represent the initial duplication of the FDH region, which appears to have arisen in a common ancestor predating the current speciation of the *Shewanella* genus (Fig. 4.2). In all species containing the duplication, *fdhA* sequences associated with the upstream FDH operon comprise a single clade (blue) while *fdhA* sequences associated with the downstream FDH operon comprise another (green), but the branching pattern cannot resolve which gene cluster came first. Unlike the majority of *Shewanella* species, *S. frigidimarina* contains a single FDH operon. The placement of *S. frigidimarina* within a clade subsequent to the original duplication suggests its FDH region was once duplicated and has since been lost (Fig. 4.2). Phylogenetic analysis also highlighted a small subset of species, which includes *S. halifaxensis*, *S. pealeana*, *S. waxsmanii*, and *S. fidelis* (red text), indicating a second duplication event resulting in three copies of the FDH gene cluster in these species (Fig. 4.2). Overall, phylogenetic analysis highlights selection for maintenance of multiple regions involved in formate oxidation in the *Shewanella* genus.

Figure 4.2: Phylogenetic analysis of FdhA across the Shewanellaceae. Duplication of FDH regions are separated by clades in either blue or green text. Species containing a triplication of the FDH region are highlighted in red. *S. frigidimarina*, which appears to have lost the duplicated region, is in black text. Evolutionary history was inferred using Maximum Likelihood (300 bootstrap replications) based on the General Time Reversible model. The tree is drawn to scale with the scale bar representing substitutions per site. The analysis involved 87 nucleotide sequences. There were a total of 2842 positions in the final dataset. Evolutionary analyses were conducted in MEGA6 (Tamura et al., 2013).

Oxidation of endogenously generated formate increases the growth rate and yield of MR-1 during anaerobic respiration

MR-1 produces formate when growing anaerobically on substrates that enter central metabolism at or above the level of pyruvate through the action of pyruvate formate-lyase (PFL), an enzyme required for growth under anaerobic conditions with lactate and fumarate (Fig. 4.1A) (Flynn et al., 2012; Hunt et al., 2010; Pinchuk et al., 2011). Despite obligatory generation, formate does not accumulate in MR-1 culture supernatants, suggesting oxidation by one or more FDH complexes(Hunt et al., 2010; Pinchuk et al., 2011). To determine the contribution of each FDH complex to formate oxidation we generated stains lacking one, two, or all three regions encoding the α, β, and γ subunits of each of the three annotated FDH clusters (ΔSO0101-0103, ΔSO4509-4511, or ΔSO4513-4515; see Fig. 4.1B).

To determine the physiological significance of formate oxidation, we examined the growth rate and yield of MR-1 and a strain with all three FDH gene clusters deleted (Δ*fdh*) in liquid culture. Strains were grown in SBM (see Materials and Methods) containing either 20 mM lactate or 20 mM pyruvate under an argon atmosphere supplemented with 40 mM fumarate. Growth in the presence of oxygen, where formate is not generated, was indistinguishable for both strains (data not shown). In contrast, when grown anaerobically with fumarate, the Δ*fdh* mutant grew slightly slower and generated less biomass than MR-1 both on lactate and pyruvate (Fig. 4.3). Under anaerobic conditions using fumarate as the electron acceptor, the generation time and final culture

density of MR-1 was comparable when grown on pyruvate (1.41 ± 0.04 hours and 0.37 ± 0.00 OD_{600}) as compared to lactate (1.34 ± 0.07 hours and 0.40 ± 0.01 OD_{600}) indicating that the oxidation of lactate to pyruvate during carbon metabolism in MR-1 does not appreciably contribute to growth rate or yield (Fig. 4.3). The oxidation of lactate to pyruvate by MR-1 occurs by way of two lactate dehydrogenases specific for either the D or L isomer (Brutinel & Gralnick, 2012; Chai et al., 2009; Pinchuk et al., 2009). While a reduced menaquinol is likely generated, the difference in redox potential between the lactate/pyruvate redox couple and the fumarate/succinate redox couple is small (-190 mV and 30 mV, respectively) and likely does not support energy conservation.

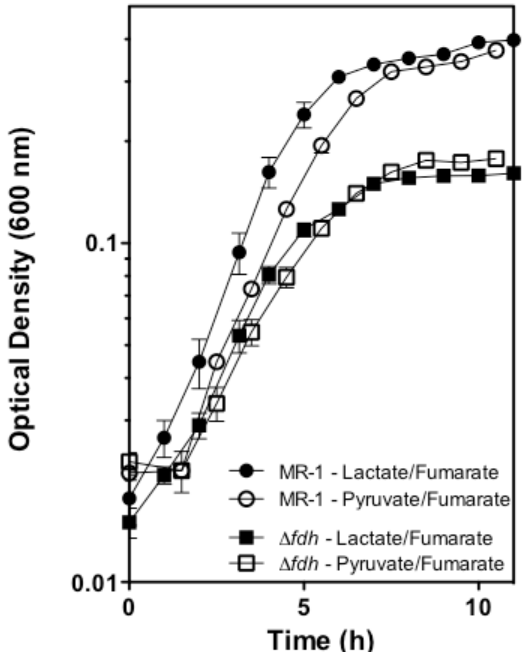

Figure 4.3: Formate oxidation contributes to growth rate and yield of MR-1. Growth curves of MR-1 (circles) and the Δ*fdh* triple mutant (squares) were performed in anoxic SBM with 20 mM lactate (closed symbols) or 20 mM pyruvate (open symbols), and 40 mM fumarate. Reported values are the average of three independent experiments and error bars represent standard error of the mean (SEM).

During anaerobic growth on lactate and fumarate (Fig. 4.1A), MR-1 catalyzed nearly stoichiometric conversion of lactate to acetate and coupled oxidation of each lactate molecule to the reduction of two molecules of fumarate (Table 4.1). MR-1 utilizes the majority of carbon for energy generation with very little being diverted to produce biomass. As had been observed previously (Pinchuk et al., 2011), formate did not accumulate in MR-1 cultures (Table 4.1). Conversely, the Δ*fdh* strain was predicted to couple lactate oxidation to fumarate reduction in a 1:1 ratio as two reducing equivalents remain with non-oxidized formate (Fig. 4.1A). The Δ*fdh* strain converted approximately 90% of the lactate linked to acetate formation to the generation of pyruvate and formate; however, the ratio of fumarate reduced was slightly higher than the stoichiometric ratio expected (Table 4.1). To determine if oxidation of pyruvate by the enzyme pyruvate dehydrogenase (PDH) and subsequent electron flow to fumarate from NADH oxidation was occurring, the E1 decarboxylase component of the PDH complex, *aceE*, was deleted in the Δ*fdh* strain background (referred to as Δ*fdh*Δ*pdh*). The Δ*fdh*Δ*pdh* strain coupled lactate utilization to fumarate reduction at ratios nearer to the 1:1 ratio expected (Table 4.1). No difference was observed in anaerobic growth rate or yield of the Δ*fdh*Δ*pdh* strain as compared the Δ*fdh* mutant (data not shown).

	20 mM Lactate/40 mM Fumarate			20 mM Pyruvate/40 mM Fumarate		
	MR-1	**Δ*fdh***	**Δ*fdh*Δ*pdh***	**MR-1**	**Δ*fdh***	**Δ*fdh*Δ*pdh***
Lactate	-20.2 ± 0.0	-14.7 ± 0.2	-12.2 ± 0.2	ND	ND	ND
Pyruvate	0.8 ± 0.0	4.0 ± 0.1	4.0 ± 0.1	-22.2 ± 0.0	-13.0 ± 0.7	-11.4 ± 0.2
Acetate	18.0 ± 0.3	12.0 ± 0.3	9.1 ± 0.1	19.7 ± 0.2	11.8 ± 0.3	8.1 ± 0.1
Formate	ND	7.1 ± 0.2	6.4 ± 0.1	ND	5.7 ± 0.6	5.8 ± 0.0
Fumarate	-39.2 ± 0.0	-18.3 ± 0.2	-14.2 ± 0.2	-20.4 ± 0.8	-6.4 ± 2.2	-2.0 ± 0.0
Succinate	38.2 ± 0.5	18.8 ± 0.6	13.6 ± 0.2	21.3 ± 0.4	4.9 ± 0.6	2.5 ± 0.1

Table 4.1: Carbon source utilization/production (mM) following anaerobic growth in SBM containing 20 mM Lactate or Pyruvate and 40 mM fumarate. Reported concentrations are averages ± SEM from three independent experiments. ND; not detected.

Because the majority of anaerobic pyruvate disproportionation by MR-1 occurs via a lyase reaction catalyzed by PFL, the only unbalanced redox reaction associated with pyruvate metabolism is the oxidation of formate (Fig. 4.1A). Therefore during anaerobic growth with pyruvate and fumarate, MR-1 couples each molecule of pyruvate converted to acetate to one molecule of fumarate reduced to succinate (Table 4.1). Since Δ*fdh* cannot oxidize formate, it was predicted to convert pyruvate to formate and acetate with no subsequent reduction of fumarate (Fig. 4.1A). Contrary to predictions, formate measured in Δ*fdh* culture supernatants was only half of that of acetate produced and a significant amount of fumarate was still reduced to succinate (Table 4.1). In the Δ*fdh*Δ*pdh* strain, ratios of formate and acetate produced were closer to the 1:1 ratio expected, and reduction of fumarate to succinate was also minimized (Table 4.1). To determine if the reduced growth rate and yield of the Δ*fdh* mutant was due to

accumulation of formate in the culture medium, we repeated the experiment with the addition of 20 mM formate. The Δ*fdh* strain showed an initial lag and grew at a slightly slower rate but to similar final yield in the presence of exogenous formate (Fig. 4.4). MR-1 was unaffected and grew similarly in both the presence and absence of added formate (Fig. 4.4).

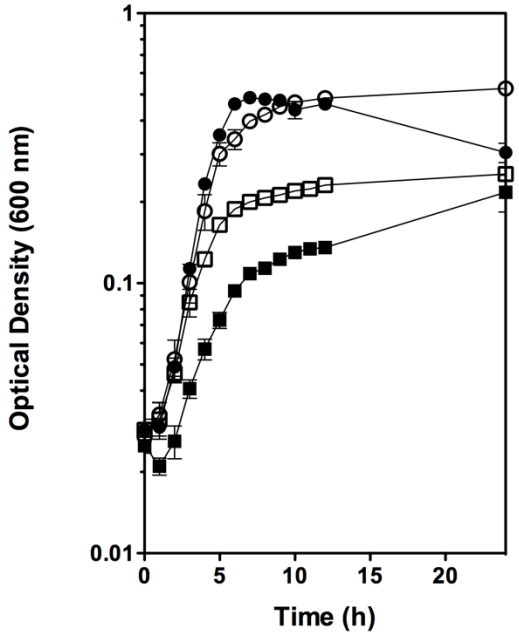

Figure 4.4: Growth of MR-1 and the Δ*fdh* triple mutant with the addition of exogenous formate. MR-1 (circles) or the Δ*fdh* triple mutant (squares) were grown in SBM with 20 mM lactate and 50 mM fumarate. Cultures were amended with 20 mM formate (closed symbols) or nothing (open symbols). Reported values are the average of at least three independent experiments and error bars represent standard error of the mean.

Oxidation of exogenous formate accelerates growth on sub-optimal carbon sources

Because the oxidation of formate clearly contributes to growth on lactate and pyruvate, we hypothesized that formate would also enhance growth on sub-optimal carbon sources. *Shewanella* spp. readily utilize NAG as the sole carbon and energy

source in the presence of oxygen (Yang et al., 2006); however, under anaerobic conditions, NAG is utilized very slowly with a generation time of 24.50 ± 0.11 hours and 37.47 ± 1.31 hours for MR-1 and the Δ*fdh* mutant, respectively (Fig. 4.5A) (Hunt et al., 2010). Augmentation of NAG grown anaerobic cultures with 20 mM formate resulted in a dramatically faster growth rate, with a generation time of 1.23 ± 0.08 hours, comparable to lactate grown cultures (Fig. 4.5A). Exogenous formate did not enhance the growth rate of Δ*fdh* on NAG, but rather arrested growth prematurely (Fig. 4.5A).

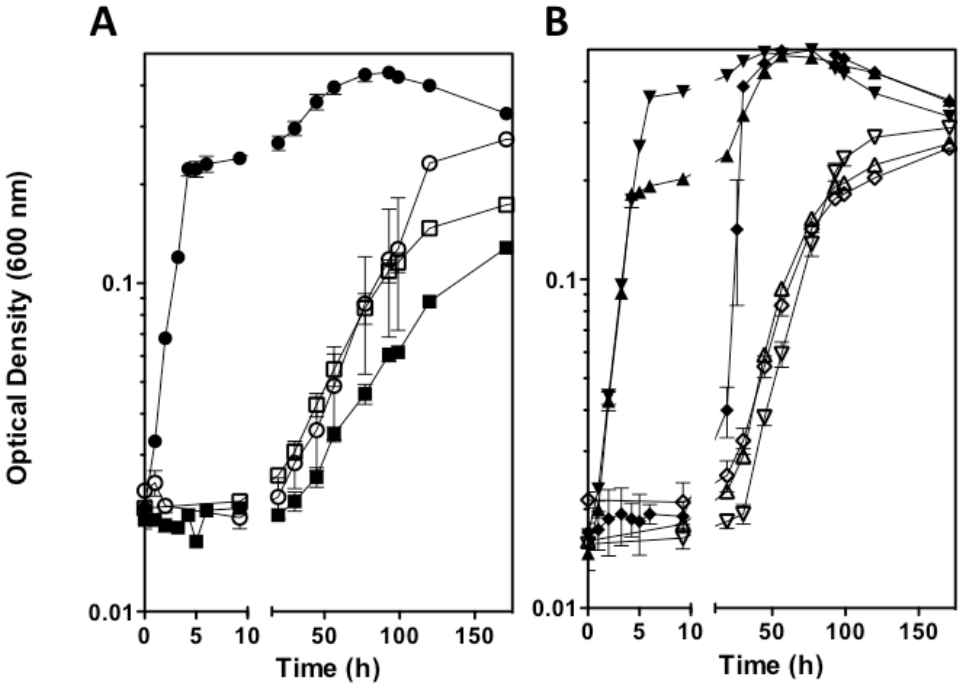

Figure 4.5: Oxidation of formate increases the growth rate of MR-1 on NAG. Growth curves were performed in the absence (open symbols) or presence (closed symbols) of 20mM formate. (A) Growth curves of MR-1 (circles) and the Δ*fdh* triple mutant (squares) were performed in anoxic SBM with 10 mM NAG and 60 mM fumarate. Note the prolonged timescale compared to growth on lactate or pyruvate in Figure 4.2. (B) Growth curves of ΔSO_4509 ΔSO_0101 (downward facing triangles), ΔSO_4513 ΔSO_0101 (upward facing triangles), and ΔSO_4509 ΔSO_4513 (diamonds) were performed as for part A. Reported values are the average of at least three independent experiments and error bars represent SEM.

The enhanced growth rate of MR-1 using NAG and fumarate supplemented with formate provides a convenient assay for physiologically relevant formate oxidation by each FDH complex. The generation time of the ΔSO0101-0103/ΔSO4509-4511 and ΔSO0101-0103/ΔSO4513-4515 mutants on NAG decreased dramatically upon addition of 20 mM formate to 1.28 ± 0.11 hours and 1.23 ± 0.01 hours, respectively, mirroring the enhanced growth rate observed in MR-1 (Fig. 4.5B). The ΔSO4509-4511/ΔSO4513-4515 strain also responded to formate, but growth rate was only partially enhanced with a generation time of 3.87 ± 0.84 hours (Fig. 4.5B). Our results suggest the complex encoded by SO0101-0103 does not contribute appreciably to the oxidation of formate during anaerobic growth on fumarate. SO0101, which is predicted to encode the catalytic subunit of the FDH complex, shares a considerable similarity at the amino acid level with FdnG (76%), the α subunit of the nitrate inducible FDH of *E. coli* (Fdh-N). Proteins encoded by SO0101-0103 may play a larger role in formate oxidation in the presence of nitrate as transcription of SO0101-0103 was found to be significantly upregulated under nitrate-reducing conditions (Beliaev et al., 2005).

Elimination of formate oxidation enables growth on pyruvate without a terminal electron acceptor

Bacteria from the genus *Shewanella* are generally thought to be respiratory organisms, requiring an electron acceptor for growth (Hau & Gralnick, 2007; Hunt et al., 2010; Nealson & Scott, 2006). It has also been reported previously that MR-1 is not capable of fermentative growth on pyruvate (Meshulam-Simon et al., 2007). Because

formate oxidation is the only unbalanced redox step associated with pyruvate metabolism, we hypothesized that deletion of the FDHs would enable anaerobic growth by *Shewanella* solely on pyruvate (Fig. 4.1A). To test this, we cultured both MR-1 and Δ*fdh* in anaerobic SBM supplemented with 20 mM pyruvate but lacking a terminal electron acceptor. We do not refer to this mode of growth as fermentation because pyruvate disproportionation occurs via a lyase reaction; hence, if the resulting formate is not oxidized, there is no need to cycle reducing equivalents. The Δ*fdh* strain was able to grow under anaerobic conditions solely on pyruvate while the MR-1 culture completed less than one doubling over 24 hours (Fig. 4.6). Analysis of culture supernatants by HPLC indicate that the Δ*fdh* strain catalyzed a nearly stoichiometric conversion of pyruvate to acetate and formate while only a small amount of pyruvate was converted to acetate by MR-1 with no terminal electron acceptor present (Table 4.2). The Δ*fdh* strain consumed less than half of the available pyruvate before growth ceased, which was not due to low levels of pyruvate oxidation by PDH, as the Δ*fdh*Δ*pdh* strain grew similar to Δ*fdh* (Fig. 4.6) and consumed similar amounts of pyruvate (Table 4.2). Inability to consume all of the available pyruvate may indicate inhibition of growth by accumulated formate or inability to cycle reducing equivalents in other metabolic pathways required for growth.

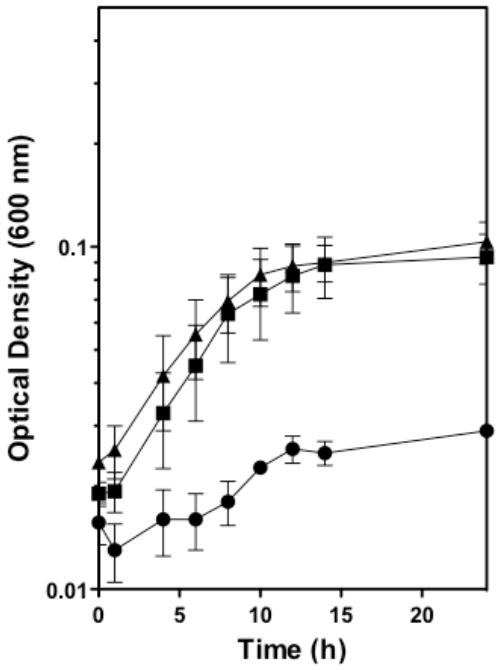

Figure 4.6: Growth of the Δ*fdh* triple mutant on pyruvate without a terminal electron acceptor. Growth curves of MR-1 (circles), the Δ*fdh* triple mutant (squares), and the Δ*fdh*Δ*pdh* triple mutant (triangles) were performed in anoxic SBM supplemented with 20 mM pyruvate. Reported values are the average of at least three independent experiments and error bars represent SEM.

	20 mM Pyruvate		
	MR-1	**Δ*fdh***	**Δ*fdh*Δ*pdh***
Pyruvate	-1.8 ± 0.4	-6.6 ± 0.3	-6.7 ± 0.6
Lactate	ND	0.1 ± 0.0	0.1 ± 0.0
Formate	ND	5.0 ± 0.0	5.2 ± 0.1
Acetate	1.4 ± 0.1	4.1 ± 1.3	5.4 ± 0.2

Table 4.2: Carbon source utilization/production (mM) following anaerobic growth in SBM containing 20 Pyruvate with no terminal electron acceptor. Reported concentrations are averages ± SEM from three independent experiments. ND; not detected.

Formate oxidation by MR-1 generates PMF under anaerobic conditions

Under anaerobic conditions, MR-1 generates ATP primarily through substrate level phosphorylation, and some of the ATP pool is utilized to generate PMF through proton pumping by the F-type ATPase (Hunt et al., 2010). Formate oxidation linked to reduction of a terminal electron acceptor should also contribute to PMF as the FDHs are predicted to reduce menaquinone in a redox loop mechanism that transports protons across the cytoplasmic membrane (Fig. 4.1A) (Simon et al., 2008). To test this, we compared growth of MR-1, the Δ*fdh* strain, Δ*atp* (a strain with a deletion of the entire ATP synthase operon SO4746-4754 (Hunt et al., 2010)), and Δ*fdh*Δ*atp* in SBM supplemented with 20 mM lactate and 40 mM fumarate. The Δ*atp* strain exhibited an initial lag phase but otherwise grew similarly to MR-1 while the Δ*fdh* strain grew at a slower rate and to a lower OD as compared to MR-1 (Fig. 4.7). Elimination of all three FDHs as well as the F-type ATPase severely inhibited growth, with strains completing less than one doubling over 13 hours (Fig. 4.7). Lower yield of the Δ*fdh* strain and severely inhibited growth of Δ*fdh*Δ*atp* with lactate and fumarate indicates that formate oxidation and proton pumping through the reversal of the F-type ATPase are the main contributors to the generation of PMF under anaerobic conditions by MR-1.

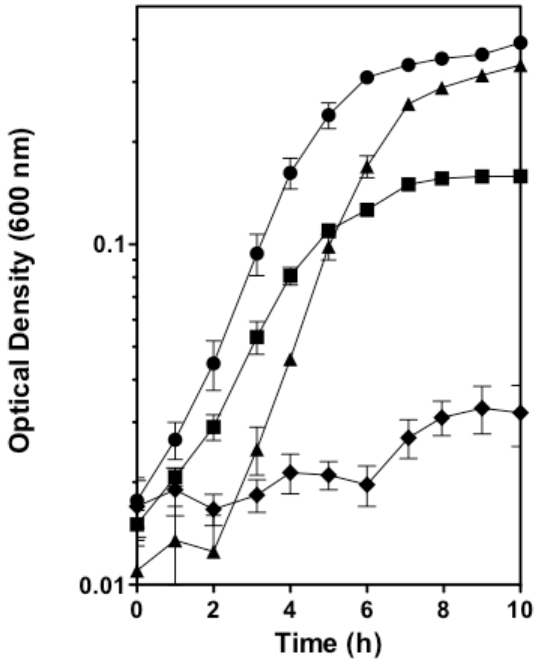

Figure 4.7: PMF is generated by the anaerobic oxidation of formate in MR-1. Growth curves of MR-1 (circles), the Δ*fdh* triple mutant (squares), the Δ*atp* mutant (triangles), and the Δ*fdh* Δ*atp* mutant (diamonds) were performed in anoxic SBM with 20 mM lactate and 40 mM fumarate. Reported values are the average of at least three independent experiments and error bars represent SEM.

Discussion

Development and rational engineering of MR-1 for applications in biotechnology requires a clear understanding of its carbon source utilization and energy metabolism. Although formate is obligately produced by MR-1 under anaerobic conditions during the disproportionation of pyruvate by PFL, little is known about the role formate plays in the ecophysiology of MR-1 or other members of the shewanellae. Beyond formate production, the presence of multiple genetic loci linked to its metabolism serves to emphasize the importance of formate in the core carbon metabolism of MR-1 and the shewanellae. To further address the role of formate oxidation, we generated mutants

lacking one, two, or all three regions encoding the α, β, and γ subunits of each of the three annotated FDH clusters (ΔSO0101-0103, ΔSO4509-4511, or ΔSO4513-4515; Fig 4.1B). We then monitored growth phenotypes of these strains during the oxidation of various carbon sources.

We have shown that oxidation of formate contributes both to growth rate and yield of MR-1 on a variety of carbon sources under anaerobic conditions with fumarate as terminal electron acceptor. During anaerobic growth with fumarate and either lactate or pyruvate, strains unable to oxidize formate (Δ*fdh*) grew at a slightly slower rate and to an overall lower yield as compared to MR-1 (Fig. 4.3). HPLC analysis indicated that, unlike MR-1, strains lacking FDH complexes accumulated formate in the supernatant, and the ratio of formate secreted was closer to the predicted 1:1 ratio with acetate when the E1 decarboxylase component of the Pdh complex, *aceE*, was also deleted (strain Δ*fdh*Δ*pdh*; Table 4.1). Previous work reported no measureable activity by PDH in MR-1 extracts under anaerobic conditions (Pinchuk et al., 2011); however, our HPLC analyses indicate that while the majority of pyruvate is routed through PFL, PDH remains active, albeit at low levels or perhaps slightly induced in the absence of PFL, under anaerobic conditions (Table 4.1). Low levels of PDH activity may be in response to the Δ*fdh* strain's inability to oxidize formate. It is also interesting to note that the amount of formate "missing" (~ 2 mM) for the Δ*fdh*Δ*pdh* strain grown anaerobically on pyruvate or lactate (based on the predicted 1:1 ratio of formate and acetate secreted) is equivalent to the concentration of "extra" fumarate reduced to succinate (~ 2 mM) (Table 4.1). Taken together, these results

indicate either i) formate is oxidized by an unidentified FDH or ii) formate is converted to another product capable of being oxidized by the cell. In *E. coli*, when medium pH drops below 6.8, the transporter FocA switches from passive formate export to active formate import (Sawers, 2005). Imported formate is then converted to dihydrogen via FHL to both control cellular pH and excess reducing power (Sawers, 2005). Recently, hydrogen production from formate was noted for MR-1, and this conversion was attributed to a predicted FHL encoded by the *hyd* operon (SO3920-3926) (Meshulam-Simon et al., 2007). It is therefore plausible that if secreted formate reaches a critical level, the Δ*fdh* and Δ*fdh*Δ*pdh* strains re-import formate and convert it to dihydrogen. Dihydrogen could then be oxidized via a hydrogenase ultimately leading to reduction of the terminal electron acceptor fumarate accounting for the similar concentrations of formate secreted by the Δ*fdh* and Δ*fdh*Δ*pdh* strains, and the sustained reduction of fumarate in the absence of formate oxidation (Table 4.1). It is also possible that once secreted formate reaches a maximal concentration, it is no longer effectively trafficked out of the cytoplasm.

Formate transport and oxidation appear to be central metabolic processes in MR-1, and the inability of the Δ*fdh* strain to oxidize formate helped to answer another main question related to the metabolism of MR-1. Pyruvate has been shown to enhance survival of MR-1 in stationary phase, and MR-1 contains lactate dehydrogenases capable of pyruvate reduction (Pinchuk et al., 2011; Pinchuk et al., 2009). Previous work has also shown that the majority of ATP is produced through substrate level phosphorylation by

MR-1 under anaerobic conditions (Hunt et al., 2010). Therefore, it has remained unclear why pyruvate cannot support fermentative growth of MR-1. Our data show that pyruvate sustains growth of the Δ*fdh* strain in anaerobic medium without a terminal electron acceptor (Fig. 4.6). Growth solely on pyruvate by Δ*fdh* suggests that, in the absence of exogenous electron acceptors, formate oxidation by MR-1 leads to an irreversible reduction of the menaquinone pool and subsequent cessation of growth. It is curious that MR-1 cultures do not simply secrete formate in the absence of terminal electron acceptor similar to the Δ*fdh* strain (Table 4.2). The inability of MR-1 to secrete formate, which would enable growth, highlights the importance of formate oxidation in the energy metabolism of MR-1 and may indicate a close proximity or even association of FDH complexes with the FocA transporter.

Exogenous formate also greatly accelerated the growth rate, likely due to enhanced PMF, of MR-1 on the sub-optimal carbon source NAG under anaerobic conditions with fumarate (Fig. 4.5A). Experiments utilizing double mutants indicate that this increase in growth rate was mainly due to activity by the FDHs encoded by SO4509-4511 and SO4513-4515 (Fig. 4.5B). While final OD was similar for mutants with SO4509-4511 or SO4513-4515 present, strains containing SO4509-4511 reached the maximum OD within the first 6 hours of growth, which may indicate a difference in efficiency or affinity for formate by each complex (Fig. 4.5B). It is interesting that the two FDH complexes that appear to have the largest effect on growth are the complexes that arose from a gene duplication event preceding current speciation of the *Shewanella* genus (Fig. 4.2).

Previous analysis of 106 bacterial genomes found that gene duplications tend to be retained when they are important for adapting to constantly changing environments (Gevers et al., 2004). Indeed, a hallmark of the *Shewanella* genus is the ability to thrive in redox-stratified environments where conditions are in a constant state of flux and may explain the occurrence of multiple paralogs enabling modularity in respiratory pathways (Coursolle & Gralnick, 2010) and now formate metabolism. Presumably, preservation of multiple FDH operons confers an evolutionary advantage to members of the *Shewanella* genus perhaps through affinity for formate across a range of available concentrations or through efficiency of formate oxidation with different terminal electron acceptors. Maintenance of the duplication or triplication of this FDH region in the vast majority of *Shewanella* serves to highlight the centrality of formate in energy conservation by this genus.

Funding Information

This work was supported by the Office of Naval Research (Awards N000141210309 and N000141310552) to JAG. RMS and NJK were supported in part by the University of Minnesota Biotechnology Training Grant Program through the National Institutes of Health.

Acknowledgements

I would like to thank Evan Brutinel, Heena Joo, Rebecca Maysonet, and Nicholas Kotloski for their help conducting experiments for this project; Professor Antony Dean

(University of Minnesota) for help with phylogenetic analysis; Dr. Jeffrey Flynn (University of Minnesota) for generating some of the FDH mutant strains. I also thank Professors Daniel Bond (University of Minnesota) and Clive Butler (University of Exeter) for helpful discussions and for critical review of the manuscript

Strain	Description	Reference
E. coli strain UQ950	DH5α host for cloning: F-*(argF-lac)169 80dlacZ58(*M15*) glnV44(*AS*) rfbD1 gyrA96(*NalR*) recA1 endA1 spoT1 thi-1 hsdR17 deoR pir+*	(Saltikov & Newman, 2003)
E. coli strain WM3064	DAP auxotroph used for conjugation: *thrB1*004 *pro thi rpsL hsdS lacZM15* RP4-1360 *(araBAD)567 dapA*1341::[*erm pir(wt)*]	(Saltikov & Newman, 2003)
S. oneidensis strain MR-1	Wild type	(Venkateswaran et al., 1999)
SOΔ0101-0103	*S. oneidensis* with an in-frame deletion of *fdnGHI* (SO0101-0103)	This study
SOΔ4509-4511	*S. oneidensis* with an in-frame deletion of *fdhABC* (SO4509-4511)	This study
SOΔ4513-4515	*S. oneidensis* with an in-frame deletion of *fdhABC* (SO4511-4513)	This study
SOΔ0101-0103Δ4509-4511	*S. oneidensis* with an in-frame deletion of *fdnGHI* (SO0101-0103) and *fdhABC* (SO4509-4511)	This study
SOΔ0101-0103Δ4513-4515	*S. oneidensis* with an in-frame deletion of *fdnGHI* (SO0101-0103) and *fdhABC* (SO4513-4515)	This study
SOΔ4509-4511Δ4513-4515	*S. oneidensis* with an in-frame deletion of *fdhABC* (SO4509-4511) and *fdhABC* (SO4513-4515)	This study
Δ*fdh*	*S. oneidensis* with an in-frame deletion of *fdnGHI* (SO0101-0103), *fdhABC* (SO4509-4511) and *fdhABC* (SO4513-4515)	This study
Δ*fdh*Δ*pdh*	*S. oneidensis* with an in-frame deletion of *fdnGHI* (SO0101-0103), *fdhABC* (SO4509-4511), *fdhABC* (SO4513-4515), and *aceE* (SO0424)	This study
Δ*fdh*Δ*atp*	*S. oneidensis* with an in-frame deletion of *fdnGHI* (SO0101-0103), *fdhABC* (SO4509-4511), *fdhABC* (SO4513-4515), and the ATP synthase operon (SO4746-4754)	This study

Table 4.3: Bacterial strains used in this study.

Primer Name	Sequence (5' to 3') or Reference
Primers for Δ0101-0103	
0101_Up_F	CATGactagtAGCGTCGTATCGCGCTGCTC
0101_Up_R	CATGgaattcGTTCATAGCGTTCTCTCACACTTTTG
0103_Dn_F	CATGgaattcCATTAATGAGTCATACAGCCGAGATA C
0103_Dn_R	CATGgagctcCGGCGAGCAGACTGTCCATC
Primers for Δ4509-4511	
4509_Up_F	CATGactagtTTGCGTCGCCATCCTAGCCTTG
4509_Up_R	CATGgaattcCATCACACACACTCCTCTGGTTAG
4511_Dn_F	CATGgaattcGACTAACTAAAGCGATATGCTAAACC C
4511_Dn_R	CATGgagctcATGTTGAGCATTTGGTCGCCCAC
Primers for Δ4513-4515	
4513_Up_F	CATGactagtCGTGTCGTGGATTGTCTGCGTG
4513_Up_F2 (for deletion construct to delete SO4513-4515 in the Δ4509-4511 background)	CATGactagtAAAGGCAACTTGCGATGAG
4513_Up_R	CATGctcgagCATCGCTGACTTCTCCTAGATTAG
4515_Dn_F	CATGctcgagGAGTAACATACTCTGATAAAACAAA ACCTC
4515_Dn_R	CATGgagctcGTGATGATAGTACTAAGTCCGCCTC
aceE (SO0424)	(Flynn et al., 2012)
ATP synthase operon (SO4746-4754)	(Hunt et al., 2010)

Table 4.4: Primers used in this study.

Chapter 5 : Hydrogenase Mutants Increase Coulombic Efficiency in Shewanella oneidensis Bioreactors

Introduction

Shewanella oneidensis strain MR-1 (hereafter referred to as MR-1) is a facultative anaerobe that thrives in redox-stratified environments due to its impressive respiratory metabolic diversity (Hau & Gralnick, 2007; Nealson & Scott, 2006). MR-1 is able to couple the oxidation of electron donors such as lactate, formate, and hydrogen, to the respiration of over 20 organic and inorganic compounds including insoluble metals (Hau & Gralnick, 2007; Nealson & Scott, 2006). The process of transferring electrons produced during anaerobic metabolism to insoluble terminal electron acceptors is termed extracellular respiration and has been well studied in MR-1 (Gralnick & Newman, 2007). Electrons generated during anaerobic metabolism by MR-1 are transferred from the quinone pool to the inner membrane tetraheme cytochrome CymA, which serves as the branch point to various acceptors (Marritt et al., 2012a; Marritt et al., 2012b; Myers & Myers, 2000) . During respiration of insoluble terminal electron acceptors, electrons are transferred from CymA to the surface of the bacterial cell via a complex of proteins collectively termed the metal reduction or Mtr pathway (Beliaev & Saffarini, 1998; Coursolle et al., 2010; Hartshorne et al., 2009). At the cell surface, electrons are either transferred directly to extracellular compounds by the Mtr complex or to redox-active flavins that facilitate electron transfer between the cell and extracellular substrates (Brutinel & Gralnick, 2012; Coursolle et al., 2010; Kotloski & Gralnick, 2013; Marsili et al., 2008; Okamoto et al., 2013; von Canstein et al., 2008).

The ability of MR-1 to couple oxidation of organic carbon and hydrogen to the reduction of insoluble metals is not only important in biogeochemical cycling but has also led to many promising applications in biotechnology (Fredrickson et al., 2008; Hau & Gralnick, 2007). Electrodes within bioelectrochemical reactors can serve as a proxy for metals used by MR-1 as terminal electron acceptors (Bretschger et al., 2007; Coursolle et al., 2010; Rabaey & Verstraete, 2005). Here, electrons are transferred through the Mtr respiratory/flavin pathway to an electrode (the anode) and can be harvested as current or used to produce hydrogen at the cathode using microbial fuel or electrolysis cells, respectively (Bretschger et al., 2007; Coursolle et al., 2010). Recent work has also shown that the Mtr conduit is reversible and hence can enable the uptake of electrons from an electrode (Ross et al., 2011). Reversal of electron flow from electrodes into microbial cells is currently being studied as a mechanism to drive reductive metabolism and the production of high value fuels and chemicals in a process termed electrosynthesis (Tremblay & Zhang, 2015).

Use of MR-1 and other organisms capable of extracellular respiration for the aforementioned biotechnology applications requires a clear understanding of the efficiency of metabolic turnover and related electron transfer reactions to and from electrodes. Coulombic efficiency (CE) relates to anodic electron transfer and is calculated as electron equivalents converted to current normalized to electron equivalents released during oxidation of the organic donor. CE decreases when electron equivalents are transferred to acceptors other than the electrode. For example, current density in MR-1

reactors is enhanced by aeration, but CE is greatly diminished due to loss of reducing equivalents to oxygen (Rosenbaum et al., 2010). Conversely, in many mixed species reactors, CE can approach or even exceed 100% due to cycling of products between the cathode and anode (Lee et al., 2009; Lee & Rittmann, 2010). For example, hydrogen cycling occurs when hydrogen produced at the cathode is oxidized by bacteria at the anode leading to increases in current density not attributable to oxidation of organic carbon sources and hence an increase in CE. Hydrogen production and utilization by microorganisms, reversible redox processes catalyzed by hydrogenases, can hamper CE calculations. Diversion of electron flux away from the anode and towards the reduction of protons forming hydrogen decreases CE. Conversely, oxidation of cathode-produced hydrogen by anode-respiring bacteria recycles current and artificially increases CE (Lee et al., 2009; Lee & Rittmann, 2010).

The genome of MR-1 contains two hydrogenase gene clusters: *hyaABCDEhypF hypBCDEA* (SO2089-2099) encodes a Group 1 [NiFe] hydrogenase and the *hy*drogenase *p*leitropy maturation proteins; *hydABfdhChydGXEF* (SO3920-3926) encodes an [FeFe] hydrogenase, maturation proteins, and a formate dehydrogenase gamma subunit (Meshulam-Simon et al., 2007). Both hydrogenase large subunits (HyaB and HydA) are periplasmically oriented, but are predicted to be bound to the inner membrane through association with other proteins encoded in each operon (Vignais & Billoud, 2007). The hydrogenase HydA functions primarily in hydrogen formation while HyaB is capable both of hydrogen production and uptake and is the dominant hydrogenase in MR-1

(Meshulam-Simon et al., 2007). Both hydrogenases are expressed during exponential and stationary phase, and hydrogen production has been observed in donor excess cultures following depletion of the electron acceptor fumarate (Kreuzer et al., 2014; Meshulam-Simon et al., 2007).

Here, we investigate the role of HyaB and HydA in hydrogen metabolism in bioelectrochemical reactors as well as current attributable to hydrogen cycling. Understanding the impacts of hydrogen metabolism on reactor efficiency and overall productivity is imperative for utilizing and engineering MR-1 for applications in biotechnology ranging from microbial fuel/electrolysis cells to electrosynthesis. Here, we show that deletion of *hyaB* and *hydA* in *Shewanella* results in higher current density and CE in single-chamber three-electrode bioreactors by diverting electron flux to the anode instead of to hydrogen production.

Materials and Methods

Bacterial Strains and Culture Conditions

Strains and plasmids used in this study are listed in Table 5.1. *Shewanella oneidensis* MR-1 has been described previously (Venkateswaran et al., 1999). *Escherichia coli* strains used for cloning (UQ950) and conjugal transfer (WM3064) were maintained on lysogeny broth (LB) agar plates containing 50 μg/mL kanamycin and/or 250 μM 2,6-diaminopimelic acid as necessary at 37°C and have been described previously (Saltikov & Newman, 2003). *S. oneidensis* strains were maintained on LB agar plates at 30°C. *Shewanella* basal media (SBM) pH 7.2 was used where indicated and

contained the following (per liter): 0.225 g K_2HPO_4, 0.225 g KH_2PO_4, 0.46 g NaCl, 0.225 g $(NH_4)_2SO_4$, 0.117 g $MgSO_4.7H_2O$, 5 mL vitamin mix, 5 ml of trace mineral mix, and 0.05% casamino acids (Hau et al., 2008). For growth assays, *S. oneidensis* strains were grown as follows. *S. oneidensis* strains were freshly streaked from -80°C glycerol stocks on LB plates and incubated for ~ 16 hours at 30°C. Single colonies from these plates were used to inoculate 5 mL of liquid LB medium shaken at 250 rpm at 30°C for 8 hours and were then sub-cultured into 5 mL of SBM supplemented with 20 mM lactate for ~16 hours shaken at 250 rpm at 30°C. For growth assays, cultures were washed twice and added to SBM containing 20 mM lactate and 40 mM fumarate in tubes sealed with butyl rubber stoppers containing an argon headspace.

Reagents and Materials

Enzymes were purchased from New England Biolabs (Ipswich, MA). Kits for gel purification and plasmid mini preps were purchased from Invitrogen (Carlsbad, CA). All related reactions were carried out according to manufacturer instructions. Media components were purchased from Becton, Dickinson and Company (Sparks, MD), and chemicals including 60% (w/w) sodium DL-lactate syrup and disodium fumarate were purchased from Sigma-Aldrich (St. Louis, MO).

Generation of Deletion Mutants

Oligonucleotide primers used to amplify regions of the MR-1 chromosome for deletion constructs are listed in Table 5.2. Regions of approximately 500 base pairs both up and downstream of the target deletion region were amplified using primers hyaB-

UF/hyaB-UR, hyaB-DF/hyaB-DR, hydA-UF/hydA-UR, and hydA-DF/hydA-DR with high fidelity polymerase Pfu Ultra (Agilent Technologies, Santa Clara, CA). Following restriction digest, up and downstream fragments were gel purified and cloned into the suicide vector pSMV3. Deletion constructs were introduced into MR-1 via conjugal transfer using *E. coli* donor strain WM3064 (Saltikov & Newman, 2003). In-frame gene deletions for *hydA* and *hyaB* were generated by homologous recombination as described previously (Saltikov & Newman, 2003). Plasmid constructs and deletion strains were sequence verified using primers hyaB-SP1/hyaB-SP-2 and hydA-SP1/hydA-SP2 at the University of Minnesota Genomics Center.

Fe(III) Citrate Reduction Assay

Real-time Fe(III) citrate reduction experiments were carried out in 96-well plates as previously described with the following modifications (Chan et al., 2015). Briefly, strains cultured for 12 hours in anaerobic SBM containing 20 mM lactate and 50 mM fumarate were washed and re-suspended in SBM to a final optical density measured at 600 nm (OD_{600}) of ~0.1. Cells were added to 96-well plates followed by a 10:1 volume of buffered solution containing sodium DL-lactate (10 mM), Fe(III) citrate (5 mM), NaCl (50 mM), K_2HPO_4 (1.3 mM), KH_2PO_4 (1.7 mM), $(NH_4)SO_4$ (1.7 mM), $MgSO_4$ (0.5 mM), HEPES (100 mM), and FerroZine reagent (2g/L). All preparations and incubations were carried out in an OMNI-LAB glove box (Vacuum Atmospheres Company) under a nitrogen atmosphere. Fe(II) concentration was assayed at 1 minute intervals at 625 nm using a SpectraMax M2 multimode microplate reader (Molecular Devices) over four

hours. Fe(II) concentration was calculated using a standard curve generated with ferrous sulfate dissolved in 0.5 N hydrochloric acid.

Bioreactor Construction

Bio-electrochemical reactors utilized in this study consisted of a 25 mL glass cone (Bioanalytical Systems, West Lafayette, IN) sealed by a silicone rubber O-ring-fitted PEEK top modified to hold electrodes and a gas line. Anaerobic conditions were maintained by flushing reactors with humidified argon purified of impurities using a heated copper column (oxygen in headspace kept below 5 ppm). The working electrode consisted of a glassy carbon electrode measuring 0.5 cm x 3 cm x 1 mm connected to a platinum wire with a Teflon bolt (McMaster Carr). The working electrode was polished with 400 grit sandpaper, rinsed in 1 N HCl and cleaned by sonication in deionized water twice for 10 min prior to use. The reference consisted of a glass body Ag/AgCl electrode in 3M KCl connected to the system via a glass capillary tube filled with 1% agarose in a 0.1 M KCl solution and capped with a vycor frit. The counter electrode consisted of a platinum wire and was shielded using glass tubing where indicated. Bioreactors were maintained at 30°C using a water bath and were stirred continuously. Electrochemical data was monitored using a 16-channel VMP® potentiostat (Bio-Logic, Claix, France).

Bioreactor Culture Preparation and Electrochemical Analysis

For bioreactor assays, single *S. oneidensis* colonies were used to inoculate LB medium incubated at 30°C, 250 rpm for ~16 hours. Strains were then sub-cultured in LB supplemented with 20 mM lactate and 40 mM fumarate under an argon headspace. When

anaerobic LB cultures reached an OD_{600} of 0.5-0.6, 1 mL of culture was added to bioreactors containing 14 mL of SBM medium containing 50 mM NaCl, 100 mM HEPES buffer, 60 mM lactate, and 40 mM fumarate. Following inoculation, the working electrode was poised at 0.240V vs SHE (Standard Hydrogen Electrode), and current was monitored for ~ 120 hours until current plateaued. Reactors, where indicated, were then washed three times with SBM containing 50 mM NaCl but lacking electron donor or acceptor and current was monitored until they reached basal levels indicating depletion of lactate. SBM containing 50 mM NaCl, 30 mM lactate, 1 μM riboflavin, and a 10 mM arabinose (internal HPLC standard) was then added to reactors and current analysis was continued for 96 hours. Supernatant was removed every 24 hours for HPLC analysis.

High Performance Liquid Chromatography

Metabolites were quantified by HPLC using Shimadzu Scientific equipment including an SCL-10A system controller, LC-10AT pump, SIL-10AF auto-injector, CTO-10A column oven, RID-10A refractive index detector, and an SPD-10A UV-Vis detector (210 nm). Mobile phase consisted of 15 mN H_2SO_4 set at a flow rate of 0.400 mL min^{-1}. Injection volumes of 50 μL were separated on an Aminex HPX-87H guard column maintained at 46°C. Reactor samples were compared to standard curves generated from known concentrations of each metabolite ($R^2 > 0.99$).

Results

Three-electrode, single-chamber bioreactors connected to a potentiostat enable real-time monitoring of current produced by MR-1 (Baron et al., 2009). In these reactors,

MR-1 cultures attach to a graphitic carbon anode, oxidize the provided electron donor, and utilize the anode as terminal electron acceptor. Electrons circuited from MR-1 to the graphitic carbon electrode are counted by a potentiostat and re-enter bioreactor medium through a platinum cathode where they reduce protons forming hydrogen. Efficiency calculations in these systems can be hampered by the fact that organisms encoding hydrogenases can i) transfer electrons to protons creating hydrogen diverting flux away from the anode and ii) can oxidize hydrogen produced at the cathode leading to a recycling of current not attributable to carbon source oxidation. To determine the effect of hydrogen metabolism on efficiency calculations in single chamber bioreactors, we monitored changes in current density for reactors with shielded cathodes and also utilized hydrogenase mutants that cannot produce or oxidize hydrogen.

Shielding the cathode leads to decreased current production in MR-1 single-chamber three-electrode bioreactors

Hydrogen cycling can occur when hydrogen produced by the cathode is oxidized by organisms at the anode leading to cycling of electron equivalents not attributable to carbon source oxidation (Fig 5.1). Shielding of the cathode, enabling hydrogen to escape to the headspace, can eliminate hydrogen cycling (Fig. 5.1). To determine the effect of cathode-produced hydrogen in MR-1 reactors, current density was monitored in three-electrode, single-chamber bioreactors with or without shielded cathodes. Cathodes were shielded by covering the platinum wire with glass tubing enabling hydrogen produced at the cathode to escape to the headspace due to its low solubility (Fig 5.1) (Lee et al.,

2009). Maximum current density decreased by ~30% in MR-1 single-chamber bioreactors when shielded cathodes were used providing evidence that hydrogen cycling may occur in MR-1 reactors (Fig. 5.2).

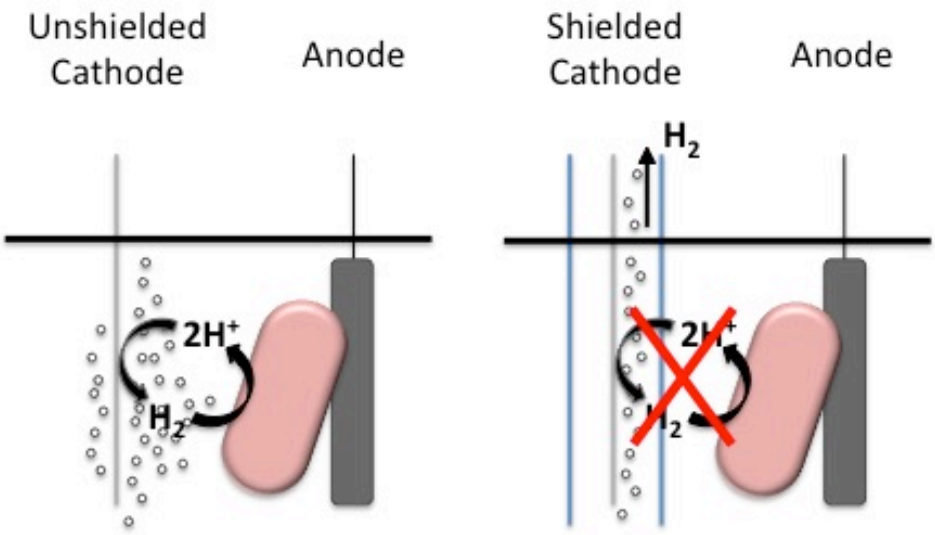

Figure 5.1: Hydrogen cycling occurs when anode-respiring bacteria oxidize hydrogen produced at the cathode. Shielding the cathode eliminates hydrogen from entering the medium and prevents hydrogen cycling.

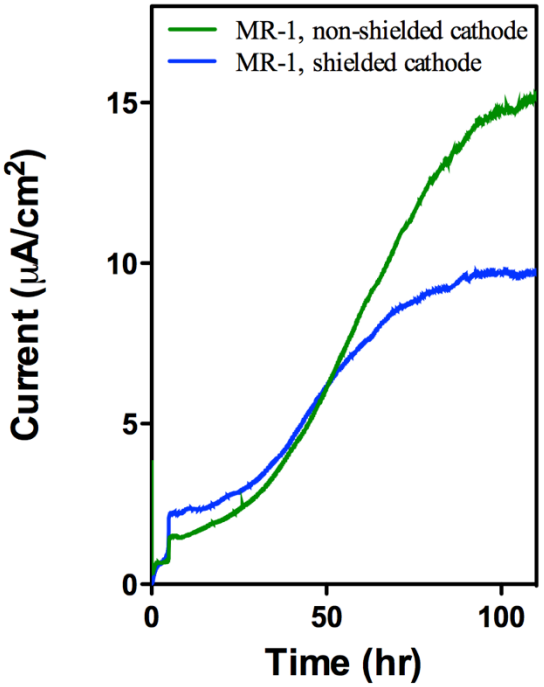

Figure 5.2: Lower current density is produced in MR-1 in bioreactors when cathodes are shielded. Current density over time for MR-1 cultures in single-chamber three-electrode bioreactors containing non-shielded (green) and shielded (blue) cathodes with reference electrodes poised at 0.24 vs. SHE. Representative data from three independent experiments are shown.

Hydrogenase mutants produce higher current density in single-chamber three-electrode bioreactors

MR-1 cells at the anode can also produce hydrogen. Electrons produced during anaerobic metabolism can either be transported through the Mtr pathway to the anode or can be transferred to hydrogenases to reduce protons forming hydrogen. Formation of hydrogen by MR-1 at the anode would decrease flux towards the electrode effectively decreasing current production per cell. To determine the role of hydrogen metabolism in current density and efficiency in single-chamber bioreactors, markerless in-frame

deletions were constructed in the regions encoding the large subunits of the two hydrogenases in the genome of MR-1 (strain referred to as Δ*hydA*Δ*hyaB*). Deletion of both hydrogenases did not adversely affect growth as Δ*hydA*Δ*hyaB* grew at the same rate and to the same yield as wild-type MR-1 under anaerobic conditions utilizing lactate and fumarate (Fig 5.3). MR-1 and Δ*hydA*Δ*hyaB* also reduced ferric citrate at the same rate (13.27 ± 5.63 mM Fe(II) hr^{-1} OD^{-1}, 13.81 ± 3.27 mM Fe(II) hr^{-1} OD^{-1}, respectively), indicating that deletion of *hyaB* and *hydA* did not adversely affect extracellular respiration. The aforementioned results suggest no phenotypic difference between MR-1 and Δ*hydA*Δ*hyaB* under fumarate and ferric citrate reducing conditions.

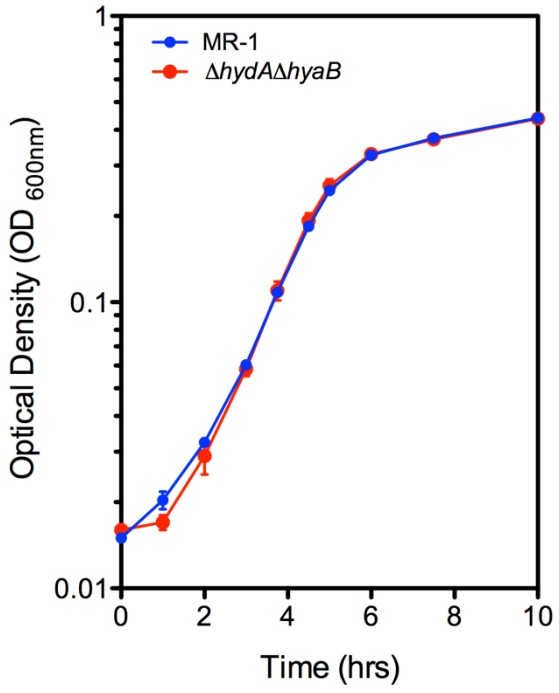

Figure 5.3: Growth of MR-1 (blue) and Δ*hydA*Δ*hyaB* (red) in anoxic SMB supplemented with 20 mM lactate and 40 mM fumarate. Data presented are averages from three independent experiments with error represented as standard error of the mean (SEM).

In contrast to ferric citrate reducing conditions, when MR-1 and Δ*hydA*Δ*hyaB* were grown with lactate in single-chamber, three-electrode bioreactors with shielded cathodes, maximum current densities were significantly higher for Δ*hydA*Δ*hyaB* (~18 $\mu A/cm^2$) as compared to MR-1 (~11 $\mu A/cm^2$) (Fig. 5.4). Following a plateau in current, reactor medium was washed three times and was replaced with SBM containing 60 mM lactate and 1 μM riboflavin (indicated by black arrow in Fig. 5.4). Following medium replacement, Δ*hydA*Δ*hyaB* reactors continued to sustain higher current densities than MR-1 (Fig 5.4). Higher maximum current densities in Δ*hydA*Δ*hyaB* reactors, as compared to MR-1, suggest that hydrogenase mutants divert more electron flux toward respiring the anode (Fig 5.4). In contrast, MR-1 cultures divert some electron flux to production of hydrogen. Similar results were observed for charge recorded by the potentiostat over time for MR-1 and for Δ*hydA*Δ*hyaB* reactors. Bioreactors containing the Δ*hydA*Δ*hyaB* strain recorded more charge over time when lactate was utilized as the electron donor as compared to MR-1 reactors (Fig 5.5).

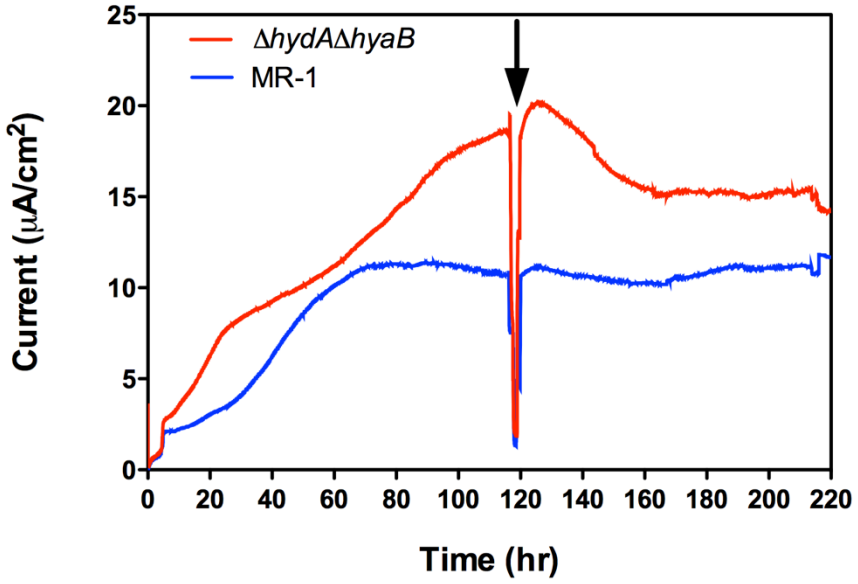

Figure 5.4: The Δ*hydA*Δ*hyaB* mutant produces higher current density than MR-1 in single-chamber three-electrode bioreactors with protected cathodes. Current density produced by Δ*hydA*Δ*hyaB* (red) or MR-1 (blue) with lactate as carbon source on graphitic carbon electrodes poised at 0.24 V vs SHE. Reactor experiments were performed three times and representative data is shown.

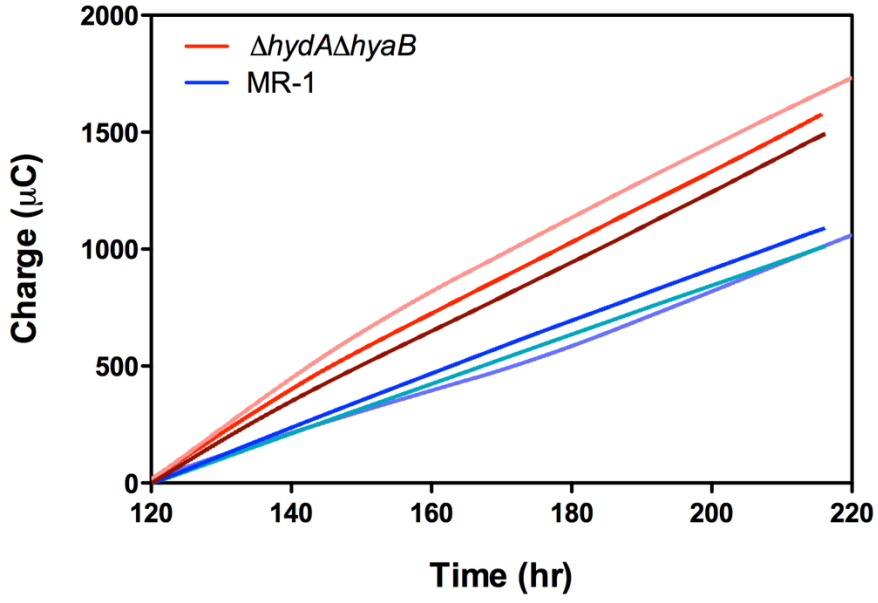

Figure 5.5: More charge is measured for reactors containing Δ*hydA*Δ*hyaB* (red shades) as compared to MR-1 (blue shades). Each line represents measured charge for one of three replicate reactors. Time in the x-axis coincides with Figure 5.4, and charge measurements were initiated after the media wash at 120 hours.

We next sought to determine if recorded charge difference were due to faster metabolic turnover by the Δ*hydA*Δ*hyaB* strain. Bioreactor medium samples were removed at 24-hour time intervals following inoculation and analyzed by HPLC. Consumed lactate is utilized both for biosynthesis and for energy conservation, so to link metabolic rate directly to respiration, we monitored the product of lactate oxidation, acetate. Acetate production rates were similar in MR-1 (0.038 ± 0.003 mM hr^{-1}) and Δ*hydA*Δ*hyaB* (0.043 ± 0.003 mM hr^{-1}) bioreactors indicating that differences in current production and charge generation were not due to variances in lactate turnover (Fig 5.6).

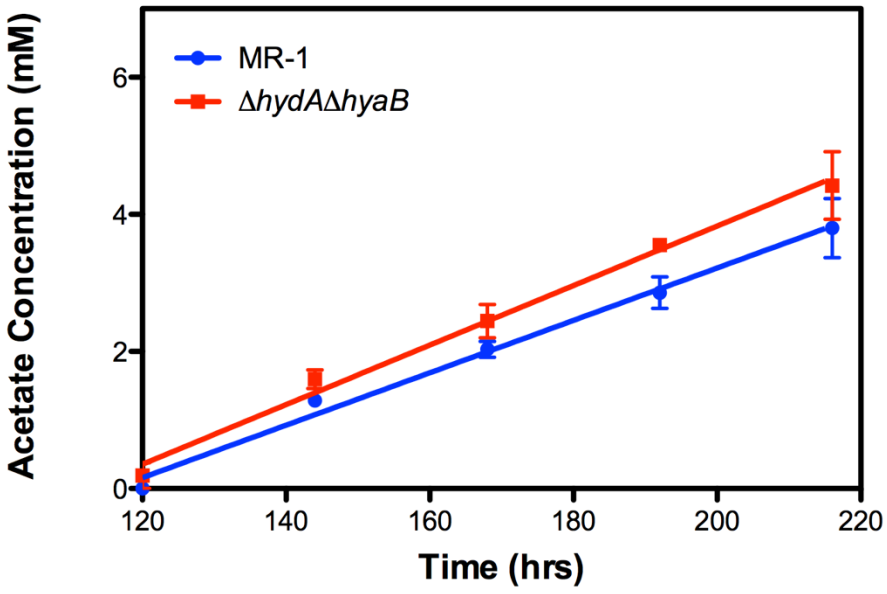

Figure 5.6: Rate of acetate production is not significantly different between MR-1 (blue) and Δ*hydA*Δ*hyaB* (red) single-chamber three-electrode bioreactors. Data represents acetate concentration measured by HPLC in reactor experiments performed in triplicate. Error is represented as SEM. Time in the x-axis coincides with Figure 5.4, and acetate concentration was measured every 24 hours after the media wash at 120 hours.

Hydrogenase mutants increase coulombic efficiency in single-chamber, three-electrode bioreactors

Using acetate production rates and current produced over time, we next calculated CE for bioreactors containing either MR-1 or Δ*hydA*Δ*hyaB* cultures. CE was calculated as mole equivalents of electrons transferred to the electrode normalized to mole equivalents of electrons released during oxidation of lactate to acetate. CE calculated for Δ*hydA*Δ*hyaB* reactors containing protected cathodes was significantly higher than MR-1 reactors with protected cathodes (Fig 5.7). Higher CE in reactors containing the Δ*hydA*Δ*hyaB* strain indicates that electron flux was diverted away from hydrogen production and towards the anode in hydrogenase mutants. CE measured for MR-1 in bioreactors with shielded cathodes was significantly lower than for MR-1 in bioreactors with un-shielded cathodes indicating hydrogen cycling by MR-1 (Fig 5.7).

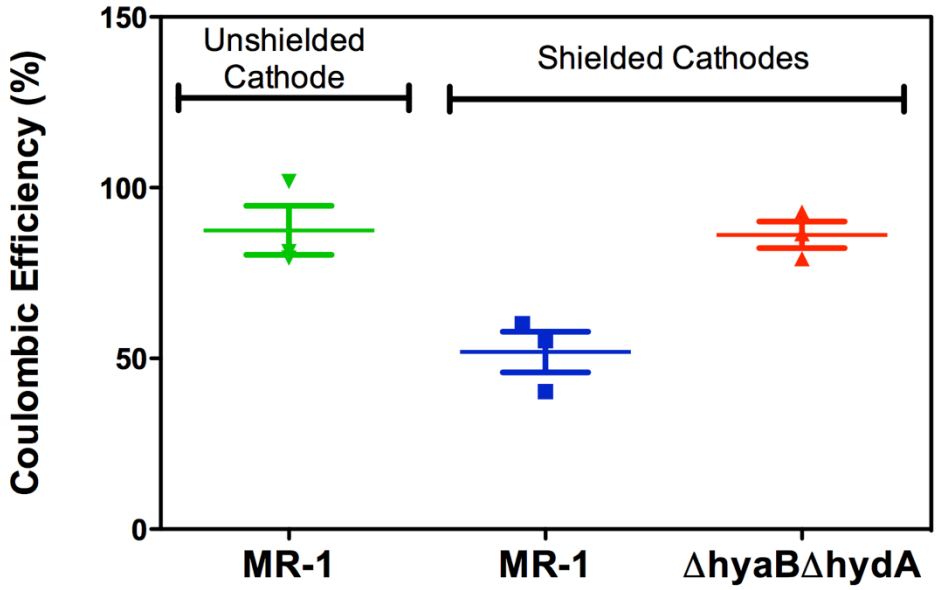

Figure 5.7: Hydrogenase mutants increase coulombic efficiency and divert electron flux towards the anode in single-chamber three-electrode bioreactors. Coulombic efficiency was measured as mole equivalents of electrons transferred to the anode normalized to mole equivalents of electrons produced by lactate oxidized to acetate for MR-1 (green) in bioreactors with unshielded cathodes, and MR-1 (blue) and Δ*hydA*Δ*hyaB* (red) in reactors with shielded cathodes. Three independent experiments are shown for each strain and reactor configuration with error representing SEM.

Discussion

In order to effectively utilize and engineer *S. oneidensis* for biotechnology applications involving reactors, it is imperative to understand metabolic turnover as well as efficiency of electron transfer to and from electrodes. Reported CE calculations for MR-1 utilizing a variety of reactor types in the literature range from 1.3-75% (majority are between 10-20%) indicating that most of the electrons generated from the oxidation of lactate by MR-1 remain unaccounted for (Bretschger et al., 2010; Kirchhofer et al., 2014; Kouzuma et al., 2012; Newton et al., 2009; Ringeisen et al., 2006; Ringeisen et al.,

2007; Rosenbaum et al., 2010; Rosenbaum et al., 2011; TerAvest & Angenent, 2014; Watson & Logan, 2010; Wu et al., 2013). Low CE in MR-1 reactors is often due to transfer of electrons to oxygen, which can leak into reactors or is intentionally sparged into the headspace to increase current production (Rosenbaum et al., 2010). Kozuma *et al.* attempted to increase CE by deleting the three terminal oxidases in MR-1, but the triple mutant was unable to produce current in reactors possibly due to oxygen toxicity (Kozuma et al., 2012). Higher CE (84 ± 7%) has been reported for MR-1 reactors by adding the conjugated oligoelectrolyte $DSSN^+$ that is thought to intercalate membranes and promote transmembrane ion conductance (Kirchhofer et al., 2014). Here, we report CE of 86.2 ± 6.8% for *Shewanella* single-chamber three-electrode bioreactors by eliminating hydrogen cycling and diverting electron flux to the anode through deletion of the hydrogenase large subunits, *hyaB* and *hydA*, in *S. oneidensis* (Fig 5.7).

Lower current densities produced with shielded versus unshielded cathodes provided evidence for hydrogen cycling in MR-1 reactors, but could also have been due to inhibition of mass ion transport to shielded cathodes which would lower electron transfer rates through reactors (Fig. 5.2). Two additional pieces of data argue against mass transport deficiencies i) Δ*hydA*Δ*hyaB* reactors with shielded cathodes achieve higher maximum current densities than MR-1 reactors with unshielded cathodes (Fig. 5.4 and 5.2) ii) differences in CE measured for MR-1 reactors with and without shielded cathodes indicate cycling of electron equivalents (Fig. 5.7).

Deletion of both hydrogenase large subunits in MR-1 increased current density and CE simultaneously in single-chamber three-electrode bioreactors (Fig. 5.4 and Fig. 5.7). The fact that MR-1 produces less current density than Δ*hydA*Δ*hyaB* (Fig. 5.4) is not entirely surprising as MR-1 thrives in a variety of environments precisely because it is a respiratory generalist (Hau & Gralnick, 2007; Nealson & Scott, 2006). MR-1 encodes a multitude of electron transport pathways to dispose of metabolic electrons enabling it to use many terminal electron acceptors, including protons, as they become available. The Δ*hydA*Δ*hyaB* mutant effectively shuts down a "leaky" pathway for electron disposal, resulting in channeling of electron flux to the anode. Elimination of hydrogenases also aids use of Δ*hydA*Δ*hyaB* for electrosynthesis studies as soluble hydrogenases have been shown to sorb to electrodes diverting cathodic electron flux (Deutzmann et al., 2015). Overall, the Δ*hydA*Δ*hyaB* strain provides a powerful chassis strain for further engineering of *Shewanella* for bioreactor applications.

Acknowledgements

I would like to acknowledge and thank Komal Joshi for her tireless work on this project. Komal and I will share first authorship when this work is published, and I could not have completed this chapter without her help.

Strain or Plasmid	Characteristics	Reference/Source
S. oneidensis strain MR-1	Wild-type	Venkateswaran et al (1999)
Δ*hydA*Δ*hyaB*	*S. oneidensis* Δ*hydA*Δ*hyaB*	This study
E. coli WM3064	DAP auxotroph *E. coli* conjugal donor strain	Saltikov and Newman (2003)
E. coli UQ950	DH5α; cloning strain	Saltikov and Newman (2003)
pSMV3	9.1 kb suicide vector; *oriR6K*, mobRP4, sacB, Km^R	Saltikov and Newman (2003)

Table 5.1:Strains used in this study.

Primer name	Sequence
Primers for *hydA* deletion:	
hydA-UF	GCATGGGCCCGCATTATCAATTCACCATAAACCC
hydA-UR	GCATACTAGTATTAATCTTGATCAGCCC
hydA-DF	GCATACTAGTGTGAAATCAGCCTCTGTC
hydA-DR	GCATGAGCTCTTTTGCTAGGCTGTCGTCCTTG
Primers for *hyaB* deletion:	
hyaB-UF	GCATGGGCCCGTGGCCGTTTTGATGCAG
hyaB-UR	GCATACTAGTTTTCAGTATGACTTCAATAAC
hyaB-DF	GCATACTAGTGATGCTGTCAATGCCCTG
hyaB-DR	GCATGAGCTCATGCGGGTTTCAGAATGG
Primers for sequence verification:	
hydA-SP1	TTCGACTCTACCTATGAAGCAATTAC
hydA-SP2	GATGTGCACATCATAGGTTAGCTG
hyaB-SP1	GTCAGCAAACCCGTGATTAACTTAG
hyaB-SP2	GATCCAACCTTGTACTAATACATCCGT

Table 5.2: Primers used in this study.

Chapter 6 : Towards Bioremediation of Methylmercury Using Silica Encapsulated Escherichia coli Harboring the mer Operon

Summary

Mercury is a highly toxic heavy metal and the ability of the neurotoxin methylmercury to biomagnify in the food chain is a serious concern for both public and environmental health globally. Because thousands of tons of mercury are released into the environment each year, remediation strategies are urgently needed and prompted this study. To facilitate remediation of both organic and inorganic forms of mercury, *Escherichia coli* was engineered to harbor a subset of genes (*merRTPAB*) from the mercury resistance (*mer*) operon. The strain was then encapsulated in silica beads resulting in a biological-based filtration material. Performing encapsulation in aerated mineral oil resulted in the production of microbeads that were smooth, spherical, and similar in diameter. Following encapsulation, *E. coli* containing *merRTPAB* retained the ability to degrade methylmercury and performed similarly to non-encapsulated cells. Due to the versatility of both the engineered mercury resistant strain and silica bead technology, this study provides a strong foundation for use of the resulting biological-based filtration material for methylmercury remediation.

Introduction

Microbial transformation of metals has a large impact on biogeochemical cycles and can alter metal distribution and partitioning in the environment. Alterations, such as change in redox state and conversion between organic and inorganic states, affect solubility and toxicity of metals and hence have great impact on environmental and public health (Barkay et al., 2003; Lin et al., 2012). Toxicity of the metal mercury is a

particular concern at present because mono-methylmercury (hereafter, methylmercury), the most common organic form, is a neurotoxin that biomagnifies in the food chain (Tchounwou et al., 2003). Five thousand to 8000 tons of mercury are estimated to be emitted into the atmosphere yearly from both human and natural sources, and anthropogenic emissions are expected to increase through 2050 (United Nations Environment Programme, 2013). Current remediation strategies exist for mercury but are prohibitively costly in many environments and other solutions are needed (Wagner-Dobler, 2013).

Bioremediation offers a potentially cost-effective and environmentally conscious approach to the problem of mercury pollution. An attractive biological-based remediation strategy for mercury pollution is utilization of the *mer*cury *r*esistance (*mer*) operon found in bacteria. The *mer* operon exists in a variety of structures and organizational forms, and a few key genes have become the central targets for remediation efforts (Wagner-Dobler, 2013). Essential to remediation of both organic and inorganic forms of mercury are the key enzymes MerB and MerA, respectively. MerB cleaves the C-Hg bond of organomercurials through protonolysis resulting in Hg(II) that is then reduced by MerA, the mercuric reductase, to volatile Hg(0) (Barkay et al., 2003; Lafrance-Vanasse et al., 2009). Other genes important to the system include *merP* and *merT* that encode for an Hg(II) transport system across the periplasm and inner membrane, and *merR* that encodes for the mercury-specific regulator of the operon (Barkay et al., 2003; Brown et al., 2003).

Previous bioremediation approaches for mercury have centered on usage of bacteria with engineered or naturally occurring *mer* operons and/or a variety of metal binding proteins. Genetic engineering has been used to introduce parts from the *mer* operon into a variety of hosts proposed for use in mercury removal from contaminated sites (Brim et al., 2000; Brim et al., 2003; Horn et al., 1994). Other studies have focused on engineering bio-sorbent strains utilizing Mer proteins and/or metal binding proteins or chelators such as metallothionein and polyphosphate kinase (Bae et al., 2001; Bae et al., 2003; Chen & Wilson, 1997; Deng & Jia, 2011; Kiyono et al., 2003; Lin et al., 2010; Pan-Hou et al., 2002; Ruiz et al., 2011; Sousa et al., 1998). Bio-sorbent strains are limited by their metal retention capacity, and because sorption is a passive process, strains must be regenerated after reaching saturation. Use of bio-sorbent strains also requires methods to separate mercury from biomass for recovery. The only method to date able to recover mercury and work at technical scale is the use of natural *mer*-containing strains of *Pseudomonas* adsorbed to silica pumice granules in packed bed bioreactors (von Canstein et al., 1999; Wagner-Dobler et al., 2000). Because adsorbed cells can easily be released in effluent water, engineered strains cannot be used with this type of system (Wagner-Dobler et al., 2000). Also, the formation of biofilm and exopolysaccharide within pumice material may limit diffusion in flow-through systems. Here we describe the use of a silica gel whole cell encapsulation system to address these challenges.

Silica encapsulation has previously been used in atrazine bioremediation (Mutlu et al., 2013; Reategui et al., 2012), providing protection of the biocatalyst, avoidance of

dispersal of organisms, and overall mechanical structure that broadens possible engineering applications. Silica gels are formed by condensation or gelation of a hydrolyzed silicon alkoxide crosslinker into a solid silica matrix. Following cross-linker hydrolysis, cells added during condensation become entrapped within the gel matrix (Mutlu et al., 2013). Recent improvements in encapsulation technology have resulted in methods retaining cell viability, which is imperative for mercury remediation since reduction of Hg(II) by MerA is an NADPH-dependent reaction (Barkay et al., 2003; Reategui et al., 2012). Encapsulated cells have been shown to retain high enzymatic activity over a period of months (Reategui et al., 2012). Optimization and modeling studies are also available to minimize material cost and pressure drop in packed beds while maintaining material strength (Mutlu et al., 2015).

Materials and Methods

Bacterial Strains and Culture Conditions

A complete list of strains used in this study can be found Table 6.2. *E. coli* strain MG1655 was kindly provided by Dr. Arkady Khodursky (University of Minnesota). *E. coli* strains UQ950 and WM3064 used for cloning and conjugal transfer have been described previously (Saltikov & Newman, 2003). For routine propagation of *E. coli*, single colonies from freshly streaked -80°C stocks were used to inoculate cultures grown for 16 hours in Luria Broth (LB) medium supplemented with 50 μg mL^{-1} kanamycin when appropriate. Unless specified otherwise, cultures were grown in LB, shaken continuously at 250 rpm, and incubated at 37°C.

Reagents and Materials

Enzymes were purchased from New England Biolabs (Ipswich, MA). Kits for gel purification and plasmid mini preps were purchased from Qiagen (Valencia, CA). All related reactions were carried out according to manufacturer instructions.

Media components, including Noble agar, were purchased from Becton, Dickinson and Company (Sparks, MD). Chemicals for encapsulation including Ludox TM40, TMOS, and Polyethylene Glycol 600 were purchased Sigma-Aldrich (St. Louis, MO). Mercuric chloride and methylmercury chloride were purchased from Fisher Chemical (Pittsburgh, PA). Due to the toxicity of mercury compounds, all safety protocols and operating procedures were reviewed by the Department of Environmental Health and Safety at the University of Minnesota.

Plasmid Construction

Plasmid pDU1358 was kindly provided by Dr. Anne Summers (University of Georgia, Athens) (Griffin et al., 1987). Plasmid pBBRBB has been described previously (Vick et al., 2011). Genes *merRTPAB* were amplified from pDU1358 in two stages to enable incorporation in the BioBrick compatible vector pBBRBB. First, a portion of *merA* and *merB* were amplified using primers merAmut-F (GTCGCGCATGTGAACGG CGAGTTCGTGCTGACCACGGGACA) and merB-R (nnACTAGTTCACGGTGTCCT AGATGACA) to mutate the internal EcoRI restriction site (bp 1024-1029) within *merA*. The resulting fragment was then gel purified and used to prime the second reaction along with primer merR-F (nnTCTAGACTACACCGCGTCGGCACCAC) to amplify

merRTPAB. This fragment was digested with XbaI and SpeI, gel purified, and cloned into the corresponding sites of pBBRBB generating plasmid pBBRBB::*mer*. Constructs in the pBBRBB backbone were moved into *E. coli* by conjugal transfer using strain WM3064.

Zone of Inhibition Plate Assays

E. coli strains were picked from single colonies into LB medium supplemented with 50 μg mL^{-1} kanamycin. Overnight cultures were diluted 10-fold, and 3 mL was added to tryptone medium agar plates (containing per liter: 15 g tryptone, 5 g NaCl, 10 g Noble agar, 1 pellet sodium hydroxide). Noble agar was used to limit agar batch variability that can confound heavy metal assays. Excess culture was removed after 5 minutes, a 6 mm paper disc was added to the center of the plate, and 10 μL of a 0.1 M $HgCl_2$ stock solution was added to each disc. $HgCl_2$ stock solutions were made fresh for each experiment. Plates were incubated at 37°C for 16 hours after which zones of inhibition were measured as the diameter of clearing around each disc.

Encapsulation

Methods for encapsulation were adapted from previous sol-gel techniques (Aukema et al., 2014; Reategui et al., 2012). Hydrolyzed cross-linker was produced by mixing TMOS with ultrapure water and 1 M HCl (1:1:0.001 vol/vol/vol) and incubating for two hours at room temperature. A solution containing colloidal silica nanoparticles (TM40), polyethylene glycol (PEG-600) and phosphate-buffered saline (PBS) was prepared prior to encapsulation (2:2:1 vol/vol/vol). Bacteria re-suspended in PBS between 0.1-0.2 g mL^{-1} were then introduced to this solution with a 1:1 volumetric ratio

to create a homogenous solution with silica interspersed between cells. Hydrolyzed cross-linker was then spiked into this solution and immediately transferred into aerated mineral oil (800 rpm, 15 min) to provide uniform viscosity throughout emulsification. After letting the silica set, beads containing the embedded bacteria were purified by phase-separation. Beads entered the dH_2O phase of the oil-water mixture and were isolated using a separatory funnel. Samples were both washed and stored in PBS overnight at 4°C prior to methylmercury testing.

Methylmercury Assays

Assays were conducted in acid-cleaned Balch tubes (Balch & Wolfe, 1976) containing 7 mL LB medium and 1 mg L^{-1} methylmercury chloride. Using previously published viability data for our encapsulation methods, encapsulated cells were inoculated at a cell density within an order of magnitude of that of the non-encapsulated cells (Reategui et al., 2012). For assays using encapsulated cells, 0.3 g of encapsulation material was added to each tube. For assays with non-encapsulated cells, overnight cultures were washed in minimal medium and inoculated to an initial optical density (OD_{600}) of ~ 0.1. Cultures were incubated at 37°C and shaken at 250 rpm. Samples were removed for analysis at times indicated.

Samples were analyzed for monomethylmercury in the University of Minnesota Mercury Analytical Laboratory using EPA method 1630 modified to eliminate sample distillation. Samples were placed in acid-cleaned 40 mL I-chem glass vials fitted with PTFE/silicone septa and brought to a final volume of 30 mL with distilled deionized

water. Samples received 0.225 mL of 2 M pH 4.5 acetate buffer and 0.03 mL of sodium tetraethylborate ethylating solution. Monomethylmercury concentrations were determined from headspace gas analysis by a Tekran model 2700 Automated MethylMercury Analyzer with Hg detection by cold vapor atomic fluorescence spectrometry (CVAFS) following capillary gas chromatography and pyrolization of ethylated Hg species.

Quality Assurance/Quality Control measures included the preparation of a calibration curve from 10 ng L^{-1} and 500 ng L^{-1} working standards at the start of each run of samples and the analysis of control check standards (0.1 and 0.5 ng L^{-1}) every 10 samples. Recoveries for control check standards averaged 98%, well within acceptable values.

Microscopy

Samples were fixed in 2% glutaraldehyde in 0.1 M sodium cacodylate buffer (pH 7.2) overnight at 4°C, rinsed in 0.1 M sodium cacodylate buffer, then placed in 1% osmium tetroxide in 0.1 M sodium cacodylate buffer overnight at 4°C. Specimens were rinsed in ultrapure water (NANOpure Infinity; Barnstead/Thermo Fisher Scientific; Waltham, Maryland), dehydrated in an ethanol series, and processed in a critical point dryer (Autosamdri-814; Tousimis; Rockville, Maryland). Material was mounted on double-sided adhesive carbon tabs on aluminum stubs, sputter-coated with gold-palladium, and observed in a scanning electron microscope (S3500N; Hitachi High Technologies America, Inc.; Schaumberg, Illinois) at an accelerating voltage of 10 kV.

Results

To develop a bioremediation strategy for both organic and inorganic forms of mercury, we began by cloning *merRTPAB* of the *mer* operon from pDU1358 (originally isolated from *Serratia marcescens*) into *E. coli* K12 resulting in strain *E. coli* pBBRBB::*mer* (Griffin et al., 1987). During amplification, the internal EcoRI restriction site in *merA* was mutated, resulting in a *mer* cassette compatible with the biobrick vector pBBRBB (Vick et al., 2011). Biobrick compatibility creates a plug-and-play vector system and facilitates addition of further remediation cassettes. Use of a modular approach in plasmid design allows the strain to be tailored to the specific needs of future remediation sites. Following construction, zone of inhibition plates were used to assess resistance to ionic forms of mercury by engineered strains. Strains were spread evenly on tryptone medium plates containing discs loaded with an $HgCl_2$ solution. Following overnight incubation, zones of inhibition were measured as the diameter of clearing around discs. *E. coli* pBBRBB::*mer* was resistant to ionic mercury as measured zones of clearing for *E. coli* pBBRBB::*mer* were comparable to the positive control *E. coli* pDU1358 and significantly smaller (p-value = 0.0002) than control strains containing empty vector (Table 6.1).

Strain	Zone of Inhibition Diameter (mm)
E. coli pDU1358	16.5 ± 0.3
E. coli pBBRBB::*mer*	16.7 ± 0.7
E. coli pBBRBB	26.5 ± 0.3

Table 6.1:Filter disc assay for mercury(II) chloride resistance in *E. coli*.

To use engineered *E. coli* pBBRBB::*mer* cells in a filtration system, the cells must be fully encapsulated in silica microbeads to prevent release of biological material. Cells were mixed with a colloidal silica nanoparticle/PEG solution and then spiked with a hydrolyzed silicon alkoxide tetramethyl orthosilicate (TMOS) solution. Transfer of this solution to aerated mineral oil enabled encapsulation of cells and resulted in the formation of smooth, spherical silica gel microbeads (Fig. 1A). Microbead structures were chosen for encapsulation because they increase surface to volume ratio for bioremediation efforts and result in a biological-based filtration material that can be used in packed bed reactors. Measurement of 20 beads using a Hitachi scanning electron microscope indicated an average bead diameter of 210 ± 60 μm. Images also indicated that gel porosity was in the nanometer range, which limits mobility of encapsulated cells (Fig. 1B). Because of the gel structure and limited space, cellular division is likely also inhibited.

Importantly, no cells were visualized on the surface of beads, and to image encapsulated cells, beads had to be crushed. Inside the gels, encapsulated cells appeared evenly dispersed within the gel matrix resulting in a highly porous material (Fig. 1B).

Encapsulated bacteria were found either as small clusters or as single cells throughout the gel. Encapsulated cells also retained normal cellular morphology and dimensions characteristic of *E. coli* (Fig. 1B). Overall, resulting microbeads were within the diameter range and bacterial loading capacity shown in previous models to both maximize diffusion and maintain mechanical strength in flow-through systems(Mutlu et al., 2015).

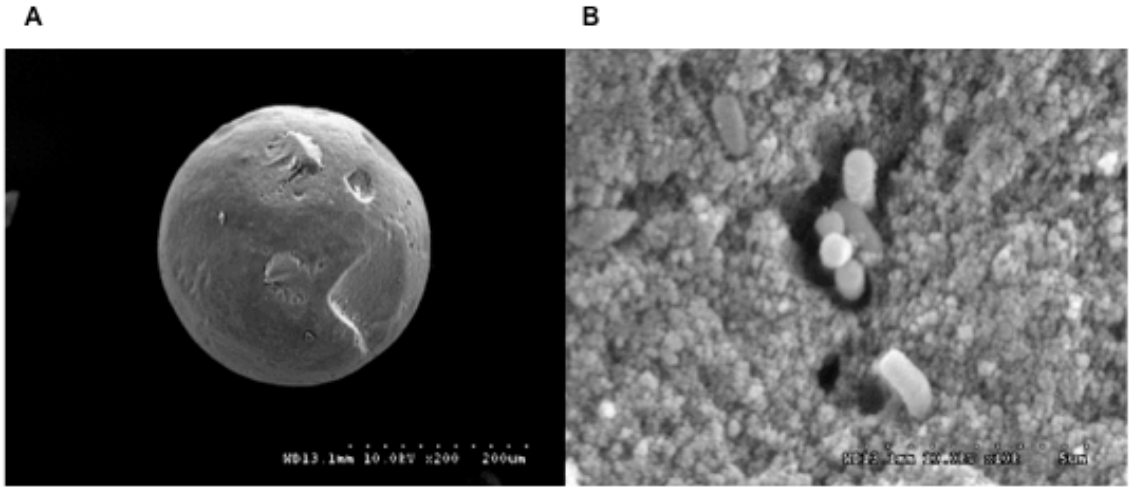

Figure 6.1:Scanning Electron Microscopy images of encapsulation silica sol gel microbeads containing *E. coli* pBBRBB::*mer*. A) Representative image depicting the smooth, spherical shape of silica microbeads following encapsulation in aerated mineral oil. Scale bar represents 200 μm B) Image of engineered *E. coli* pBBRBB::*mer* cells within encapsulation beads. Scale bar represents 5 μm.

To assess potential for degradation of methylmercury by *E. coli* pBBRBB::*mer*, both encapsulated and non-encapsulated cells were incubated in LB medium in the presence of 1 mg L^{-1} methylmercury chloride, which is a concentration 1000-fold greater than typically seen in contaminated environments and gold mining tailings ponds and thus a stringent test of our approach for methylmercury remediation(Guedron, Cossa,

Grimaldi, & Charlet, 2011; Leopold, Foulkes, & Worsfold, 2010). Samples were removed at various time points and analyzed for methylmercury concentration using a Tekran model 2700 Automated MethylMercury Analyzer with mercury detection by cold vapor atomic fluorescence spectrometry (CVAFS). Abiotic encapsulation beads and *E. coli* containing empty vector pBBRBB were included as negative controls.

E. coli pBBRBB::*mer* was efficient at remediation of methylmercury chloride prior to encapsulation. Non-encapsulated *E. coli* pBBRBB::*mer* was able to remediate greater than 99% of methylmercury chloride from solution after only 4 hours of incubation (Fig. 2A). The rate constant for degradation of methylmercury chloride by *E. coli* pBBRBB::*mer* was 0.96 ± 0.07 hr-^{1} with a measured half-life for methylmercury chloride of 0.72 ± 0.07 hours (Fig. 2A). Abiotic samples, as well as tubes containing non-encapsulated *E. coli* harboring an empty vector, showed slight decreases in the concentration of methylmercury after 24 hours (-0.16 ± 0.05 mg L^{-1} and -0.20 ± 0.05 mg L^{-1}, respectively), and are likely due to photodecomposition of methylmercury (Zhang & Hsu-Kim, 2010)(Fig. 2A). Taken together, these results indicate that the dramatically enhanced rate of methylmercury chloride degradation by *E. coli* pBBRBB::*mer* is due to Mer-mediated activity in engineered cells.

We next sought to determine if the rate of methylmercury degradation by encapsulated *E. coli* pBBRBB::*mer* was inhibited since encapsulation is likely to provide a diffusion barrier to degradation(Yeom, Mutlu, Aksan, & Wackett, Epub 2015 Jul 17). Methylmercury degradation rates were similar between non-encapsulated and

encapsulated cells. The rate constant for degradation of methylmercury chloride by encapsulated *E. coli* pBBRBB::*mer* was 0.87 ± 0.04 hr^{-1} with a measured half-life for methylmercury chloride of 0.80 ± 0.04 hours (Fig. 2B). Over 97% remediation of methylmercury chloride was achieved using encapsulated *E. coli* pBBRBB::*mer* after 4 hours of incubation (Fig. 2B). These results suggest that encapsulation did not diminish the ability of *E. coli* pBBRBB::*mer* to degrade methylmercury.

Abiotic encapsulation beads were also incubated in the presence of methylmercury chloride to determine if the beads alone absorbed significant amounts of this compound. Only small concentrations of methylmercury chloride were absorbed by abiotic silica gel beads (-0.27 ± 0.06 mg L^{-1}) as well as beads containing *E. coli* with the empty vector control (-0.20 ± 0.05 mg L^{-1}) after 24 hours (Fig. 2B). Absorption of methylmercury chloride by silica gel beads would aid in remediation efforts but would also hamper efforts to capture and potentially recycle elemental mercury using incorporated activated charcoal filters in scale-up packed bed reactors.

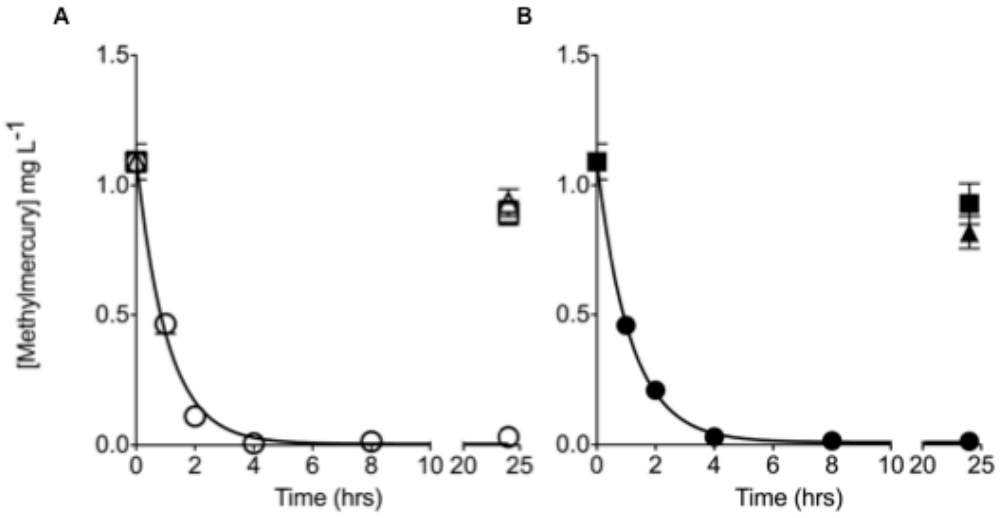

Figure 6.2: Degradation of methylmercury chloride by A) Non-encapsulated (open symbols) and B) Encapsulated (closed symbols) *E. coli* pBBRBB::*mer* (circles) and *E. coli* pBBRBB (squares). Degradation of methylmercury chloride in abiotic medium (open triangle) and sorption by abiotic beads (closed triangle) were included as controls. Data presented is for experiments performed at least in triplicate with error bars represented as SEM

Strain	**Genotype/Characteristics**	**Reference**
***E. coli* K12 strain MG1655**	Wild Type	Kindly provided by Dr. Arkady Khodursky (University of Minnesota)
***E. coli* strain UQ950**	DH5α host for cloning: F-*(argF-lac)169 80dlacZ58(*M15*) glnV44(*AS*) rfbD1 gyrA96(*NalR*) recA1 endA1 spoT1 thi-1 hsdR17 deoR pir+*	(Saltikov & Newman, 2003)
***E. coli* strain WM3064**	DAP auxotroph used for conjugation: *thrB1*004 *pro thi rpsL hsdS lacZM15* RP4- 1360 *(araBAD)567 dapA*1341::[*erm pir(wt)*]	(Saltikov & Newman, 2003)

Table 6.2: Strains utilized in this study.

Discussion

Because mercury cannot be transformed into a non-toxic state, remediation efforts have focused on conversion of organic and ionic forms to the less toxic elemental form Hg(0). Ultimately, the goal of any mercury remediation strategy is to capture the elemental form thereby enabling safe disposal and the potential to recycle materials. Encapsulation of bacterial cells containing the *mer* operon provide a possible answer to the challenges involved in mercury remediation since encapsulation enables use of engineered cells and the filtration material can be incorporated in flow-through systems.

By incorporating a subset of the *mer* operon in *E. coli* and encapsulating cells in silica microbeads, a remediation platform targeting both ionic and organic forms of mercury was developed. Performing encapsulation in aerated mineral oil resulted in the production of smooth, spherical beads that could be incorporated into packed bed reactor wastewater treatment facilities (Fig. 1). Encapsulated *E. coli* pBBRBB::*mer* performed similarly to non-encapsulated cells, and was able to remediate high methylmercury concentrations to below detection levels after approximately 4 hours (Fig. 2). Encapsulation, by providing protection to the biocatalysts and overall mechanical structure, broadens possible engineering applications for the remediation of mercury.

Mercury pollution is widespread, and its effects are not limited to areas near the source of pollution. Since mercury can travel thousands of miles through the atmosphere before being deposited back in the environment, it has become an issue of global concern. Remediation methods are needed that can target multiple arenas including industry,

mining tailing ponds, and open bodies of water. This study provides a foundation for methods to encapsulate *mer*-containing bacteria in silica sol-gel materials to offer a versatile option that can be tailored to various mercury-polluted sites. Further work in this area is being targeted at refactoring the *mer* operon to increase turnover rates, testing other genera such as encapsulated *Pseudomonas* species for the remediation of methylmercury, and determination of long-term cell escape rates from beads.

Acknowledgements

This project was conducted by the 2014 iGEM team at the University of Minnesota and was supported by the Office of Naval Research (Award N000141210309 to JAG) and the University of Minnesota MnDRIVE initiative: Advancing industry, conserving our environment. We would like to thank Dr. Anne Summers (University of Georgia) for providing pDU1358, safety protocols, and project guidance. We would also like to thank Professor Alptekin Aksan and Dr. Baris Mutlu (University of Minnesota) for initial discussions concerning encapsulation protocols, and Gail Celio (University of Minnesota Imaging Center) for assistance with microscopy.

Chapter 7 : Conclusions and Future Directions

Chapters 2 and 3:

Experiments conducted in Chapters 2 and 3 highlight the utility of engineered laboratory co-cultures as model systems for the study of interspecies interaction and cooperation. In Chapter 2, a co-culture was engineered using the bacteria *Shewanella oneidensis* and *Geobacter sulfurreducens*, both important organisms for a variety of applications in biotechnology. In this system, *S. oneidensis* was engineered to metabolize glycerol and secrete acetate via the pGUT2 plasmid enabling commensal cross-feeding as acetate provided a carbon source for *G. sulfurreducens*. In the commensal co-culture, complete oxidation of glycerol to carbon dioxide occurred only in the presence of both species and was coupled by both to fumarate respiration.

Deletion of the gene encoding fumarate reductase (*fccA*) in *S. oneidensis* pGUT2 altered the interaction between *Shewanella* and *Geobacter* from a commensal relationship to an obligate mutualism resulting in a complete shift in metabolic strategy and a novel approach to energy generation by the community. Instead of oxidizing glycerol, both organisms in the obligate co-culture converted fumarate to malate and subsequently utilized malate as a carbon source. Growth linked to malate catabolism in the obligate co-culture required the presence of both *Shewanella* and *Geobacter*. Targeted deletions in putative malate-uptake pathways or in acetate production in *Shewanella* significantly inhibited growth rate and yield in obligate co-cultures. Importantly, predicted pathways for malate uptake and consumption are not redox-balanced in *Shewanella*, and the

presence of *Geobacter* to accept reducing equivalents from *Shewanella* strains may explain obligate co-culture growth.

The transfer of reducing equivalents enabling obligate co-culture growth, a process termed interspecies electron transfer, was studied further in Chapter 3. In Chapter 3, *S. oneidensis* pGUT2 and *G. sulfurreducens* were cultured together in single-chamber, three-electrode bioreactors containing gold anodes enabling real-time monitoring of co-culture metabolism. In this system, the supplied carbon source (glycerol) could only be metabolized by *S. oneidensis* pGUT2, while the terminal electron acceptor (gold anode) could only be respired by *G. sulfurreducens*. Current was produced, stemming from glycerol oxidation coupled to gold anode respiration, only when *S. oneidensis* pGUT2 and *G. sulfurreducens* were co-cultured because each species required activity mediated by the other. *S. oneidensis* pGUT2 oxidized glycerol and secreted acetate as a carbon source for *G. sulfurreducens* only if *G. sulfurreducens* accepted reducing equivalents from *Shewanella* and transferred electrons to the gold anode. Targeted gene deletions were used to identify pathways enabling interspecies electron transfer between *S. oneidensis* pGUT2 and *G. sulfurreducens* in bioreactor systems. Deletion of the flavin exporter *bfe* in *S. oneidensis* pGUT2 significantly decreased current production by *S. oneidensis* Δ*bfe* pGUT2/*G. sulfurreducens* co-culture reactors and was restored to levels near that of the original obligate co-culture when exogenous flavins were added. The model laboratory co-culture of *S. oneidensis* pGUT2 and *G. sulfurreducens* enabled identification of a new mechanism mediating interspecies electron transfer—transfer via

redox-active flavin shuttles. Flavins can be reversibly oxidized and reduced and thus can "shuttle" electrons between *Shewanella* and *Geobacter*. Flavin-mediated interspecies electron transfer may also have important implications in environmental communities as many species have been shown recently to secrete flavins.

The various co-cultures engineered using *Shewanella* and *Geobacter* provide model laboratory communities consisting of bacteria with well-defined genetic and metabolic systems. As such, these co-cultures can serve as chassis communities for further engineering. For example, a co-culture of *S. oneidensis* and *G. sulfurreducens* could be used to expand carbon source utilization in fuel cells or in electrosynthesis applications to divide metabolic labor among community members and overcome limitations inherent to individual strains.

Shewanella and *Geobacter* co-cultures also provide powerful tools to study evolution of interaction over time. Further studies are planned or are currently underway using *Shewanella* and *Geobacter* co-cultures to study how genetic backgrounds and metabolism change or affect interaction in communities. Successive transfers of co-culture communities would enable determination of metabolic change associated with each strain due to the presence of the other. Because *S. oneidensis* and *G. sulfurreducens* were originally isolated from different environments, evolution of interactions can be monitored from the initial point of contact. We are also developing genetic tools for co-cultures. An undergraduate working with me in the laboratory, Rachel Soble, has been developing methods combining classical transposon mutagenesis with high-throughput

sequencing (Tn-seq) to quantify genetic fitness related to each gene in the chromosomes of *S. oneidensis* and *G. sulfurreducens* related to co-culture growth. In this method, transposon mutant libraries are generated for each species and are pooled to create a parent library. Parent libraries are then outgrown both alone and in co-culture, and mutant ratios are determined for each condition by sequencing transposon-genomic DNA junctions using the Illumina platform. Mutant ratios provide a fitness score relative to growth rate under the conditions tested. Tn-seq is a powerful hypothesis-generating tool to identify mutations that are beneficial, neutral, or deleterious to growth of a population under the conditions tested. Tn-seq will allow us to determine a "fitness score" for each gene in *S. oneidensis* and *G. sulfurreducens* as they relate to growth in co-culture. Clean deletions will then be generated to verify Tn-seq results. *Shewanella* and *Geobacter* co-cultures can also be used to study negative interactions in communities. For example, using the commensal co-culture, competitive interactions can be studied by limiting concentrations of the shared resource fumarate. One can then study population dynamics attributable to limited resources over successive generations. As highlighted here, the model laboratory co-cultures of *Shewanella* and *Geobacter* have spurred several other projects in the laboratory and are allowing us to test multiple hypotheses based on interaction in communities.

Chapter 4:

Experiments in Chapter 4 demonstrate that anaerobic formate metabolism in *S. oneidensis* generates proton motive force and prevents growth without a terminal electron

acceptor. The chromosome of *S. oneidensis* encodes three complete formate dehydrogenase complexes and a putative formate hydrogenlyase, which raised several questions as to the role of formate metabolism in *Shewanella* physiology. One of the FDH operons appeared to have arisen due to a gene duplication event, and to look further into the history of the region, phylogenetic analysis was conducted. The resulting phylogenetic tree indicated that duplication of the FDH region had occurred in a common ancestor predating current speciation of the *Shewanella* genus. Selection for maintenance of multiple FDH regions in the majority of *Shewanella* further indicated importance of formate metabolism. Using combinatorial deletions in the FDH regions, we demonstrated that formate oxidation contributed to growth rate and yield of *S. oneidensis* on a variety of carbon sources, and that exogenous formate could accelerate *S. oneidensis* growth on sub-optimal carbon sources. The triple FDH mutant alone and in combination an ATPase mutant enabled us to demonstrate that formate oxidation and proton pumping by the F-type ATPase were the main contributors to proton motive force (pmf) in *S. oneidensis* under anaerobic conditions. Formate oxidation leading to translocation of protons generating pmf was proposed to occur via a redox loop mechanism with CymA. Future work and structural data for FDH and CymA are required to determine coupling sites and confirm the redox loop mechanism. Deletion of all three FDH operons also enabled growth of *S. oneidensis* on pyruvate without the addition of a terminal electron acceptor, a mode of growth never before observed in *S. oneidensis*, suggesting that either a

feedback mechanism or inability to cycle reducing equivalents prevent fermentative growth.

A brief bioinformatic analysis was also presented in Chapter 4 concerning the putative formate hydrogenlyase (FHL) predicted as part of the *hyd* locus in *S. oneidensis*. FHL complexes catalyze the disproportionation of formate to carbon dioxide and hydrogen. Previous research has shown hydrogen production in the presence of formate providing evidence for formate hydrogenlyase activity in *S. oneidensis* (Meshulam-Simon, Behrens, Choo, & Spormann, 2007). The predicted FHL region encoded by the *hyd* locus is annotated as containing *fdhC* and hence does not encode the catalytic subunit necessary to oxidize formate. Interestingly, locus SO0988 in *S. oneidensis* is annotated as an orphan FDH catalytic subunit and does not encode a TAT pathway signal sequence indicating its protein product remains in the cytoplasm (as would be expected for the catalytic subunit of FHL). Domain analysis indicated that the N-terminal portion of the protein encoded by SO0988 contained multiple Fe-S cluster domains and the C-terminal portion was 58% similar at the amino acid level to Fdh-H, the catalytic subunit of the *Escherichia coli* FHL. The protein products of SO0988 and the *hyd* locus may encode FHL in *S. oneidensis* and warrant further work as this would provide the first evidence for an FHL comprised of an [Fe-Fe] hydrogenase and an unknown biochemical pathway for hydrogen production from formate.

Chapter 5:

Work performed in Chapter 5 demonstrated the impact of hydrogen metabolism on both current production and coulombic efficiency (charge recovery) in *S. oneidensis* bioelectrochemical systems. Hydrogenases catalyze the reversible reduction of protons forming hydrogen. The inherent reversibility of hydrogen metabolism poses two problems in bioelectrochemical reactors i) transfer of electrons to protons diverts electron flux away from the electrode and decreases current production and coulombic efficiency ii) oxidation of hydrogen produced at the cathode by anode-respiring bacteria (hydrogen cycling) leads to re-circuiting of charge increasing overpotential and required applied voltages. Deletion of both hydrogenase large subunits in *S. oneidensis* (Δ*hydA*Δ*hyaB*) increased current density and led to charge recoveries of ~86%, the highest reported for *S. oneidensis* to date. In order to effectively utilize and further engineer *Shewanella* for biotechnology applications, it is imperative to understand metabolic turnover, respiratory pathways, and efficiency of electron transfer to and from terminal electron acceptors. Hydrogenases presented a "leaky" pathway for electron flux out of *Shewanella* and deletion enabled channeling of flux towards electrodes. We also developed methods to shield cathodes and eliminate hydrogen cycling, which may prove useful in reactor applications using bacteria that lack genetic systems.

Chapter 6:

Work described in Chapter 6 highlighted a project conducted by the 2014 University of Minnesota iGEM competition team (international Genetically Engineered

Machine) focused on mercury bioremediation. Mercury is a potent neurotoxin and microbial-catalyzed transformations can alter its distribution in the environment. To develop a bioremediation strategy for both organic and ionic forms of mercury, the team cloned *merRTPAB* of the mercury resistance (*mer*) operon from plasmid pDU1358 (originally from *Serratia marcescens*) into *E. coli*. The engineered *E. coli* strain was then encapsulated using silica sol gel technology developed by Professors Lawrence Wackett and Alptekin Aksan from the University of Minnesota. Encapsulating *E. coli* harboring *merRTPAB* (*E. coli* pBBRBB::*mer*) generated a biological-based filtration material for use in remediation strategies. Encapsulated *E. coli* pBBRBB::*mer* was able to remediate methylmercury, degrading 97% from a 1 mg L^{-1} laboratory sample after 4 hours. *E. coli* pBBRBB::*mer* and encapsulation methods provide a platform technology for mercury remediation. Further studies should be conducted to determine cell viability and remediation capacity over time. Also, further engineering of *mer*RTPAB could potentially increase turnover rates by the *E. coli* pBBRBB::*mer* strain.

References

Abbas, C. A., & Sibirny, A. A. (2011). Genetic control of biosynthesis and transport of riboflavin and flavin nucleotides and construction of robust biotechnological producers. *Microbiology and Molecular Biology Reviews, 75*(2), 321-360. doi:10.1128/MMBR.00030-10

Aklujkar, M., Coppi, M. V., Leang, C., Kim, B. C., Chavan, M. A., Perpetua, L., Giloteaux, L., Liu, A., & Holmes, D. E. (2013). Proteins involved in electron transfer to Fe(III) and Mn(IV) oxides by *Geobacter sulfurreducens* and *Geobacter uraniireducens*. *Microbiology-Sgm, 159*, 515-535. doi:10.1099/mic.0.064089-0

Alperin, M., & Hoehler, T. (2010). The ongoing mystery of sea-floor methane. *Science, 329*(5989), 288-289. doi:10.1126/science.1189966

Aukema, K. G., Kasinkas, L., Aksan, A., & Wackett, L. P. (2014). Use of silica-encapsulated *Pseudomonas* sp strain NCIB 9816-4 in biodegradation of novel hydrocarbon ring structures found in hydraulic fracturing waters. *Applied and Environmental Microbiology, 80*(16), 4968-4976. doi:10.1128/AEM.01100-14

Bae, W., Mehra, R., Mulchandani, A., & Chen, W. (2001). Genetic engineering of *Escherichia coli* for enhanced uptake and bioaccumulation of mercury. *Applied and Environmental Microbiology, 67*(11), 5335-5338. doi:10.1128/AEM.67.11.5335-5338.2001

Bae, W., Wu, C., Kostal, J., Mulchandani, A., & Chen, W. (2003). Enhanced mercury biosorption by bacterial cells with surface-displayed MerR. *Applied and Environmental Microbiology, 69*(6), 3176-3180. doi:10.1128/AEM.69.6.3176-3180.2003

Balasubramanian, R., Levinson, B. T., & Rosenzweig, A. C. (2010). Secretion of flavins by three species of methanotrophic bacteria. *Applied and Environmental Microbiology, 76*(21), 7356-7358. doi:10.1128/AEM.00935-10

Balch, W., & Wolfe, R. (1976). New approach to cultivation of methanogenic bacteria: 2-mercaptoethanesulfonic acid (HS-CoM)-dependent growth of *Methanobacterium*

ruminantium in a pressurized atmosphere. *Applied and Environmental Microbiology, 32*(6), 781-791.

Barkay, T., Miller, S., & Summers, A. (2003). Bacterial mercury resistance from atoms to ecosystems. *FEMS Microbiology Reviews, 27*(2-3), 355-384. doi:10.1016/S0168-6445(03)00046-9

Baron, D., LaBelle, E., Coursolle, D., Gralnick, J. A., & Bond, D. R. (2009). Electrochemical measurement of electron transfer kinetics by *Shewanella oneidensis* MR-1. *Journal of Biological Chemistry, 284*(42), 28865-28873. doi:10.1074/jbc.M109.043455

Beliaev, A., Klingeman, D., Klappenbach, J., Wu, L., Romine, M., Tiedje, J., Nealson, K., Fredrickson, J., & Zhou, J. (2005). Global transcriptome analysis of *Shewanella oneidensis* MR-1 exposed to different terminal electron acceptors. *Journal of Bacteriology, 187*(20), 7138-7145. doi:10.1128/JB.187.20.7138-7145.2005

Beliaev, A., & Saffarini, D. (1998). *Shewanella putrefaciens mtrB* encodes an outer membrane protein required for Fe(III) and Mn(IV) reduction. *Journal of Bacteriology, 180*(23), 6292-6297.

Beliaev, A., Saffarini, D., McLaughlin, J., & Hunnicutt, D. (2001). MtrC, an outer membrane decahaem *c* cytochrome required for metal reduction in *Shewanella putrefaciens* MR-1. *Molecular Microbiology, 39*(3), 722-730. doi:10.1046/j.1365-2958.2001.02257.x

Biebl, H., & Pfennig, N. (1978). Growth yields of green sulfur bacteria in mixed cultures with sulfur and sulfate reducing bacteria. *Archives of Microbiology, 117*(1), 9-16. doi:10.1007/BF00689344

Boetius, A., Ravenschlag, K., Schubert, C., Rickert, D., Widdel, F., Gieseke, A., Amann, R., Jorgensen, B., Witte, U., & Pfannkuche, O. (2000). A marine microbial consortium apparently mediating anaerobic oxidation of methane. *Nature, 407*(6804), 623-626. doi:10.1038/35036572

Bond, D., Holmes, D., Tender, L., & Lovley, D. (2002). Electrode-reducing microorganisms that harvest energy from marine sediments. *Science, 295*(5554), 483-485. doi:10.1126/science.1066771

Brenner, K., You, L., & Arnold, F. H. (2008). Engineering microbial consortia: a new frontier in synthetic biology. *Trends in Biotechnology, 26*(9), 483-489. doi:10.1016/j.tibtech.2008.05.004

Bretschger, O., Cheung, A., Mansfeld, F., & Nealson, K. H. (2010). Comparative microbial fuel cell evaluations of *Shewanella* spp. *Electroanalysis, 22*(7-8), 883-894. doi:10.1002/elan.200800016

Bretschger, O., Obraztsova, A., Sturm, C., Chang, I., Gorby, Y., Reed, S., Culley, D., Reardon, C., Barua, S., Romine, M., & Nealson, K. H. (2007). Current production and metal oxide reduction by *Shewanella oneidensis* MR-1 wild type and mutants. *Applied and Environmental Microbiology, 73*(21), 7003-7012. doi:10.1128/AEM.01087-07

Brim, H., McFarlan, S., Fredrickson, J., Minton, K., Zhai, M., Wackett, L., & Daly, M. (2000). Engineering *Deinococcus radiodurans* for metal remediation in radioactive mixed waste environments. *Nature Biotechnology, 18*(1), 85-90.

Brim, H., Venkateswaran, A., Kostandarithes, H., Fredrickson, J., & Daly, M. (2003). Engineering *Deinococcus geothermalis* for bioremediation of high-temperature radioactive waste environments. *Applied and Environmental Microbiology, 69*(8), 4575-4582. doi:10.1128/AEM.69.8.4575-4582.2003

Brown, N., Stoyanov, J., Kidd, S., & Hobman, J. (2003). The MerR family of transcriptional regulators. *FEMS Microbiology Reviews, 27*(2-3), 145-163. doi:10.1016/S0168-6445(03)00051-2

Brutinel, E. D., & Gralnick, J. A. (2012a). Preferential utilization of D-lactate by *Shewanella oneidensis*. *Applied and Environmental Microbiology, 78*(23), 8474-8476. doi:10.1128/AEM.02183-12

Brutinel, E. D., & Gralnick, J. A. (2012b). Shuttling happens: soluble flavin mediators of extracellular electron transfer in *Shewanella*. *Applied Microbiology and Biotechnology, 93*(1), 41-48. doi:10.1007/s00253-011-3653-0

Bryant, M. P., Wolin, E. A., Wolin, M. J., & Wolfe, R. S. (1967). *Methanobacillus omelianskii,* a symbiotic association of two species of bacteria. *Arch Mikrobiol, 59*((1/3)), 20-31. doi:10.1007/BF00406313

Bull, J. J., & Harcombe, W. R. (2009). Population dynamics constrain the cooperative evolution of cross-feeding. *Plos One, 4*(1), e4115. doi:10.1371/journal.pone.0004115

Butler, J. E., Young, N. D., & Lovley, D. R. (2010). Evolution of electron transfer out of the cell: comparative genomics of six *Geobacter* genomes. *Bmc Genomics, 11*, 40. doi:10.1186/1471-2164-11-40

Caccavo, F., Lonergan, D., Lovley, D., Davis, M., Stolz, J., & McInerney, M. (1994). *Geobacter sulfurreducens* sp-nov, a hydrogen-oxidizing and acetate-oxidizing dissimilatory metal-reducing microorganism. *Applied and Environmental Microbiology, 60*(10), 3752-3759.

Carpentier, W., Sandra, K., De Smet, I., Brige, A., De Smet, L., & Van Beeumen, J. (2003). Microbial reduction and precipitation of vanadium by *Shewanella oneidensis*. *Applied and Environmental Microbiology, 69*(6), 3636-3639. doi:10.1128/AEM.69.6.3636-3639.2003

Chai, Y., Kolter, R., & Losick, R. (2009). A widely conserved gene cluster required for lactate utilization in *Bacillus subtilis* and its involvement in biofilm formation. *Journal of Bacteriology, 191*(8), 2423-2430. doi:10.1128/JB.01464-08

Chan, C., Levar, C., Zacharoff, L., Badalamenti, J., & Bond, D. R. (2015). Scarless genome editing and stable inducible expression vectors for *Geobacter sulfurreducens*. *Appl.Environ.Microbiol., 81*(20), 7178-7186. doi:doi:10.1128/AEM.01967-15

Chen, S., Rotaru, A., Shrestha, P., Malvankar, N., Liu, F., Fan, W., Nevin, K., & Lovley, D. R. (2014). Promoting interspecies electron transfer with biochar. *Scientific Reports, 4*, 5019. doi:10.1038/srep05019

Chen, S., & Wilson, D. (1997). Construction and characterization of *Escherichia coli* genetically engineered for bioremediation of Hg2+-contaminated environments. *Applied and Environmental Microbiology, 63*(6), 2442-2445.

Coppi, M., Leang, C., Sandler, S., & Lovley, D. (2001). Development of a genetic system for *Geobacter sulfurreducens*. *Applied and Environmental Microbiology, 67*(7), 3180-3187. doi:10.1128/AEM.67.7.3180-3187.2001

Coursolle, D., Baron, D., Bond, D., & Gralnick, J. A. (2010). The Mtr respiratory pathway is essential for reducing flavins and electrodes in *Shewanella oneidensis*. *Journal of Bacteriology, 192*(2), 467-474. doi:10.1128/JB.00925-09

Coursolle, D., & Gralnick, J. A. (2010). Modularity of the Mtr respiratory pathway of *Shewanella oneidensis* strain MR-1. *Molecular Microbiology, 77*(4), 995-1008. doi:10.1111/j.1365-2958.2010.07266.x

Covington, E., Gelbmann, C., Kotloski, N., & Gralnick, J. A. (2010). An essential role for UshA in processing of extracellular flavin electron shuttles by *Shewanella oneidensis*. *Molecular Microbiology, 78*(2), 519-532. doi:10.1111/j.1365-2958.2010.07353.x

Crossley, R., Gaskin, D., Holmes, K., Mulholland, F., Wells, J., Kelly, D., van Vliet, A., &Walton, N. J. (2007). Riboflavin biosynthesis is associated with assimilatory ferric reduction and iron acquisition by *Campylobacter jejuni*. *Applied and Environmental Microbiology, 73*(24), 7819-7825. doi:10.1128/AEM.01919-07

De Roy, K., Marzorati, M., Van den Abbeele, P., Van de Wiele, T., & Boon, N. (2014a). Synthetic microbial ecosystems: an exciting tool to understand and apply microbial communities. *Environmental Microbiology, 16*(6), 1472-1481. doi:10.1111/1462-2920.12343

De Windt, W., Boon, N., Van den Bulcke, J., Rubberecht, L., Prata, F., Mast, J., Hennebel, T., & Verstraete, W. (2006). Biological control of the size and reactivity of catalytic Pd(0) produced by *Shewanella oneidensis. Antonie Van Leeuwenhoek International Journal of General and Molecular Microbiology, 90*(4), 377-389. doi:10.1007/s10482-006-9088-4

Denef, V., Mueller, R., & Banfield, J. F. (2010). AMD biofilms: using model communities to study microbial evolution and ecological complexity in nature. *Isme Journal, 4*(5), 599-610. doi:10.1038/ismej.2009.158

Deng, X., & Jia, P. (2011). Construction and characterization of a photosynthetic bacterium genetically engineered for Hg2+ uptake. *Bioresource Technology, 102*(3), 3083-3088. doi:10.1016/j.biortech.2010.10.051

Deutzmann, J., Sahin, M., & Spormann, A. M. (2015). Extracellular enzymes facilitate electron uptake in biocorrosion and bioelectrosynthesis. *Mbio, 6*(2), e00496. doi:10.1128/mBio.00496-15

Ding, Y., Hixson, K., Aklujkar, M., Lipton, M., Smith, R., Lovley, D., & Mester, T. (2008). Proteome of *Geobacter sulfurreducens* grown with Fe(III) oxide or Fe(III) citrate as the electron acceptor. *Biochimica Et Biophysica Acta-Proteins and Proteomics, 1784*(12), 1935-1941. doi:10.1016/j.bbapap.2008.06.011

Ding, Y., Hixson, K., Giometti, C., Stanley, A., Esteve-Nunez, A., Khare, T., Tollaksen, S., Zhu, W., Adkins, J., Lipton, M., & Lovley, D. R. (2006). The proteome of dissimilatory metal-reducing microorganism *Geobacter sulfurreducens* under various growth conditions. *Biochimica Et Biophysica Acta-Proteins and Proteomics, 1764*(7), 1198-1206. doi:10.1016/j.bbapap.2006.04.017

Dmytruk, K., Voronovsky, A., & Sibirny, A. A. (2006). Insertion mutagenesis of the yeast *Candida famata* (*Debaryomyces hansenii*) by random integration of linear DNA fragments. *Current Genetics, 50*(3), 183-191. doi:10.1007/s00294-006-0083-0

Dolfing, J. (2014). Syntrophy in microbial fuel cells. *Isme Journal, 8*(1), 4-5. doi:10.1038/ismej.2013.198

Dong, X., Plugge, C., & Stams, A. (1994). Anaerobic degradation of propionate by a mesophilic acetogenic bacterium in coculture and triculture with different methanogens. *Applied and Environmental Microbiology, 60*(8), 2834-2838.

D'Onofrio, A., Crawford, J., Stewart, E., Witt, K., Gavrish, E., Epstein, S., Clardy, J., & Lewis, K. (2010). Siderophores from neighboring organisms promote the growth of uncultured bacteria. *Chemistry & Biology, 17*(3), 254-264. doi:10.1016/j.chembiol.2010.02.010

Dunham, M. J. (2007). Synthetic ecology: A model system for cooperation. *Proceedings of the National Academy of Sciences of the United States of America, 104*(6), 1741-1742. doi:10.1073/pnas.0611067104

Edgar, R. (2004). MUSCLE: multiple sequence alignment with high accuracy and high throughput. *Nucleic Acids Research, 32*(5), 1792-1797. doi:10.1093/nar/gkh340

Endy, D. (2005). Foundations for engineering biology. *Nature, 438*(7067), 449-453. doi:10.1038/nature04342

Falkowski, P., Fenchel, T., & Delong, E. F. (2008). The microbial engines that drive Earth's biogeochemical cycles. *Science, 320*(5879), 1034-1039. doi:10.1126/science.1153213

Fassbinder, F., Kist, M., & Bereswill, S. (2000). Structural and functional analysis of the riboflavin synthesis genes encoding GTP cyclohydrolase II (*ribA*), DHBP synthase (*ribBA*), riboflavin synthase (*ribC*), and riboflavin deaminase/reductase (*ribD*) from *Helicobacter pylori* strain P1. *FEMS Microbiology Letters, 191*(2), 191-197. doi:10.1016/S0378-1097(00)00389-X

Faust, K., & Raes, J. (2012). Microbial interactions: from networks to models. *Nature Reviews Microbiology, 10*(8), 538-550. doi:10.1038/nrmicro2832

Felsenstein, J. (1985). Confidence-limits on phylogenies - an approach using the bootstrap. *Evolution, 39*(4), 783-791. doi:10.2307/2408678

Flynn, C., Hunt, K., Gralnick, J., & Srienc, F. (2012). Construction and elementary mode analysis of a metabolic model for *Shewanella oneidensis* MR-1. *Biosystems, 107*(2), 120-128. doi:10.1016/j.biosystems.2011.10.003

Flynn, J., Ross, D., Hunt, K., Bond, D., & Gralnick, J. A. (2010). Enabling unbalanced fermentations by using engineered electrode-interfaced bacteria. *Mbio, 1*(5), e00190. doi:10.1128/mBio.00190-10

Foster, K., & Bell, T. (2012). Competition, not cooperation, dominates interactions among culturable microbial species. *Current Biology, 22*(19), 1845-1850. doi:10.1016/j.cub.2012.08.005

Franzosa, E., Hsu, T., Sirota-Madi, A., Shafquat, A., Abu-Ali, G., Morgan, X., & Huttenhower, C. (2015). Sequencing and beyond: integrating molecular 'omics' for microbial community profiling. *Nature Reviews Microbiology, 13*(6), 360-372. doi:10.1038/nrmicro3451

Fredrickson, J., Romine, M., Beliaev, A., Auchtung, J., Driscoll, M., Gardner, T., Nealson, K., Osterman, A., Pinchuk, G., Reed, J., Rodionov, D., Rodrigues, J.,

Saffarini, D., Serres, M., Spormann, A., Zhulin, I., & Tiedje, J. M. (2008). Towards environmental systems biology of *Shewanella*. *Nature Reviews Microbiology, 6*(8), 592-603. doi:10.1038/nrmicro1947

Fuller, S., McMillan, D., Renz, M., Schmidt, M., Burke, I., & Stewart, D. I. (2014). Extracellular electron transport-mediated Fe(III) reduction by a community of alkaliphilic bacteria that use flavins as electron shuttles. *Applied and Environmental Microbiology, 80*(1), 128-137. doi:10.1128/AEM.02282-13 ER

Gevers, D., Vandepoele, K., Simillion, C., & Van de Peer, Y. (2004). Gene duplication and biased functional retention of paralogs in bacterial genomes. *Trends in Microbiology, 12*(4), 148-154. doi:10.1016/j.tim.2004.02.007

Gralnick, J., & Newman, D. K. (2007). Extracellular respiration. *Molecular Microbiology, 65*(1), 1-11. doi:10.1111/j.1365-2958.2007.05778.x

Griffin, H., Foster, T., Silver, S., & Misra, T. (1987). Cloning and DNA-sequence of the mercuric-resistance and organomercurial-resistance determinants of plasmid PDU1358. *Proceedings of the National Academy of Sciences of the United States of America, 84*(10), 3112-3116. doi:10.1073/pnas.84.10.3112

Grobkopf, T., & Soyer, O. S. (2014). Synthetic microbial communities. *Current Opinion in Microbiology, 18*, 72-77. doi:10.1016/j.mib.2014.02.002

Guedron, S., Cossa, D., Grimaldi, M., & Charlet, L. (2011). Methylmercury in tailings ponds of Amazonian gold mines (French Guiana): Field observations and an experimental flocculation method for *in situ* remediation. *Applied Geochemistry, 26*(2), 222-229. doi:10.1016/j.apgeochem.2010.11.022

Harcombe, W. (2010). Novel cooperation experimentally evolved between species. *Evolution, 64*(7), 2166-2172. doi:10.1111/j.1558-5646.2010.00959.x

Hartshorne, R., Reardon, C., Ross, D., Nuester, J., Clarke, T., Gates, A., Mills, P., Fredrickson, J., Zachara, J., Shi, L., Beliaev, A., Marshall, M., Tien, M., Brantley, S., Butt, J., & Richardson, D. J. (2009). Characterization of an electron conduit between bacteria and the extracellular environment. *Proceedings of the National Academy of Sciences of the United States of America, 106*(52), 22169-22174. doi:10.1073/pnas.0900086106

Hau, H., Gilbert, A., Coursolle, D., & Gralnick, J. A. (2008). Mechanism and consequences of anaerobic respiration of cobalt by *Shewanella oneidensis* strain MR-1. *Applied and Environmental Microbiology, 74*(22), 6880-6886. doi:10.1128/AEM.00840-08

Hau, H., & Gralnick, J. A. (2007). Ecology and biotechnology of the genus *Shewanella*. *Annual Review of Microbiology, 61*, 237-258. doi:10.1146/annurev.micro.61.080706.093257

Heidelberg, J., Paulsen, I., Nelson, K., Gaidos, E., Nelson, W., Read, T., Eisen, J., Seshadri, R., Ward, N., Methe, B., Clayton, R., Meyer, T., Tsapin, A., Scott, J., Beanan, M., Brinkac, L., Daugherty, S., DeBoy, R., Dodson, R., Durkin, A., Haft, D., Kolonay, J., Madupu, R., Peterson, J., Umayam, L., White, O., Wolf, A., Vamathevan, J., Weidman, J., Impraim, M., Lee, K., Berry, K., Lee, C., Mueller, J., Khouri, H., Gill, J., Utterback, T., McDonald, L., Feldblyum, T., Smith, H., Venter, C., Nealson, K., & Fraser, C. (2002). Genome sequence of the dissimilatory metal ion-reducing bacterium *Shewanella oneidensis*. *Nature Biotechnology, 20*(11), 1118-1123. doi:10.1038/nbt749

Hillesland, K., Lim, S., Flowers, J., Turkarslan, S., Pinel, N., Zane, G., Elliott, N., Qin, Y., Wu, L., Baliga, N., Zhou, J., Wall, J., & Stahl, D. A. (2014). Erosion of functional independence early in the evolution of a microbial mutualism. *Proceedings of the National Academy of Sciences of the United States of America, 111*(41), 14822-14827. doi:10.1073/pnas.1407986111 ER

Hillesland, K., & Stahl, D. A. (2010). Rapid evolution of stability and productivity at the origin of a microbial mutualism. *Proceedings of the National Academy of Sciences of the United States of America, 107*(5), 2124-2129. doi:10.1073/pnas.0908456107

Holmes, D., Chaudhuri, S., Nevin, K., Mehta, T., Methe, B., Liu, A., Ward, J., Woodard, T., Webster, J., & Lovley, D. R. (2006). Microarray and genetic analysis of electron transfer to electrodes in *Geobacter sulfurreducens*. *Environmental Microbiology, 8*(10), 1805-1815. doi:10.1111/j.1462-2920.2006.01065.x

Hong, Y., & Gu, J. (2010). Physiology and biochemistry of reduction of azo compounds by *Shewanella* strains relevant to electron transport chain. *Applied Microbiology and Biotechnology, 88*(3), 637-643. doi:10.1007/s00253-010-2820-z

Horn, J., Brunke, M., Deckwer, W., & Timmis, K. (1994). *Pseudomonas putida* strains which constitutively overexpress mercury resistance for biodetoxification of organomercurial pollutants. *Applied and Environmental Microbiology, 60*(1), 357-362.

Hunt, K., Flynn, J., Naranjo, B., Shikhare, I., & Gralnick, J. A. (2010). Substrate level phosphorylation is the primary source of energy conservation during anaerobic respiration of *Shewanella oneidensis* strain MR-1. *Journal of Bacteriology, 192*(13), 3345-3351. doi:10.1128/JB.00090-10

Huttenhower, C., Gevers, D., Knight, R., Abubucker, S., Badger, J., Chinwalla, A., . . . Human Microbiome Project Consortium. (2012). Structure, function and diversity of the healthy human microbiome. *Nature, 486*(7402), 207-214. doi:10.1038/nature11234

Jormakka, M., Tornroth, S., Byrne, B., & Iwata, S. (2002). Molecular basis of proton motive force generation: Structure of Formate Dehydrogenase-N. *Science, 295*(5561), 1863-1868. doi:10.1126/science.1068186

Kaden, J., Galushko, A., & Schink, B. (2002). Cysteine-mediated electron transfer in syntrophic acetate oxidation by cocultures of *Geobacter sulfurreducens* and *Wolinella succinogenes*. *Archives of Microbiology, 178*(1), 53-58. doi:10.1007/s00203-002-0425-3

Kaeberlein, T., Lewis, K., & Epstein, S. (2002). Isolating "uncultivable" microorganisms in pure culture in a simulated natural environment. *Science, 296*(5570), 1127-1129. doi:10.1126/science.1070633

Kane, A., Bond, D., & Gralnick, J. A. (2013). Electrochemical analysis of *Shewanella oneidensis* engineered to bind gold electrodes. *ACS Synthetic Biology, 2*(2), 93-101. doi:10.1021/sb300042w

Kato, S., Hashimoto, K., & Watanabe, K. (2012). Microbial interspecies electron transfer via electric currents through conductive minerals. *Proceedings of the National Academy of Sciences of the United States of America, 109*(25), 10042-10046. doi:10.1073/pnas.1117592109

Kembel, S. W., Jones, E., Kline, J., Northcutt, D., Stenson, J., Womack, A. M., Bohannan, B., Brown, G., & Green, J. L. (2012). Architectural design influences the diversity and structure of the built environment microbiome. *Isme Journal, 6*(8), 1469-1479. doi:10.1038/ismej.2011.211

Kim, H., Boedicker, J., Choi, J., & Ismagilov, R. F. (2008). Defined spatial structure stabilizes a synthetic multispecies bacterial community. *Proceedings of the National Academy of Sciences of the United States of America, 105*(47), 18188-18193. doi:10.1073/pnas.0807935105

Kirchhofer, N., Chen, X., Marsili, E., Sumner, J., Dahlquist, F., & Bazan, G. C. (2014). The conjugated oligoelectrolyte DSSN plus enables exceptional coulombic efficiency via direct electron transfer for anode-respiring *Shewanella oneidensis* MR-1-a mechanistic study. *Physical Chemistry Chemical Physics, 16*(38), 20436-20443. doi:10.1039/c4cp03197k

Kiyono, M., Omura, H., Omura, T., Murata, S., & Pan-Hou, H. (2003). Removal of inorganic and organic mercurials by immobilized bacteria having *mer-ppk* fusion plasmids. *Applied Microbiology and Biotechnology, 62*(2-3), 274-278. doi:10.1007/s00253-003-1282-y

Kotloski, N., & Gralnick, J. A. (2013). Flavin electron shuttles dominate extracellular electron transfer by *Shewanella oneidensis*. *Mbio, 4*(1), e00553. doi:10.1128/mBio.00553-12

Kouzuma, A., Hashimoto, K., & Watanabe, K. (2012a). Influences of aerobic respiration on current generation by *Shewanella oneidensis* MR-1 in single-chamber microbial fuel cells. *Bioscience Biotechnology and Biochemistry, 76*(2), 270-275. doi:10.1271/bbb.110633

Kouzuma, A., Kato, S., & Watanabe, K. (2015). Microbial interspecies interactions: recent findings in syntrophic consortia. *Frontiers in Microbiology, 6*, 477. doi:10.3389/fmict.2015.00477

Kovach, M., Elzer, P., Hill, D., Robertson, G., Farris, M., Roop, R., & Peterson, K. (1995). 4 new derivatives of the broad-host-range cloning vector PBBR1mcs, carrying different antibiotic-resistance cassettes. *Gene, 166*(1), 175-176. doi:10.1016/0378-1119(95)00584-1

Kreuzer, H., Hill, E., Moran, J., Bartholomew, R., Yang, H., & Hegg, E. L. (2014). Contributions of the [NiFe]-and [FeFe]-hydrogenase to H_2 production in *Shewanella oneidensis* MR-1 as revealed by isotope ratio analysis of evolved H_2. *FEMS Microbiology Letters, 352*(1), 18-24. doi:10.1111/1574-6968.12361

Lafrance-Vanasse, J., Lefebvre, M., Di Lello, P., Sygusch, J., & Omichinski, J. G. (2009). Crystal structures of the organomercurial lyase MerB in its free and mercury-bound forms: Insights into the mechanism of methylmercury degradation. *Journal of Biological Chemistry, 284*(2), 938-944. doi:10.1074/jbc.M807143200

Lederberg, J. (1946). Proceedings of local branches of the society of American bacteriologists. *Journal of Bacteriology, 52*, 501-504.

Lee, H., & Rittmann, B. E. (2010). Significance of biological hydrogen oxidation in a continuous single-chamber microbial electrolysis cell. *Environmental Science & Technology, 44*(3), 948-954. doi:10.1021/es9025358

Lee, H., Torres, C. I., Parameswaran, P., & Rittmann, B. E. (2009). Fate of H_2 in an upflow single-chamber microbial electrolysis cell using a metal-catalyst-free cathode. *Environmental Science & Technology, 43*(20), 7971-7976. doi:10.1021/es900204j

Leonhartsberger, S., Korsa, I., & Bock, A. (2002). The molecular biology of formate metabolism in enterobacteria. *Journal of Molecular Microbiology and Biotechnology, 4*(3), 269-276.

Leopold, K., Foulkes, M., & Worsfold, P. (2010). Methods for the determination and speciation of mercury in natural waters-A review. *Analytica Chimica Acta, 663*(2), 127-138. doi:10.1016/j.aca.2010.01.048

Levar, C., Chan, C., Mehta-Kolte, M., & Bond, D. R. (2014). An inner membrane cytochrome required only for reduction of high redox potential extracellular electron acceptors. *Mbio, 5*(6), e02034. doi:10.1128/mBio.02034-14

Lin, C., Yee, N., & Barkay, T. (2012). Microbial transformation in the mercury cycle. In G. Liu, C. Yong & N. O'Driscoll (Eds.), *Environmental chemistry and toxicology of mercury* (pp. 155-191). Hoboken: John Wiley and Sons.

Lin, K., Chien, M., Hsieh, J., & Huang, C. (2010). Mercury resistance and accumulation in *Escherichia coli* with cell surface expression of fish metallothionein. *Applied Microbiology and Biotechnology, 87*(2), 561-569. doi:10.1007/s00253-010-2466-x

Little, A., Robinson, C., Peterson, S., Raffa, K., & Handelsman, J. (2008). Rules of engagement: Interspecies interactions that regulate microbial communities. *Annual Review of Microbiology, 62*, 375-401. doi:10.1146/annurev.micro.030608.101423

Liu, F., Rotaru, A., Shrestha, P., Malvankar, N., Nevin, K., & Lovley, D. R. (2012). Promoting direct interspecies electron transfer with activated carbon. *Energy & Environmental Science, 5*(10), 8982-8989. doi:10.1039/c2ee22459c

Liu, Y., Kim, H., Franklin, R., & Bond, D. R. (2010). Gold line array electrodes increase substrate affinity and current density of electricity-producing *G. sulfurreducens* biofilms. *Energy & Environmental Science, 3*(11), 1782-1788. doi:10.1039/c0ee00242a

Lloyd, J., Leang, C., Myerson, A., Coppi, M., Cuifo, S., Methe, B., Sandler, S., & Lovley, D. (2003). Biochemical and genetic characterization of PpcA, a periplasmic *c*-type cytochrome in *Geobacter sulfurreducens*. *Biochemical Journal, 369*, 153-161. doi:10.1042/BJ20020597

Lovley, D. R., Ueki, T., Zhang, T., Malvankar, N. S., Shrestha, P. M., Flanagan, K., Aklujkar, M., Butler, J., Giloteaux, L., Rotaru, A., Holmes, D., Franks, A., Orellana, R., Risso, C., & Nevin, K. P. (2011). *Geobacter*: The microbe electric's physiology, ecology, and practical applications. *Advances in Microbial Physiology, Vol 59, 59*, 1-100. doi:10.1016/B978-0-12-387661-4.00004-5

Lovley, D., GiovannoniI, S., White, D., Champine, J., Phillips, E., Gorby, Y., & Goodwin, S. (1993). *Geobacter metallireducens* gen-nov sp-nov, a microorganism capable of coupling the complete oxidation of organic compounds to the reduction of iron and other metals. *Archives of Microbiology, 159*(4), 336-344. doi:10.1007/BF00290916

Lovley, D., Holmes, D., & Nevin, K. (2004). Dissimilatory Fe(III) and Mn(IV) reduction. *Advances in Microbial Physiology, Vol.49, 49*, 219-286. doi:10.1016/S0065-2911(04)49005-5

Lovley, D., Stolz, J., Nord, G., & Phillips, E. (1987). Anaerobic production of magnetite by a dissimilatory iron-reducing microorganism. *Nature, 330*(6145), 252-254. doi:10.1038/330252a0

Mahadevan, R., Palsson, B. O., & Lovley, D. R. (2011). *In situ* to *in silico* and back: elucidating the physiology and ecology of *Geobacter* spp. using genome-scale modelling. *Nature Reviews Microbiology, 9*(1), 39-50. doi:10.1038/nrmicro2456

Marritt, S., Lowe, T., Bye, J., McMillan, D., Shi, L., Fredrickson, J., Zachara, J., Richardson, D., Cheesman, M., Jeuken, L., & Butt, J. N. (2012). A functional description of CymA, an electron-transfer hub supporting anaerobic respiratory flexibility in *Shewanella*. *Biochemical Journal, 444*, 465-474. doi:10.1042/BJ20120197

Marritt, S., McMillan, D., Shi, L., Fredrickson, J., Zachara, J., Richardson, D., Jeuken, L., & Butt, J. N. (2012). The roles of CymA in support of the respiratory flexibility of *Shewanella oneidensis* MR-1. *Biochemical Society Transactions, 40*, 1217-1221. doi:10.1042/BST20120150

Marsili, E., Baron, D., Shikhare, I., Coursolle, D., Gralnick, J., & Bond, D. R. (2008). *Shewanella* secretes flavins that mediate extracellular electron transfer. *Proceedings of the National Academy of Sciences of the United States of America, 105*(10), 3968-3973. doi:10.1073/pnas.0710525105

McGlynn, S., Chadwick, G., Kempes, C., & Orphan, V. J. (2015). Single cell activity reveals direct electron transfer in methanotrophic consortia. *Nature, 526*(7574), 531-NIL_146.

Mehta-Kolte, M., & Bond, D. R. (2012). *Geothrix fermentans* secretes two different redox-active compounds to utilize electron acceptors across a wide range of redox potentials. *Applied and Environmental Microbiology, 78*(19), 6987-6995. doi:10.1128/AEM.01460-12

Meshulam-Simon, G., Behrens, S., Choo, A. D., & Spormann, A. M. (2007). Hydrogen metabolism in *Shewanella oneidensis* MR-1. *Applied and Environmental Microbiology, 73*(4), 1153-1165. doi:10.1128/AEM.01588-06

Methe, B., Nelson, K., Eisen, J., Paulsen, I., Nelson, W., Heidelberg, J., . . . Fraser, C. (2003). Genome of *Geobacter sulfurreducens*: Metal reduction in subsurface environments. *Science, 302*(5652), 1967-1969. doi:10.1126/science.1088727

Milucka, J., Ferdelman, T. G., Polerecky, L., Franzke, D., Wegener, G., Schmid, M., Lieberwirth, I., Wagner, M., Widdel, F., & Kuypers, M. M. M. (2012). Zero-valent sulphur is a key intermediate in marine methane oxidation. *Nature, 491*(7425), 541-+. doi:10.1038/nature11656

Mitchell, P. (1961). Coupling of phosphorylation to electron and hydrogen transfer by a chemi-osmotic type of mechanism. *Nature, 191*((4784)), 144-148. doi:10.1038/191144a0

Morris, B., Henneberger, R., Huber, H., & Moissl-Eichinger, C. (2013). Microbial syntrophy: interaction for the common good. *FEMS Microbiology Reviews, 37*(3), 384-406. doi:10.1111/1574-6976.12019

Morris, J., Lenski, R., & Zinser, E. R. (2012). The black queen hypothesis: Evolution of dependencies through adaptive gene loss. *Mbio, 3*(2), e00036. doi:10.1128/mBio.00036-12

Mutlu, B., Yeom, S., Tong, H., Wackett, L., & Aksan, A. (2013). Silicon alkoxide cross-linked silica nanoparticle gels for encapsulation of bacterial biocatalysts. *Journal of Materials Chemistry A, 1*(36), 11051-11060. doi:10.1039/c3ta12303k

Mutlu, B., Yeom, S., Wackett, L., & Aksan, A. (2015). Modelling and optimization of a bioremediation system utilizing silica gel encapsulated whole-cell biocatalyst. *Chemical Engineering Journal, 259*, 574-580. doi:10.1016/j.cej.2014.07.130

Myers, C., Carstens, B., Antholine, W., & Myers, J. (2000). Chromium(VI) reductase activity is associated with the cytoplasmic membrane of anaerobically grown *Shewanella putrefaciens* MR-1. *Journal of Applied Microbiology, 88*(1), 98-106. doi:10.1046/j.1365-2672.2000.00910.x

Myers, J., & Myers, C. (2000). Role of the tetraheme cytochrome CymA in anaerobic electron transport in cells of *Shewanella putrefaciens* MR-1 with normal levels of menaquinone. *Journal of Bacteriology, 182*(1), 67-75.

Nealson, K., & Scott, J. (2006). In Dworkin, M Falkow, S Rosenberg, E Schleifer, KH Stackebrandt,E. (Ed.), Ecophysiology of the Genus *Shewanella*. New York: Springer. doi:10.1007/0-387-30746-x_45

Nealson, K., Moser, D., & Saffarini, D. (1995). Anaerobic electron-acceptor chemotaxis in *Shewanella putrefaciens*. *Applied and Environmental Microbiology, 61*(4), 1551-1554.

Nei, M., & Kumar, S. (2000). Molecular evolution and phylogenetics. Oxford & New York: Oxford University Press.

Newton, G., Mori, S., Nakamura, R., Hashimoto, K., & Watanabe, K. (2009). Analyses of current-generating mechanisms of *Shewanella loihica* PV-4 and *Shewanella oneidensis* MR-1 in microbial fuel cells. *Applied and Environmental Microbiology, 75*(24), 7674-7681. doi:10.1128/AEM.01142-09

Nilsson, A., Koskiniemi, S., Eriksson, S., Kugelberg, E., Hinton, J., & Andersson, D. (2005). Bacterial genome size reduction by experimental evolution. *Proceedings of the National Academy of Sciences of the United States of America, 102*(34), 12112-12116. doi:10.1073/pnas.0503654102

Okamoto, A., Hashimoto, K., Nealson, K., & Nakamura, R. (2013). Rate enhancement of bacterial extracellular electron transport involves bound flavin semiquinones. *Proceedings of the National Academy of Sciences of the United States of America, 110*(19), 7856-7861. doi:10.1073/pnas.1220823110

Orcutt, B., & Meile, C. (2008). Constraints on mechanisms and rates of anaerobic oxidation of methane by microbial consortia: process-based modeling of ANME-2 archaea and sulfate reducing bacteria interactions. *Biogeosciences, 5*(6), 1587-1599.

Orphan, V. J. (2009). Methods for unveiling cryptic microbial partnerships in nature. *Current Opinion in Microbiology, 12*(3), 231-237. doi:10.1016/j.mib.2009.04.003

Orphan, V., House, C., Hinrichs, K., McKeegan, K., & DeLong, E. (2001). Methane-consuming archaea revealed by directly coupled isotopic and phylogenetic analysis. *Science, 293*(5529), 484-487. doi:10.1126/science.1061338

Pande, S., Merker, H., Bohl, K., Reichelt, M., Schuster, S., de Figueiredo, L. F., Kaleta, C., & Kost, C. (2014). Fitness and stability of obligate cross-feeding interactions that emerge upon gene loss in bacteria. *Isme Journal, 8*(5), 953-962. doi:10.1038/ismej.2013.211

Pan-Hou, H., Kiyono, M., Omura, H., Omura, T., & Endo, G. (2002). Polyphosphate produced in recombinant *Escherichia coli* confers mercury resistance. *FEMS Microbiology Letters, 207*(2), 159-164. doi:10.1111/j.1574-6968.2002.tb11045.x

Phillips, D., Joseph, C., Yang, G., Martinez-Romero, E., Sanborn, J., & Volpin, H. (1999). Identification of lumichrome as a *Sinorhizobium* enhancer of alfalfa root respiration and shoot growth. *Proceedings of the National Academy of Sciences of the United States of America, 96*(22), 12275-12280. doi:10.1073/pnas.96.22.12275

Pinchuk, G., Geydebrekht, O., Hill, E., Reed, J., Konopka, A., Beliaev, A., & Fredrickson, J. K. (2011). Pyruvate and lactate metabolism by *Shewanella oneidensis* MR-1 under fermentation, oxygen limitation, and fumarate respiration conditions. *Applied and Environmental Microbiology, 77*(23), 8234-8240. doi:10.1128/AEM.05382-11

Pinchuk, G., Rodionov, D., Yang, C., Li, X., Osterman, A., Dervyn, E., Geydebrekht, O., Reed, S., Romine, M., Collart, F., Scott, J., Fredrickson, J., & Beliaev, A. S. (2009). Genomic reconstruction of *Shewanella oneidensis* MR-1 metabolism reveals a previously uncharacterized machinery for lactate utilization. *Proceedings of the National Academy of Sciences of the United States of America, 106*(8), 2874-2879. doi:10.1073/pnas.0806798106

Rabaey, K., & Verstraete, W. (2005). Microbial fuel cells: novel biotechnology for energy generation. *Trends in Biotechnology, 23*(6), 291-298. doi:10.1016/j.tibtech.2005.04.008

Raes, J., & Bork, P. (2008). Molecular eco-systems biology: towards an understanding of community function. *Nature Reviews Microbiology, 6*(9), 693-699. doi:10.1038/nrmicro1935

Rappe, M., & Giovannoni, S. (2003). The uncultured microbial majority. *Annual Review of Microbiology, 57*, 369-394. doi:10.1146/annurev.micro.57.030502.090759

Reategui, E., Reynolds, E., Kasinkas, L., Aggarwal, A., Sadowsky, M. J., Aksan, A., & Wackett, L. P. (2012). Silica gel-encapsulated AtzA biocatalyst for atrazine biodegradation. *Applied Microbiology and Biotechnology, 96*(1), 231-240. doi:10.1007/s00253-011-3821-2

Ringeisen, B., Henderson, E., Wu, P., Pietron, J., Ray, R., Little, B., Biffinger, J., & Jones-Meehan, J. (2006). High power density from a miniature microbial fuel cell using *Shewanella oneidensis* DSP10. *Environmental Science & Technology, 40*(8), 2629-2634. doi:10.1021/es052254w

Ringeisen, B., Ray, R., & Little, B. (2007). A miniature microbial fuel cell operating with an aerobic anode chamber. *Journal of Power Sources, 165*(2), 591-597. doi:10.1016/j.jpowsour.2006.10.026

Rodriguez-Celma, J., Vazquez-Reina, S., Orduna, J., Abadia, A., Abadia, J., Alvarez-Fernandez, A., & Lopez-Millan, A. (2011). Characterization of flavins in roots of Fe-deficient strategy I plants, with a focus on *Medicago truncatula*. *Plant and Cell Physiology, 52*(12), 2173-2189. doi:10.1093/pcp/pcr149

Rollefson, J., Levar, C., & Bond, D. R. (2009). Identification of genes involved in biofilm formation and respiration via mini-Himar transposon mutagenesis of *Geobacter sulfurreducens*. *Journal of Bacteriology, 191*(13), 4207-4217. doi:10.1128/JB.00057-09

Rondon, M., August, P., Bettermann, A., Brady, S., Grossman, T., Liles, M., Loiacono, K., Lynch, B., MacNeil, I., Minor, C., Tiong, C., Gilman, M., Osburne, M., Clardy, J., Handelsman, J., & Goodman, R. (2000). Cloning the soil metagenome: a strategy for accessing the genetic and functional diversity of uncultured microorganisms. *Applied and Environmental Microbiology, 66*(6), 2541-2547. doi:10.1128/AEM.66.6.2541-2547.2000

Rosenbaum, M., Bar, H., Beg, Q., Segre, D., Booth, J., Cotta, M., & Angenent, L. T. (2011). *Shewanella oneidensis* in a lactate-fed pure-culture and a glucose-fed co-culture with *Lactococcus lactis* with an electrode as electron acceptor. *Bioresource Technology, 102*(3), 2623-2628. doi:10.1016/j.biortech.2010.10.033

Rosenbaum, M., Cotta, M., & Angenent, L. T. (2010). Aerated *Shewanella oneidensis* in continuously fed bioelectrochemical systems for power and hydrogen production. *Biotechnology and Bioengineering, 105*(5), 880-888. doi:10.1002/bit.22621

Ross, D., Flynn, J., Baron, D., Gralnick, J., & Bond, D. R. (2011). Towards electrosynthesis in *Shewanella*: Energetics of reversing the Mtr pathway for reductive metabolism. *Plos One, 6*(2), e16649. doi:10.1371/journal.pone.0016649

Rotaru, A., Shrestha, P., Liu, F., Ueki, T., Nevin, K., Summers, Z., & Lovley, D. R. (2012). Interspecies electron transfer via hydrogen and formate rather than direct electrical connections in cocultures of *Pelobacter carbinolicus* and *Geobacter sulfurreducens*. *Applied and Environmental Microbiology, 78*(21), 7645-7651. doi:10.1128/AEM.01946-12

Ruebush, S., Brantley, S., & Tien, M. (2006). Reduction of soluble and insoluble iron forms by membrane fractions of *Shewanella oneidensis* grown under aerobic and anaerobic conditions. *Applied and Environmental Microbiology, 72*(4), 2925-2935. doi:10.1128/AEM.72.4.2925-2935.2006

Ruiz, O., Alvarez, D., Gonzalez-Ruiz, G., & Torres, C. (2011). Characterization of mercury bioremediation by transgenic bacteria expressing metallothionein and polyphosphate kinase. *Bmc Biotechnology, 11*, 82. doi:10.1186/1472-6750-11-82

Saltikov, C., & Newman, D. (2003). Genetic identification of a respiratory arsenate reductase. *Proceedings of the National Academy of Sciences of the United States of America, 100*(19), 10983-10988. doi:10.1073/pnas.1834303100

Sawers, R. (2005). Formate and its role in hydrogen production in *Escherichia coli*. *Biochemical Society Transactions, 33*, 42-46.

Schink, B. (1997). Energetics of syntrophic cooperation in methanogenic degradation. *Microbiology and Molecular Biology Reviews, 61*(2), 262-&.

Schink, B., & Stams, A. J. M. (2006). In Dworkin, M Falkow, S Rosenberg, E Schleifer, KH Stackebrandt,E. (Ed.), *Syntrophism among Prokaryotes*. New York: Springer. doi:10.1007/0-387-30742-7_11

Shou, W., Ram, S., & Vilar, J. M. G. (2007). Synthetic cooperation in engineered yeast populations. *Proceedings of the National Academy of Sciences of the United States of America, 104*(6), 1877-1882. doi:10.1073/pnas.0610575104

Shrestha, P., & Rotaru, A. (2014). Plugging in or going wireless: strategies for interspecies electron transfer. *Frontiers in Microbiology, 5*, 237. doi:10.3389/fmicb.2014.00237

Sieber, J., McInerney, M., & Gunsalus, R. P. (2012). Genomic insights into syntrophy: The paradigm for anaerobic metabolic cooperation. *Annual Review of Microbiology, Vol 66, 66*, 429-452. doi:10.1146/annurev-micro-090110-102844

Simon, J., van Spanning, R., & Richardson, D. J. (2008). The organisation of proton motive and non-proton motive redox loops in prokaryotic respiratory systems. *Biochimica Et Biophysica Acta-Bioenergetics, 1777*(12), 1480-1490. doi:10.1016/j.bbabio.2008.09.008

Smith, J., Nevin, K., & Lovley, D. R. (2015). Syntrophic growth via quinone-mediated interspecies electron transfer. *Frontiers in Microbiology, 6*, 121. doi:10.3389/fmicb.2015.00121

Song, H., Ding, M., Jia, X., Ma, Q., & Yuan, Y. (2014). Synthetic microbial consortia: from systematic analysis to construction and applications. *Chemical Society Reviews, 43*(20), 6954-6981. doi:10.1039/c4cs00114a

Sousa, C., Kotrba, P., Ruml, T., Cebolla, A., & De Lorenzo, V. (1998). Metalloadsorption by *Escherichia coli* cells displaying yeast and mammalian metallothioneins anchored to the outer membrane protein LamB. *Journal of Bacteriology, 180*(9), 2280-2284.

Stams, A., & Plugge, C. M. (2009). Electron transfer in syntrophic communities of anaerobic bacteria and archaea. *Nature Reviews Microbiology, 7*(8), 568-577. doi:10.1038/nrmicro2166

Stenchuk, N., Kutsiaba, V., Kshanovskaia, B., & Fedorovich, D. (2001). Effect of *rib83* mutation on riboflavin biosynthesis and iron assimilation in *Pichia guilliermondii*. *Mikrobiologiia, 70*(6), 753-758.

Summers, Z., Fogarty, H., Leang, C., Franks, A. E., Malvankar, N., & Lovley, D. R. (2010). Direct exchange of electrons within aggregates of an evolved syntrophic coculture of anaerobic bacteria. *Science, 330*(6009), 1413-1415. doi:10.1126/science.1196526

Tamura, K., Stecher, G., Peterson, D., Filipski, A., & Kumar, S. (2013). MEGA6: Molecular evolutionary genetics analysis version 6.0. *Molecular Biology and Evolution, 30*(12), 2725-2729. doi:10.1093/molbev/mst197

Tchounwou, P., Ayensu, W., Ninashvili, N., & Sutton, D. (2003). Environmental exposure to mercury and its toxicopathologic implications for public health. *Environmental Toxicology, 18*(3), 149-175. doi:10.1002/tox.10116

Teal, T., Lies, D., Wold, B., & Newman, D. K. (2006). Spatiometabolic stratification of *Shewanella oneidensis* biofilms. *Applied and Environmental Microbiology, 72*(11), 7324-7330. doi:10.1128/AEM.01163-06

TerAvest, M., & Angenent, L. T. (2014). Oxidizing electrode potentials decrease current production and coulombic efficiency through cytochrome *c* inactivation in *Shewanella oneidensis* MR-1. *Chemelectrochem, 1*(11), 2000-2006. doi:10.1002/celc.201402128

Thiele, J., & Zeikus, J. (1988). Control of interspecies electron flow during anaerobic digestion: Significance of formate transfer versus hydrogen transfer during syntrophic methanogenesis in flocs. *Applied and Environmental Microbiology, 54*(1), 20-29.

Tremblay, P., & Zhang, T. (2015). Electrifying microbes for the production of chemicals. *Frontiers in Microbiology, 6*, UNSP 201. doi:10.3389/fmicb.2015.00201

United Nations Environment Programme. (2013). Global mercury assessment 2013: Sources, emissions, releases and environmental transport. Geneva: UNEP Chemicals Branch.

Venkateswaran, K., Moser, D., Dollhopf, M., Lies, D., Saffarini, D., MacGregor, B., Ringelberg, D., White, D., Nishijima, M., Sano, H., Burghardt, J., Stackebrandt, E., & Nealson, K. H. (1999). Polyphasic taxonomy of the genus *Shewanella* and

description of *Shewanella oneidensis* sp. nov. *International Journal of Systematic Bacteriology, 49*, 705-724.

Venter, J., Remington, K., Heidelberg, J., Halpern, A., Rusch, D., Eisen, J., Wu, D., Paulsen, I., Nelson, K., Nelson, W., Fouts, D., Levy, S., Knap, A., Lomas, M., Nealson, K., White, O., Peterson, J., Hoffman, J., Parsons, R., Baden-Tillson, H., Pfannkoch, C., Rogers, Y., & Smith, H. (2004). Environmental genome shotgun sequencing of the Sargasso Sea. *Science, 304*(5667), 66-74. doi:10.1126/science.1093857

Vick, J., Johnson, E., Choudhary, S., Bloch, S., Lopez-Gallego, F., Srivastava, P., Tikh, I., Wawrzyn, G., & Schmidt-Dannert, C. (2011). Optimized compatible set of BioBrick™ vectors for metabolic pathway engineering. *Applied Microbiology and Biotechnology, 92*(6), 1275-1286. doi:10.1007/s00253-011-3633-4

Vignais, P., & Billoud, B. (2007). Occurrence, classification, and biological function of hydrogenases: An overview. *Chemical Reviews, 107*(10), 4206-4272. doi:10.1021/cr050196r

von Canstein, H., Li, Y., Timmis, K., Deckwer, W., & Wagner-Dobler, I. (1999). Removal of mercury from chloralkali electrolysis wastewater by a mercury-resistant *Pseudomonas putida* strain. *Applied and Environmental Microbiology, 65*(12), 5279-5284.

von Canstein, H., Ogawa, J., Shimizu, S., & Lloyd, J. R. (2008). Secretion of flavins by *Shewanella* species and their role in extracellular electron transfer. *Applied and Environmental Microbiology, 74*(3), 615-623. doi:10.1128/AEM.01387-07

Wagner-Dobler, I., von Canstein, H., Li, Y., Timmis, K., & Deckwer, W. (2000). Removal of mercury from chemical wastewater by microoganisms in technical scale. *Environmental Science & Technology, 34*(21), 4628-4634. doi:10.1021/es0000652

Wagner-Dobler, I. (2013). In WagnerDobler I. (Ed.), *Current Research for Bioremediation of Mercury*. Wymondham: Caister Academic Press.

Waite, A., & Shou, W. (2012). Adaptation to a new environment allows cooperators to purge cheaters stochastically. *Proceedings of the National Academy of Sciences of the United States of America, 109*(47), 19079-19086. doi:10.1073/pnas.1210190109

Watson, V., & Logan, B. E. (2010). Power production in MFCs inoculated with *Shewanella oneidensis* MR-1 or mixed cultures. *Biotechnology and Bioengineering, 105*(3), 489-498. doi:10.1002/bit.22556

Wegener, G., Krukenberg, V., Riedel, D., Tegetmeyer, H., & Boetius, A. (2015). Intercellular wiring enables electron transfer between methanotrophic archaea and bacteria. *Nature, 526*(7574), 587-NIL_315.

Whitman, W., Coleman, D., & Wiebe, W. (1998). Prokaryotes: The unseen majority. *Proceedings of the National Academy of Sciences of the United States of America, 95*(12), 6578-6583. doi:10.1073/pnas.95.12.6578

Wintermute, E., & Silver, P. A. (2010). Emergent cooperation in microbial metabolism. *Molecular Systems Biology, 6*, 407. doi:10.1038/msb.2010.66

Worst, D., Gerrits, M., Vandenbroucke-Grauls, C., & Kusters, J. (1998). *Helicobacter pylori ribBA*-mediated riboflavin production is involved in iron acquisition. *Journal of Bacteriology, 180*(6), 1473-1479.

Wu, D., Xing, D., Lu, L., Wei, M., Liu, B., & Ren, N. (2013). Ferric iron enhances electricity generation by *Shewanella oneidensis* MR-1 in MFCs. *Bioresource Technology, 135*, 630-634. doi:10.1016/j.biortech.2012.09.106

Yang, C., Rodionov, D. A., Li, X., Laikova, O. N., Gelfand, M. S., Zagnitko, O. P., Romine, M., Obraztsova, A., Nealson, K., & Osterman, A. L. (2006). Comparative genomics and experimental characterization of N-acetylglucosamine utilization pathway of *Shewanella oneidensis*. *Journal of Biological Chemistry, 281*(40), 29872-29885. doi:10.1074/jbc.M60505220

Yang, G., Bhuvaneswari, T., Joseph, C., King, M., & Phillips, D. (2002). Roles for riboflavin in the *Sinorhizobium* - Alfalfa association. *Molecular Plant-Microbe Interactions, 15*(5), 456-462. doi:10.1094/MPMI.2002.15.5.456

Yang, T., Coppi, M., Lovley, D., & Sun, J. (2010). Metabolic response of *Geobacter sulfurreducens* towards electron donor/acceptor variation. *Microbial Cell Factories, 9*, 90. doi:10.1186/1475-2859-9-90

Yeom, S., Mutlu, B., Aksan, A., & Wackett, L. P. (Epub 2015 Jul 17). Bacterial cyanuric acid hydrolases for water treatment. *Appl Environ Microbiol,* doi:DOI: 10.1128/AEM.02175-15

Zacharoff, L., Chan, C., & Bond, D. R. (2016). Reduction of low potential electron acceptors requires the CbcL inner membrane cytochrome of *Geobacter sulfurreducens*. *Bioelectrochemistry, 107*, 7-13. doi:doi.org/10.1016/j.bioelechem.2015.08.003

Zengler, K., & Palsson, B. O. (2012). A road map for the development of community systems (CoSy) biology. *Nature Reviews Microbiology, 10*(5), 366-372. doi:10.1038/nrmicro2763

Zhang, T., & Hsu-Kim, H. (2010). Photolytic degradation of methylmercury enhanced by binding to natural organic ligands. *Nature Geoscience, 3*(7), 473-476. doi:10.1038/NGEO892